TAPHONOMIC, TAXONOMIC, AND BEHAVIORAL DIVERSITY OF WORMWORLD FOSSIL ASSEMBLAGES FROM EDIACARAN UNITS OF THE WESTERN UNITED STATES

A Dissertation
Submitted to the Graduate Faculty
of the
North Dakota State University
of Agriculture and Applied Science

By

Gretchen Rose O'Neil

In Partial Fulfillment of the Requirements
for the Degree of
DOCTOR OF PHILOSOPHY

Major Program:
Environmental and Conservation Sciences

September 2020

Fargo, North Dakota

North Dakota State University
Graduate School

Title

TAPHONOMIC, TAXONOMIC, AND BEHAVIORAL DIVERSITY OF WORMWORLD FOSSIL ASSEMBLAGES FROM EDIACARAN UNITS OF THE WESTERN UNITED STATES

By

Gretchen Rose O'Neil

The Supervisory Committee certifies that this ***disquisition*** complies with North Dakota State University's regulations and meets the accepted standards for the degree of

DOCTOR OF PHILOSOPHY

SUPERVISORY COMMITTEE:

Dr. Lydia Tackett
Chair

Dr. Jon Sweetman

Dr. Benjamin Laabs

Dr. Steve Travers

Approved:

11/16/2020
Date

Dr. Craig Stockwell
Department Chair

ABSTRACT

The western United States Deep Spring and Wood Canyon formations contain a variety of late Ediacaran fossils, representing the enigmatic Ediacara biota and a metazoan worm-like fauna. The latter, dubbed “Wormworld”, is comprised of a number of tube-dwelling organisms whose tubes were preserved through pervasive pyritization and carbonaceous compressions, as well as abundant horizontal burrows and grazing traces. One particular site, within Ancient Bristlecone Pine Forest presents a challenge that is not faced at the other localities, as it contains abundant tube-shaped fossils that are lacking in morphological characteristics due to poor preservation. Through investigations into what remains of the fossils and the potential preservational pathways that could produce such fossils, it is possible to use the findings to identify additional tube worm assemblages that may have been overlooked due to the assumed restriction on exceptional preservation based on sedimentology. Alternatively, trace fossils in the area appear to be more readily preserved and abundant, allowing for investigations into trends in frequency and faunal occurrences leading into the Cambrian Explosion. These traces and the trace maker activities are of a particular interest, as they represent the first communities of established bioturbators, which helped oxygenate the seafloor and mix the previously stratified microbial mat-rich substrate. The trace fossils on the surface of the beds represented ichnotaxa that are well-known in Cambrian deposits. However, petrographic thin sectioning revealed an unexpected fossil, *Lamonte trevallis*, previously only reported from South China. The presence of *Lamonte trevallis* is evidence for more advanced, complex Cambrian-like feeding behaviors occurring prior to the Precambrian–Cambrian boundary. The diversity of the Ediacaran fossils from the western United States places it among the established Ediacaran exceptional preservation localities and justifies the designation of the Deep Spring/Wood Canyon assemblage as an Ediacaran Lagerstätte.

ACKNOWLEDGEMENTS

I would like to thank those that have helped me and supported me during this process Lydia Tackett, Annaka Clement, and Sara Gibbs-Schnucker from North Dakota State University, Tara Selly, James Schiffbauer, Sarah Jacquet, Stephanie Rosbach, and Mikaela Pulsipher from the University of Missouri and Scott Mata for assistance in fieldwork and research. I'd also like to thank Simon Darroch of Vanderbilt University for feedback and input during manuscript preparation. I'd like to thank my family, especially my parents and grandparents, for being so supportive of my academic pursuits. I'd like to thank the Geology and Environmental and Conservation Sciences departments at North Dakota State University. I would like to thank NDSU, the Geological Society of America, the Society for Sedimentary Geology, and the National Science Foundation for funding this research. Finally, I would like to thank Roy and Gary for their invaluable input during the writing process.

DEDICATION

This dissertation is dedicated to the brightest beacons of light and hope, Joe Biden, Kamala Harris, and Britney Jean Spears.

TABLE OF CONTENTS

LIST OF TABLES

LIST OF FIGURES

LIST OF ABBREVIATIONS

ABPF……...Ancient Bristlecone Pine Forest

EEI……environmental engineering intensity

CHAPTER 1: INTRODUCTION TO THE EDIACARAN AND THE WORMWORLD FAUNA

1.1. Introduction

Divided into three consecutive faunal assemblages, the Avalon (635–558 Mya), the White Sea (~558–550 Mya), and the Nama (~550–539? Mya), the Ediacaran Period (635–539? Mya) witnesses the introduction, radiation, and suggested biotic replacement of unique, dominantly non-metazoan forms (Fig. 1.1) (Laflamme et al., 2013; Darroch et al., 2015; Darroch et al., 2018; Cribb et al., 2019). The strange organisms represent the earliest macroscopic forms of life in the fossil record and are typically preserved as casts and molds of collapsed soft-bodied frondose, lobate, and radial forms (Figs. 1.2 and 1.3). The lack of analogues in the Paleozoic fossil record has led to most of the Ediacara biota being classified strictly by morphotype (based on preserved morphological similarities), as opposed to taxonomic lineages outside of *incertae cedis*. There are a few controversial outliers, with forms like *Kimberella* (Fig. 1.3C), which has been suggested to be a probable mollusk, and *Parvancorina* (Fig. 1.3D), which resembles the arthropod body plan (Martin, 2000; Lin et al., 2006).

The Ediacara biota are, in a sense, the archetype of the Ediacaran Period—a group of non-analogous forms in a non-analogous ecosystem. In the final ~12 million years of the Ediacaran, during the Nama assemblage, a small, abundant new fauna came to fruition, called the 'Wormworld' fauna by Schiffbauer et al., 2016 (Fig. 1.1). As opposed to the majority of the Ediacara biota, the Wormworld fauna are considered as true metazoans that are much more similar in morphology and ecology to the Cambrian fauna than to their Ediacaran predecessors (Darroch et al., 2015; Cribb et al., 2019).

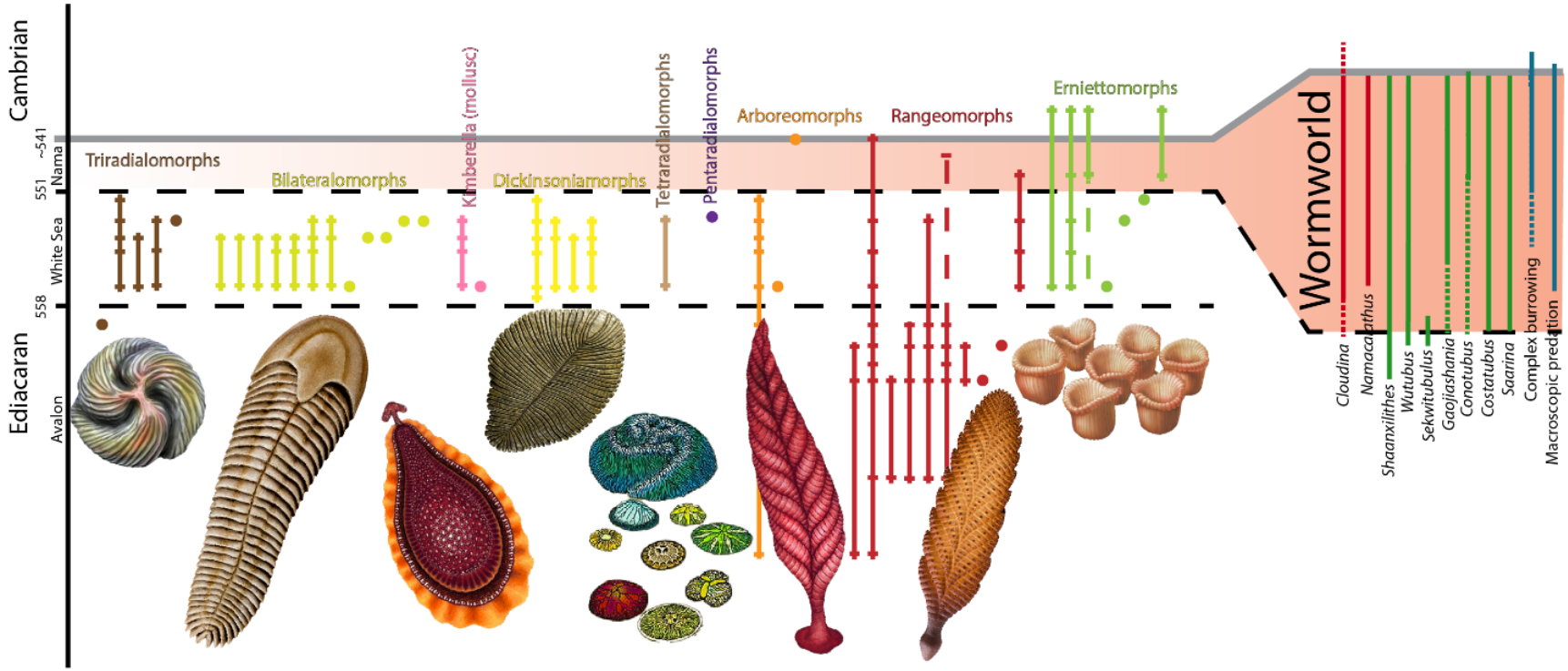

Figure 1.1. Ediacaran diversity through time. Bars represent ranges of known taxa, with horizontal dashes marking dated occurrences. Circles indicate taxa with only one known occurrence. Modified from Laflamme et al. (2013) Figure 3 and Darroch et al. (2018) Figure 2. Reconstructions by Franz Anthony (*Kimberella* and *Charnia/Charniodiscus*), Apokryltaros (Trilobozoa), Nobu Tamura (*Tribrachidium*), Matteo De Stefano/MUSE (*Charnia* and *Spriggina*), Bengt Olofsson (*Dickinsonia*), and Dave Mazierski (Ernietta).

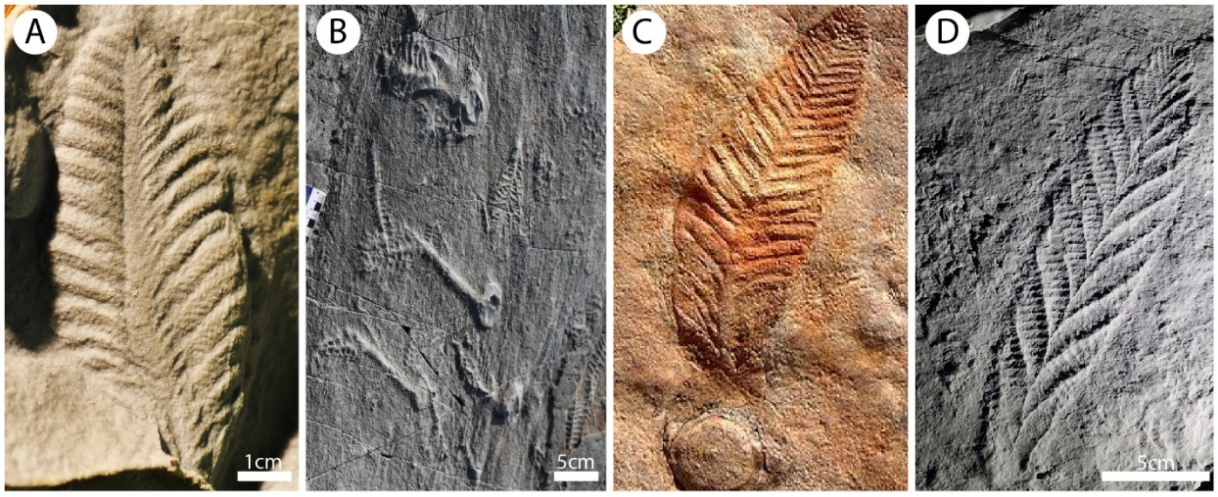

Figure 1.2. Ediacara biota taxa with a frondose morphology. A) *Rangea* (image by G. Retallack, licensed under Creative Commons Attribution-Share Alike 4.0 International license); B) Various fronds including *Charniodiscus procerus* (image by G. Narbonne); C) *Charniodiscus spinosus* (from the South Australian Museum, Adelaide); D) *Charnia masoni* (from the Bradgate Formation, Charnwood Forest)

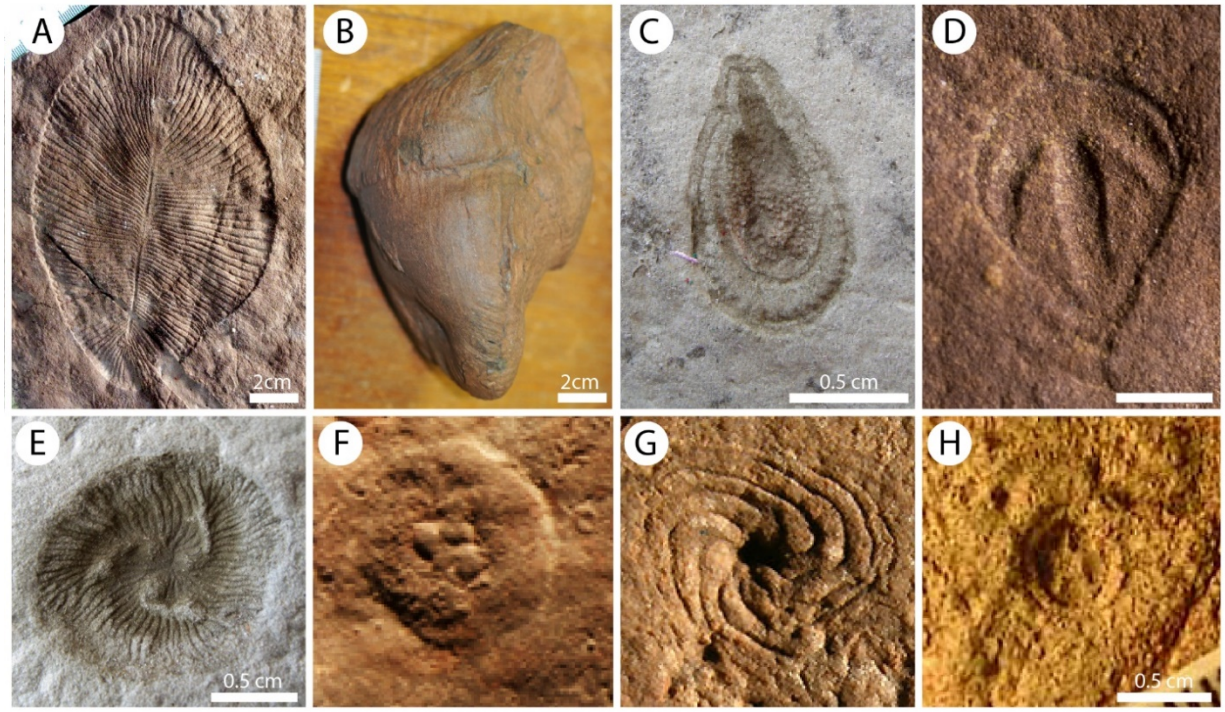

Figure 1.3. Non-frondose Ediacara biota. A) *Dickinsonia costata* (from Australia); B) *Ernietta plateauensis* (image by G. Retallack, collected from the Dabis Formation, Namibia, licensed under Creative Commons Attribution-Share Alike 4.0 International license); C) *Kimberella quadrata* (image by Aleksey Nagovitsyn); D) *Parvancorina* (from Coutts et al., 2018, North Ediacara Conservation Park (NECP) Bed-1, SAM P49380), E) *Tribrachidium* (image by Aleksey Nagovitsyn), F) *Hallidaya*, South Australia (image by G. Retallack); G) *Eoandromeda* (from Zhu et al., 2008); H) *Arkarua* (source unlisted).

Beyond the possibility that the Wormworld fauna are the earliest full metazoan communities represented in the fossil record, their place in geologic time is exceptionally important. The Wormworld fauna are flanked by the old Ediacaran ecosystem and the bustling Cambrian, where almost all known animal phyla appeared during the ~25 million-year period at the beginning of the Cambrian commonly known as the Cambrian Explosion (Erwin et al., 2011; Schiffbauer et al., 2016).

The causes or "triggers" of the Cambrian Explosion have been highly debated, dating back as far as Charles Darwin (Schopf, 2000). Although many causes have been suggested, there will likely never be a true consensus. However, Schiffbauer et al. (2016) presents a model for a series of "switches", or a combination of specific biological, ecological, and environmental drivers, all intertwined, where had one switch not flipped in the exact order and time that it did, the radiation of metazoan life in the Cambrian may never have occurred. The biological drivers, or what we know of them from the fossil record, are overwhelming placed within the late Ediacaran Wormworld (Schiffbauer et al., 2016). Additionally, many of the ecological and environmental changes appear to have been biotically driven, emphasizing the importance of this late Ediacaran fauna.

The Wormworld fauna is diverse, with representatives preserved as body fossils of tube-dwelling worms and traces of burrowers and grazers (Fig. 1.4) (Schiffbauer et al., 2016). The growing amount of data continues to clarify the role these organisms played in the ushering in of the Cambrian Explosion and each newly described fossil occurrence of the Wormworld organisms, as well as the use of new analytical techniques, amplifies the evolutionary importance of the latest Ediacaran ecosystem.

1.2. Life in the Ediacaran

1.2.1. The Ediacara biota

The earliest members of the Ediacara biota appear in the Avalon assemblage and include quilted frondose Ediacara rangeomorphs (similar in form to *Rangea*), the frondose arboreomorphs (arborea = tree), *Charniodiscus* and *Charnia*, as well as the triradialomorph (triradial = three rays), *Triforillonia* (Fig. 1.2) (Ford, 1958; Gehling et al., 2000). The White Sea assemblage preserves an apparent radiation of Ediacaran forms. Along with the rangeomorphs, arboreomorphs, and triradialomorphs, the White Sea contains the appearances of the dickinsoniamorph (similar in form to *Dickinsonia*), erniettomorph (similar in form to *Ernietta*), kimberellomorph (similar in form to

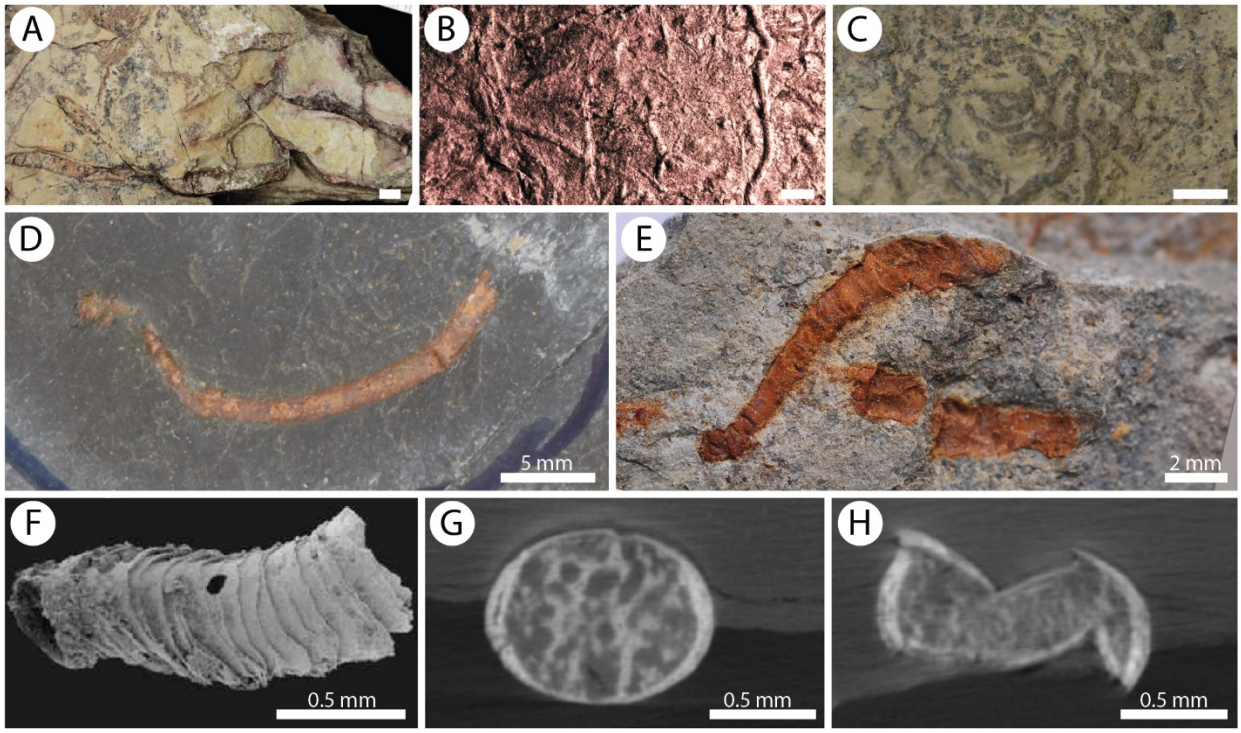

Figure 1.4. Fossils of the Ediacaran Wormworld. A–B) the burrowing trace, *Planolites*, from the Wood Canyon Fm., CA; C) The grazing trace, *Gordia marina*, from the Wood Canyon Fm., CA; D) Cloudinomorph from the Deep Spring Fm., NV; E) The tubicolous body fossil, *Conotubus hemiannulatus* from the Dengying Fm., South China (image by Y. Cai); F) The biomineralized tubicolous body fossil, *Cloudina*, with evidence of boring predation from the Dengying Fm., South China (from Bengtson and Zhao, 1992); G–H) Cross-section through *Costatubus bibendi*, showing evidence of partial biomineralization from the Wood Canyon Fm., NV. (from Selly et al., 2019).

Kimberella), bilaterialomorph (bilateral symmetry), and the tetra-, and penta-radialomorph morphoclades (Fig. 1.3). The final assemblage, the Nama, has a notable loss of diversity, with only the rangeomorphs and erniettomorphs remaining of the Ediacara biota (Fig. 1.1, 1.2A–B). Thetemporal occurrence of the Nama Assemblage, being just prior to the largest diversification event in Earth's history, the Cambrian Explosion, amplifies the importance of studying the biotic transitions occurring through this final gasp of the Precambrian. Darroch et al. (2015) provided evidence for the gradual disappearance of the Ediacara biota during the Nama through comparative studies with Avalon and White Sea assemblages focused on sampling density and worst and best-case scenario diversity values. The results indicate a gradual loss of diversity of the Ediacara biota, as opposed to a rapid mass extinction or a taphonomic or sampling bias. This supports the idea of a biotic replacement model, where the dominant fauna is pushed out by more successful faunal elements (Fig. 1.5) (Darroch et al., 2015; Darroch et al., 2018).

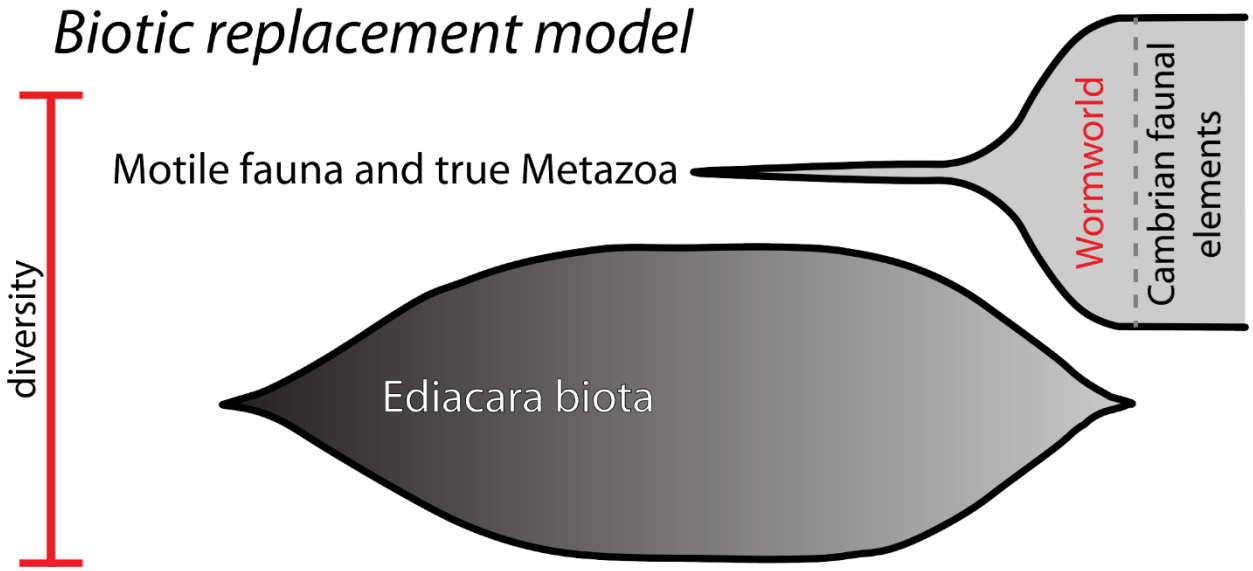

Figure 1.5. Biotic replacement model (modified from Darroch et al. 2018).

1.2.2. The 'Wormworld' fauna

Beyond the Ediacara biota, the Nama assemblage is rich in other fossils, with an evident transition to a metazoan-grade worm-like fauna as the Ediacara biota fades away (Figure 1.5).

Tubicolous (tube-dwelling worm) body fossils and bilaterian-grade trace fossils, comprising the Wormworld fauna, occurring in the final ~12 million years of the Ediacaran provide insight into the newly introduced competitive fauna evolving alongside the Ediacara biota (Schiffbauer et al., 2016; Darroch et al. 2020). Several ecological innovations have been attributed to the Wormworld organisms, the most prominent being macrobiomineralization, burrowing, and predation (Becker-Kerber et al., 2017; Darroch et al., 2020). Motility and active feeding also become prominent within the Wormworld fauna, although two of the Ediacara biota, *Kimberella* and *Dickinsonia* have been found with evidence of potential musculature, motility, and radula-like grazing behaviors (ex. *Dickinsonia* death march, *Kimberichnus*, etc.) (Gehling et al., 2014; Hoekzema et al., 2017).

Figure 1.6. Reconstruction of the Ediacaran Wormworld (from Schiffbauer et al. 2016). Artwork by Stacy Turpin Cheavens (Dept. of Orthopaedic Surgery, University of Missouri), reconstructions include *Conotubus*, *Gaojiashania*, *Wutubus*, *Ernietta*, and simple horizontal traces.

Complex trace making behaviors and advanced faunal interactions occurring within the Wormworld fauna shaped the seafloor, preparing it for the impending diversification of metazoans in the early Cambrian. As new behaviors were introduced, the Wormworld fauna drove major changes in the marine ecosystem ultimately playing a part in building the modern Ecological

Pyramid (Schiffbauer et al., 2016). During the final ~12 million years of the Ediacaran, evidence for primary consumer bilaterian behaviors began to appear, with simple, horizontal mat-ground dwelling traces like *Planolites* and *Palaeophycus* becoming commonplace (O'Neil et al., *in review*). The motility of the trace making organisms began to alter the mat-ground system, driving low-impact mixing and oxygenation of the substrate (Buatois et al., 2018). The introduction of the Nama trace making behaviors was paired with the introduction of secondary consumers in the form of soft-bodied tubicolous worm-like organisms known as cloudinomorphs (Schiffbauer et al., 2016; Selly et al., 2019), named for their morphological similarity to the early biomineralizer and possible derived form, *Cloudina* (Fig. 1.4F).

The cloudinomorph namesake, *Cloudina*, is the first member of the morphoclade to exhibit full biomineralization, with evidence of possible partial biomineralization in *Costatubus* (Fig. 1.4G–H) (Selly et al., 2019). The stability of the *Cloudina* shells allowed for the preservation of the earliest evidence of predation in the fossil record, with several specimens from South China being preserved with bore holes through the biomineralized shell (Fig. 1.4F) (Hua et al., 2003). Hua et al., (2003) noted that, in specimens containing bore holes, the location of the holes is not random, and most typically occurs towards the lower, mat-sticking funnels, distanced at approximately 4 to 5 times the tube diameter. Almost all specimens have only one bore hole, with some having the occasional partial bore hole from aborted attempts at drilling. The consistency in bore hole location towards the base of the shell and the lack of multiple holes indicates that the (unpreserved) predator was successful and likely drilled to kill, targeting the tube-dwelling worm at the base of the tube (Hua et al., 2003).

1.3. Ediacaran Preservation

Preservational conditions in the Ediacaran were unlike the rest of the known fossil record. The base of the Ediacaran Period corresponds to the end of the Marinoan Snowball Earth glaciation, as the major fluctuations in climate during the Cryogenian subsided, which had likely played a role in limiting the evolution of macroscopic life (Long et al., 2019). The first fossils present in the aftermath of Marinoan were microscopic fossils of potential embryos and sponges, indicating that ocean conditions at this time could maintain viable life (Long et al., 2019). Not long after, the Ediacara biota came to fruition in a marine ecosystem previously untouched by macroscopic life forms. Without macroscopic motile organisms, the substrate was covered in thick matgrounds, now preserved as stromatolites, wrinkle structures, and "elephant skin" textures (Hagadorn and Bottjer, 1997; Bailey et al., 2006; Gehling and Droser, 2009). Oxygen levels were low, especially in the deeper ocean, where the Avalon biota are believed to have lived and microbial communities thrived, resulting in the unique Ediacaran "Death Mask" preservation (Fig. 1.7, Gehling, 1999).

The model for "Death mask" preservation was first proposed by Gehling (1999) to explain the preservation of the completely soft-bodied Ediacara organisms in sandstone deposits with such highly detailed morphologies. The model suggests that the organisms' preservation was facilitated by the abundant matgrounds on which the Ediacara biota lived. Burial of the matground and the matground biota, potentially due to storm deposition, led to the buried soft-bodied lifeforms being encased between the microbial mat and the overlying sediment. Sediment loading caused the bodies to collapse, resulting in convex epirelief casts and concave hyporelief sandstone molds. The molds are often found with an "elephant skin" texture caused by the presence of microbial mats. The lack of bioturbation prior to the terminal Ediacaran kept the enclosing sediment from being

disturbed and oxygenated, as well as preventing any sort of scavenging. Following the burial, a new microbial mat would begin to form on top of the sediment and was eventually inhabited by a new community of Ediacarans (Gehling, 1999). The Death Mask preservational model, however, is not able to explain much of the preservation in the latest Ediacaran, which contains fully three-dimensional Ediacara biota fossils.

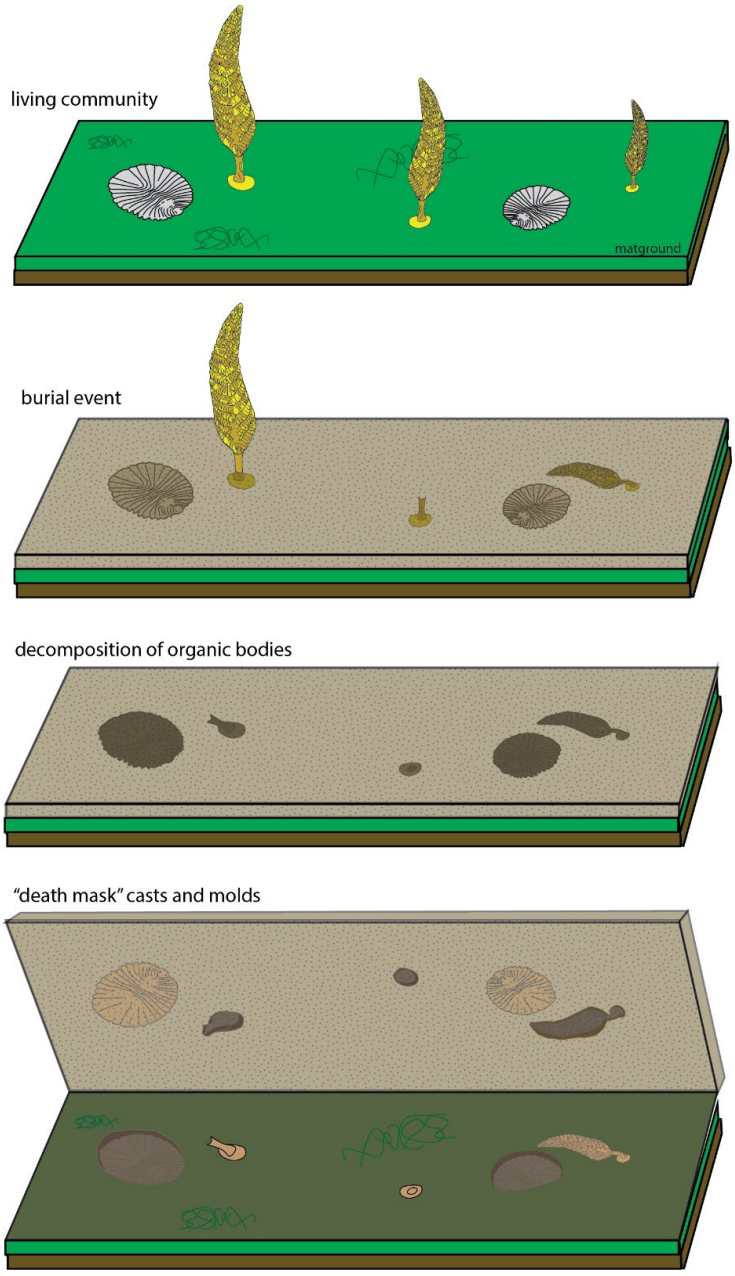

Figure 1.7. Model for Ediacaran Death Mask preservation. Based on Gehling (1999) and Meyer (2010).

A shift to shallower environments during the White Sea not only changed the environmental conditions of preservation, but likely facilitated the radiation of Ediacara forms and early bioturbators. However, bioturbation was sparse and shallow, limited to grazing traces (*Kimberella* and *Kimberichnus*) and low-impact, horizontal burrows, and microbial matgrounds continued to thrive sustaining the "death mask" preservation style. Bioturbation further altered the seafloor, resulting in new preservational conditions, or the potential destruction of the previous preservational conditions (Laflamme et al., 2013). In the Nama, Ediacara biota fossil preservation changes from the classic "death mask" to three-dimensional sediment filled "sacs" (Elliott et al., 2016).

The cloudinomorphs and related non-biomineralized tubicolous fossils are believed to have had tubes built from rigid organic matter (Hong et al., 2007). The preservation of the organic tubes varies greatly from the completely soft-bodied Ediacara biota, resulting in the organic tube material facilitating new preservational modes through mineral replacement of the rigid organic matter and carbonaceous compression replication, like that of the Cambrian Burgess Shale (Gaines et al., 2012). Level of biomineralization, resource availability, and the speed of burial are believed to have greatly influenced the type of preservation and replacement minerals even within the same fossil assemblage, as seen in the Gaojiashan Lagerstätte of South China (Cai et al., 2007; Schiffbauer et al., 2014).

Ediacaran trace fossils are dominated by infilled burrows and ridges of surficial traces. Lining of the burrows and the redistribution of sediment, as well as the stability of the remaining matground allowed for exceptional preservation of the simple Ediacaran traces (Buatois et al., 2014). Preservation of dwelling behaviors can also be observed in cross-sections of fossiliferous

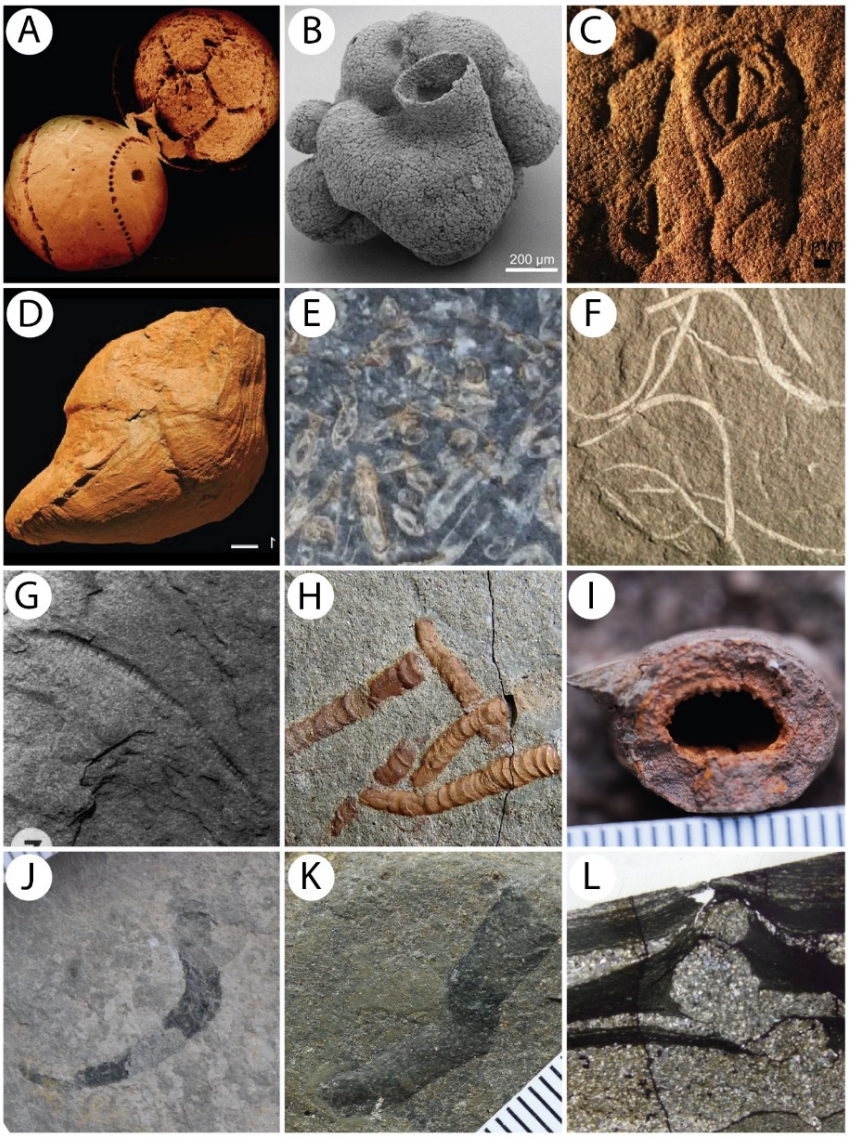

Figure 1.8. Various Ediacaran preservation styles. A) Phosphatized embryos from the Doushantuo Formation, South China; B) Phosphatized sponge from the Doushantuo Formation, South China; C) Elephant skin texture with *Parvancorina* from the Ediacara Member, South Australia; D) full three-dimensional Ediacara biota preservation of *Ernietta* from the Nama Group, Namibia (Elliott et al., 2016); E) Biomineralized *Cloudina* hash (image by Rachel Wood); F) Algae preserved through aluminosilicification (Dornbos et al., 2016); G) Cast/mold preservation of a cloudinomorph tube from the Wood Canyon Formation, California (Hagadorn and Waggoner, 2000); H) Three-dimensional pyritization of *Conotubus* from the Gaojiashan Lagerstätte of South China (image by Yaoping Cai); I) Cross-section through a three-dimensional pyritized *Conotubus* from the Gaojiashan Lagerstätte of South China (image by Yaoping Cai); J) Kerogenized (carbonaceous compression) *Conotubus* from the Gaojiashan Lagerstätte of South China (image by Yaoping Cai); K) Kerogenized (carbonaceous compression) *Conotubus* with aluminosilicate coating from the Gaojiashan Lagerstätte of South China (image by Yaoping Cai); L) Cross-section through *Lamonte trevallis* burrows stabilized by microbial mat laminae (O'Neil et al., 2020).

specimens, as the infilled, semi-infaunal to infaunal burrows are often preserved in three-dimensions.

1.3.1. Early phosphatization

Prior to the earliest occurrences of the Ediacara biota, in the earliest Avalon assemblage, phosphatized fossils of embryos, acritarchs, and sponges have been described from the Doushantuo Formation in South China (Fig. 1.8A–B) (Muscente et al., 2015). High phosphate levels in the shallow, high energy environments of the early Ediacaran facilitated the mineralization of completely soft-bodied, otherwise extremely fragile organisms (Chen et al., 2009; Schiffbauer et al., 2012). This mode of preservation is often referred to as Doushantuo-type preservation.

1.3.2. Ediacara biota preservation

The soft-bodied Ediacara biota lacked rigidity, leading to a dominantly cast/mold preservation style. However, the preservation is not typical of most cast/mold fossils, as the conditions of burial and the environment were not by any means "typical". That is evidenced by the Death Mask preservation brought about by the combination of the thick microbial mat-grounds, low-oxygen conditions, and a lack of motile grazers and predators (Gehling, 1999). Most Death Mask fossils are of exceptional quality, with preservation of intricate external (and potentially internal, Dzik, 2003) morphological characteristics, creating a unique snapshot of an otherwise difficult-to-impossible to preserve biota.

1.3.3. Flinders and Fermeuse-style preservation

Flinders-style preservation is based on the unique preservation of the Avalon biota from the Flinders Ranges in South Australia. Fossils are preserved on the underside of coarse, shoreface sandstones, with the counterpart preserved on the top of the underlying bed (Bobrovskiy, 2019).

The underlying beds are often found with a crinkled, microbially mediated, grooved texture, referred to as “elephant skin”. The presence of the elephant skin texture and other mat-related morphologies, like wrinkle structures, indicated that the organisms were subjected to burial while living in mat-bound communities (Hagadorn and Bottjer, 1997; Bailey et al., 2006; Gehling and Droser, 2009). The resulting preservation is often referred to as the Ediacaran “death mask” (Gehling, 1999). Fermeuse-style preservation is named for the Avalon biota fossils from the Fermeuse Formation in Newfoundland, Canada. The preservation style is similar to Flinders-style, but occurs in deeper sediments (Bobrovskiy, 2019).

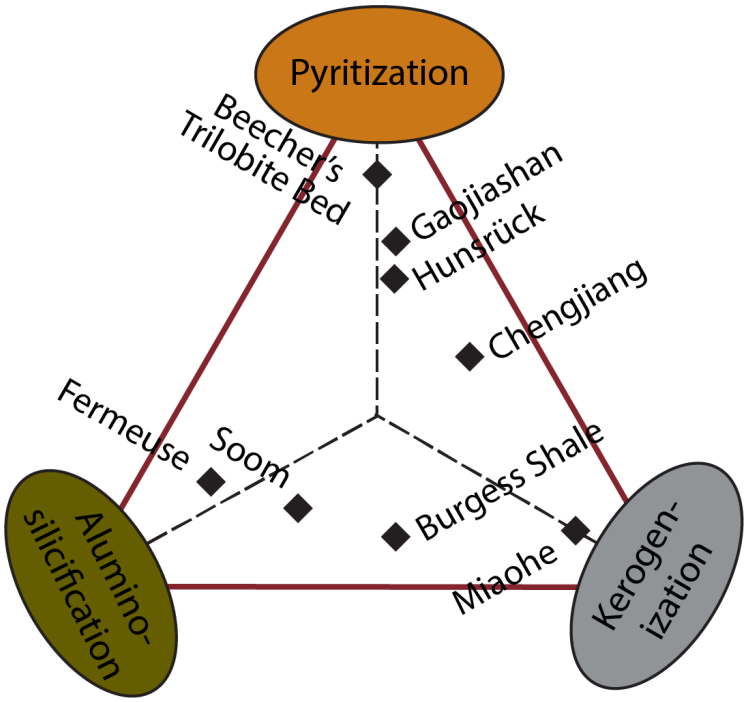

Figure 1.9. Pyritization, aluminosilicification, kerogenization ternary diagram. The diagram shows the approximate ratio of taphonomic pathways (pyritization, aluminosilicification, kerogenization) from Lagerstätte fossil localities. Diagram is modified from Cai et al. (2012).

1.3.4. ‘Wormworld’ preservation

The preservation of the Wormworld organisms varies not only between localities, but also within singular sections. The biomineralized taxa are most common, as the preservation potential is higher than that of the more labile, non-mineralized tissue. The morphoclade namesake,

Cloudina, is preserved in mass numbers, with some aggregates of specimens showing possible evidence of reef-like structures (Penny et al., 2014), although this interpretation remains debated (Mehra and Maloof, 2018). The non-biomineralized forms are much more difficult to preserve and require unique taphonomic conditions. The varying taphonomic pathways have led to difficulties in classification and association of the non-biomineralized (and lightly biomineralized) forms, with preservational limitations on certain morphological characteristics.

1.3.5. Burgess Shale Type preservation

The Burgess Shale represents one of the most diverse and exceptionally preserved assemblages of Cambrian fauna fossils. The fossils are dominantly carbonaceous compression with some evidence of authigenic clay growth on the surface of the fossils and rare pyrite growth (Gaines et al., 2012). This type of preservation is important, as it replicates the soft-tissue often lost in the preservation process and incorporates the preservational model that is common in the Wormworld organisms.

1.3.6. Cast/Mold

Cast and mold preservation of Wormworld organisms is rare due to the lack of hard parts, but potential casts and molds of biomineralized taxa have been recorded (Hagadorn and Waggoner, 2000).

1.3.7. Gaojiashan preservation

Preservation of the Wormworld organisms from the Gaojiashan Lagerstätte in South China present a unique combination of taphonomic modes that allow for the exceptional preservation of these difficult to preserve fossils. A taphonomic model proposed by Schiffbauer et al. (2014), outlines how pyritization (replacement of organic matter through pervasive pyritization), kerogenization (replication of tissues as carbonaceous compressions), and aluminosilicification

(growth of authigenic clay minerals during kerogenization) occur along the same taphonomic pathway, with preservation type being controlled by sedimentation rate and the size of the bacterial sulfate reduction zone. Pyritization and kerogenization (with associated clay minerals) can occur independently or consecutively depending on the burial conditions.

Pyritization is the most commonly occurring mode of preservation in the Wormworld fauna. Pyritized fossils are preserved in three-dimensions and often preserve a high level of detail, especially within specimens from the Gaojiashan Lagerstätte, where rapid initial burial promoted the precipitation of pyrite within the bacterial sulfate reduction zone (Fig. 1.10) (Schiffbauer et al., 2014). Kerogenization of fossils occurs with rapid sedimentation continuing after the initial burial of the fossil tissues with a limited bacterial sulfate reduction zone. In the case of kerogenization, fossil preservation occurs dominantly in the methanogenesis zone, with only a short time in the bacterial sulfate reduction zone, resulting in only a slight amount of pyrite growth (Fig. 1.10) (Schiffbauer et al., 2014). During aluminosilicification, authigenic clay minerals form a thin coating over the carbonaceous compression of a kerogenized fossil (Ye et al., 2017). This process is poorly understood but is intertwined with the processes of kerogenization and pyritization.

1.3.8. Trace fossils

Ediacaran trace fossils are dominantly simple, horizontal burrows and grazing traces. Burrows are often preserved in three-dimensions, and cross-cutting along the sample surface. The most common burrows are *Planolites* and *Palaeophycus*, distinguished by the infill sediment, being different or the same as the host rock, respectively (O'Neil et al., *in prep*). While *Planolites* and *Palaeophycus* are often three-dimensional in cross-section, the burrows only lightly penetrate the sample surface. However, another trace fossil, *Lamonte trevallis*, known from the Wood

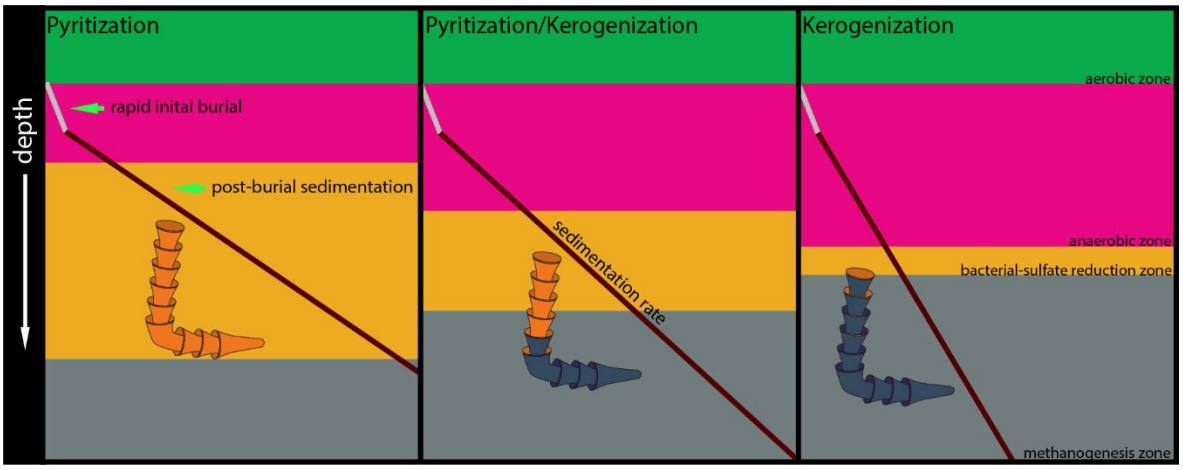

Figure 1.10. Pyritization–Kerogenization–Aluminosilicification taphonomic pathway model (modified from Schiffbauer et al. 2014). The blue area represents the aerobic zone, the pink area represents the anaerobic zone, the orange area represents the bacterial-sulfate reduction zone, and the grey area represents the methanogenesis zone. The grey line indicates rapid initial burial of the organism and the slope of the corresponding maroon line represents the rate of post-burial sedimentation. The pyritization pathway results from slow post-burial sedimentation leading to preservation occurring dominantly in the bacterial sulfate reduction zone. The pyritization–kerogenization pathway results from somewhat rapid post-burial sedimentation with a restricted bacterial sulfate reduction zone leading to partial preservation within the bacterial sulfate reduction zone and the methanogenesis zone. The kerogenization pathway results from rapid post-burial sedimentation with an extremely limited bacterial sulfate reduction zone leading to a dominantly kerogenized fossil with little residual pyrite.

Canyon Formation and Deep Spring Formations of the Death Valley region, California, USA and the Dengying Formation in South China (an additional unpublished occurrence in Namibia is also known from personal communications) appears similar to *Planolites* and *Palaeophycus* on the surface, but shows complex mat-targeted feeding behaviors in cross-section (Chen et al., 2013; Meyer et al., 2014; O'Neil et al., 2020). The grazing traces *Helminthopsis*, *Helminthoidichnites*, and *Gordia* are also known from the latest Ediacaran and appear as surficial meandering grooves (Cribb et al., 2019; O'Neil et al., *in prep*).

A suite of complex trace fossils from the terminal Ediacaran have recently been described from the Nama Group in Namibia (Smith et al., 2017; Darroch et al., 2020). The expansive trace assemblage is likely the most diverse from known Ediacaran localities and preserves a number of

highly complex Cambrian-like behaviors. The trace fossils exist within the same beds as the noted loss of diversity in the Nama Group Lagerstätte of Namibia (Darroch et al., 2015).

1.4. Ediacaran Fossil Localities

Although Ediacaran fossils have been found in a number of localities worldwide, a subset of these localities are known for the superior condition and/or diversity of the fossils. These localities have been heavily studied and continue to produce new research, shaping the Ediacaran assemblages of which they represent.

1.4.1. Mistaken Point, Newfoundland, Canada

Located on the Avalon Peninsula in southwestern Newfoundland, CA, Mistaken Point contains the most diverse Avalon assemblage in the world. Fossils are preserved via "death mask" preservation, with exceptional preservation of soft-bodied frondose rangeomorphs and arboreomorphs, and triradialmorphs. Mistaken Point's age is estimated to be between 580–560 Ma, with the fossils of the Mistaken Point Formation estimated to be at around 565 Ma (Benus, 1988), making it the oldest Ediacara biota fossil locality. Also located on the Avalon Peninsula are the older Drook and Briscal formations, with the Drook Formation dated at 578 Ma and the Briscal Formation between the Drook and the E-surface at Mistaken Point estimated at 565 Ma (Laflamme et al., 2012). The Drook Formation contains the large, enigmatic *Ivesheadia*, which has been interpreted as a preservational remnant of an Ediacara biota fossil. Among Ivesheadia are a number of small frondose forms and holdfast structures (Liu et al., 2011, 2012). The Briscal Formation contains the rangeomorph, *Culmofrons plumosa*, although with significantly lower diversity than the younger Mistaken Point assemblage (Laflamme et al, 2012).

1.4.2. White Sea, Russia

The White Sea assemblage, located in the Southeastern part of the White Sea area in Russia, contains one of the most diverse group of Ediacara biota fossils, with approximately 20 described taxa including *Kimberella* and *Dickinsonia* (Bottjer and Clapham, 2006, Droser and Gehling, 2015). The majority of the soft-bodied organisms are preserved through Flinders-style "death mask" preservation associated with microbial mat textures (Gehling, 1999). Fossils are preserved in the Zimnie Gory and Verkhovka formations and are believed to be preserved in near *in situ* communities that appear to be constrained by the presence of microbial mats (Zakrevskaya, 2014).

1.4.3. Ediacara Hills, Australia

The namesake of the Ediacaran, the Ediacara Hills, is located in South Australia and contains Ediacara biota fossils preserved within the Ediacara Member of the Precambrian–Cambrian age Rawnsley Quartzite. The Ediacara Hills preserves the White Sea fauna in Flinders-style "death mask" preservation. Fossils are found with evidence of microbial mats and shrinkage cracks (Reid et al., 2019).

1.4.4. Nama Group, Namibia

The Nama Group of Namibia preserves end-Ediacaran Nama biota fossils, including *Ernietta*, an erniettomorph fossil commonly found in the same units as Ediacaran Wormworld fossils (Hagadorn and Waggoner, 2000; Smith et al., 2017). The fossiliferous Nama units are separated into two sub basins, the Witsputs in the south and the Zaris to the north. The Ediacara biota are preserved as infilled three-dimensional fossils. The Nama Group also contains a diverse suite of Ediacaran complex trace fossils (Cribb et al., 2019; Darroch et al., 2020).

1.4.5. Gaojiashan Lagerstätte, South China

The Gaojiashan Lagerstätte is located in South China near the village of Gaojiashan. The Lagerstätte is contained within the Dengying Formation and contains a variety of extremely well-preserved soft-bodied taxa from the Ediacaran Wormworld (Cai et al., 2010). The most common Wormworld taxa, *Conotubus* and *Gaojiashania* are preserved through pyritization and kerogenization, but the Gaojiashan Lagerstätte also contains a number of other less common tube fossils (Cai et al., 2007; Schiffbauer et al., 2014). The high density of the tubes and the incredible condition places the Gaojiashan in the forefront of the Wormworld assemblages. The fossils are considered to be preserved in "near-life" communities that were smothered during subsequent storm events (Cai et al., 2010). Trace fossils, including *Lamonte trevallis*, have also been described from the Gaojiashan Lagerstätte (Meyer et al., 2014).

1.5. Death Valley Region, United States: A Burgeoning Ediacaran Lagerstätten

The western United States contains two fossiliferous Ediacaran–Cambrian boundary-spanning formations, the Wood Canyon and Deep Spring (1.11). The formations are part of two successions, the White-Inyo and the Nopah Range. The successions are temporally correlative, with the White-Inyo Reed Dolomite and Deep Spring formations reflected as the Stirling Quartzite and lower member of the Wood Canyon formation in the Nopah Range (Stewart. 1970). The earlier Precambrian units, the Reed Dolomite and Stirling Quartzite contain rare fossils, but are largely depauperate. Due to sedimentological restrictions, the fossils are limited largely to more easily preservable taxa, including *Cloudina* (called *Wyattia* by Taylor, 1966) from the Reed Dolomite on White Mountain and the Stirling Quartzite at Mt. Dunfee in Nevada (Langille, 1974; Grant, 1990; Corsetti and Hagadorn, 2000). Both traces and Ediacaran biota body fossils from the Deep Spring and Wood Canyon have been described in the literature since the 1960s. The soft-bodied

tubicolous Wormworld taxa, however, were not described until 2016 from the Mt. Dunfee fossil beds (Smith et al., 2016). Since the publication of the Mt. Dunfee tubicolous fossils, focus on outcrops of the Wood Canyon and Deep Spring formations has grown, yielding several tube morphologies, adding to the known diversity of the Ediacaran Wormworld (Smith et al., 2016; Selly et al., 2019, Schiffbauer et al., 2020).

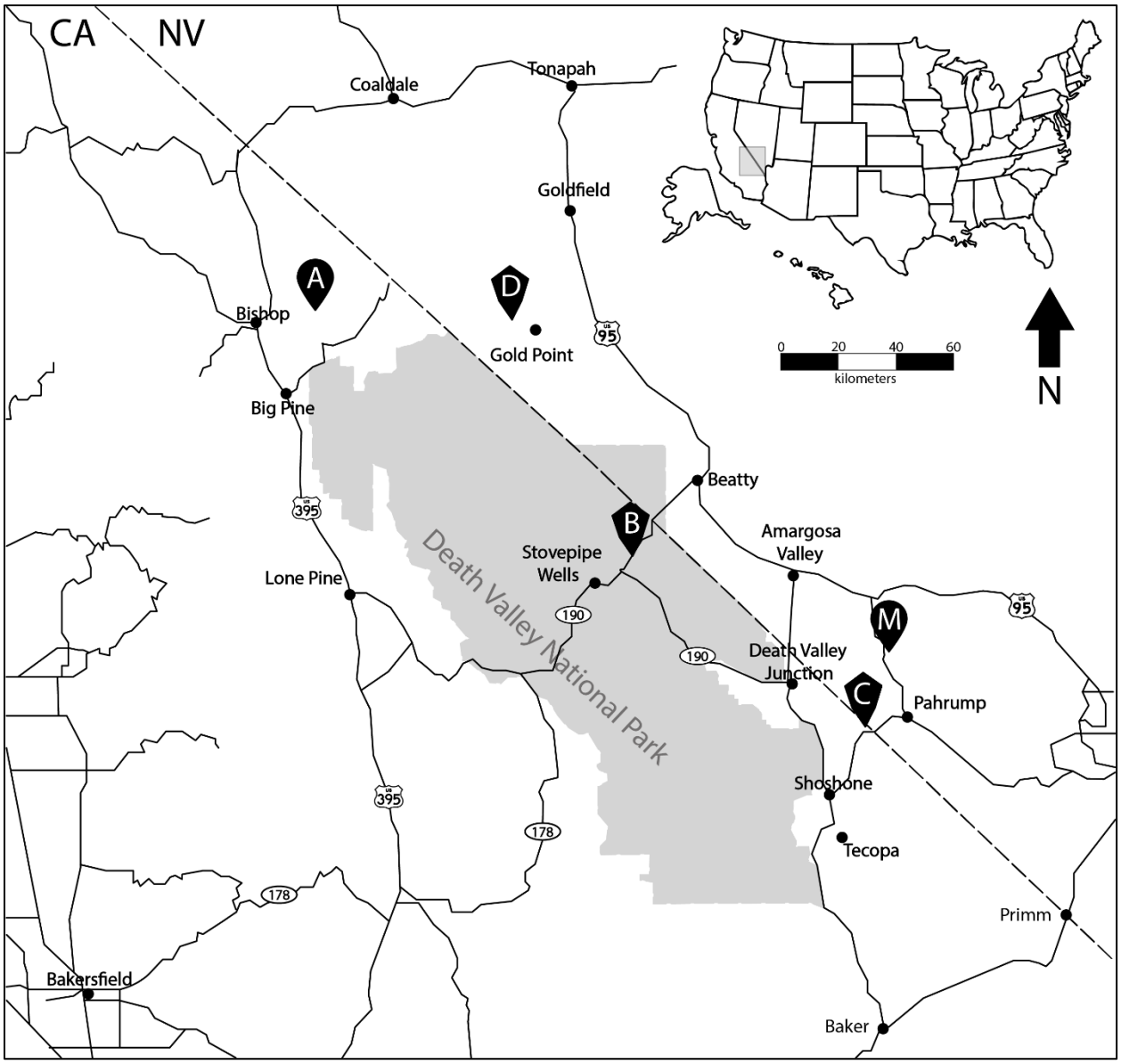

Figure 1.11. Map of Ediacaran fossil containing units of the Deep Spring (circle marker) and Wood Canyon (diamond marker) formations. A = Ancient Bristlecone Pine Forest, M = Montgomery Mountains, D = Mt. Dunfee, C = Chicago Pass, B = Boundary Canyon.

Connections between and among sections of the two formations are tedious, as sedimentology and fossil occurrences are greatly varied. Fossil localities in California, like the Wood Canyon Formation sections at Chicago Pass and Boundary Canyon, are abundant in traces, but only rare occurrences of body fossils have been observed (Fig. 1.11, 1.12). Alternatively, the Deep Spring Formation at Mt. Dunfee and the Wood Canyon Formation of the Montgomery Mountains contain exceptionally preserved specimens of the rare tubicolous body fossils, while containing few traces (Fig. 1.11, 1.12). Another section of the Deep Spring Formation, detailed in Chapter 2, occurs within the boundary of the Ancient Bristlecone Pine Forest in California and contains poorly preserved representatives of Wormworld trace and tubicolous body fossils. It is possible that the fossil assemblage at Ancient Bristlecone, and additional sections containing poor preservation, could play an important role in understanding the total diversity and community makeup of the Ediacaran Wormworld if preservation is being limited by sedimentology. Addressing this issue requires a full investigation into the fossil diversity, sedimentology, environments, and taphonomy of the known Ediacaran fossil assemblages, with particular focus on the difficult-to-preserved Wormworld organisms and the transition from the Ediacara biota to the Wormworld fauna and eventual Cambrian Explosion.

1.5.1. The Wood Canyon Formation

The Wood Canyon Formation is a Precambrian–Cambrian unit in the southern Great Basin region along the California–Nevada border to the northwest of Las Vegas, NV. The formation is a mixed siliciclastic–carbonate system with three members, the lower, middle, and upper. The three members are bounded by the underlying Stirling Quartzite, a light pink/brown Precambrian quartzite unit and the overlying Zabriske Formation, a light-colored quartzite unit

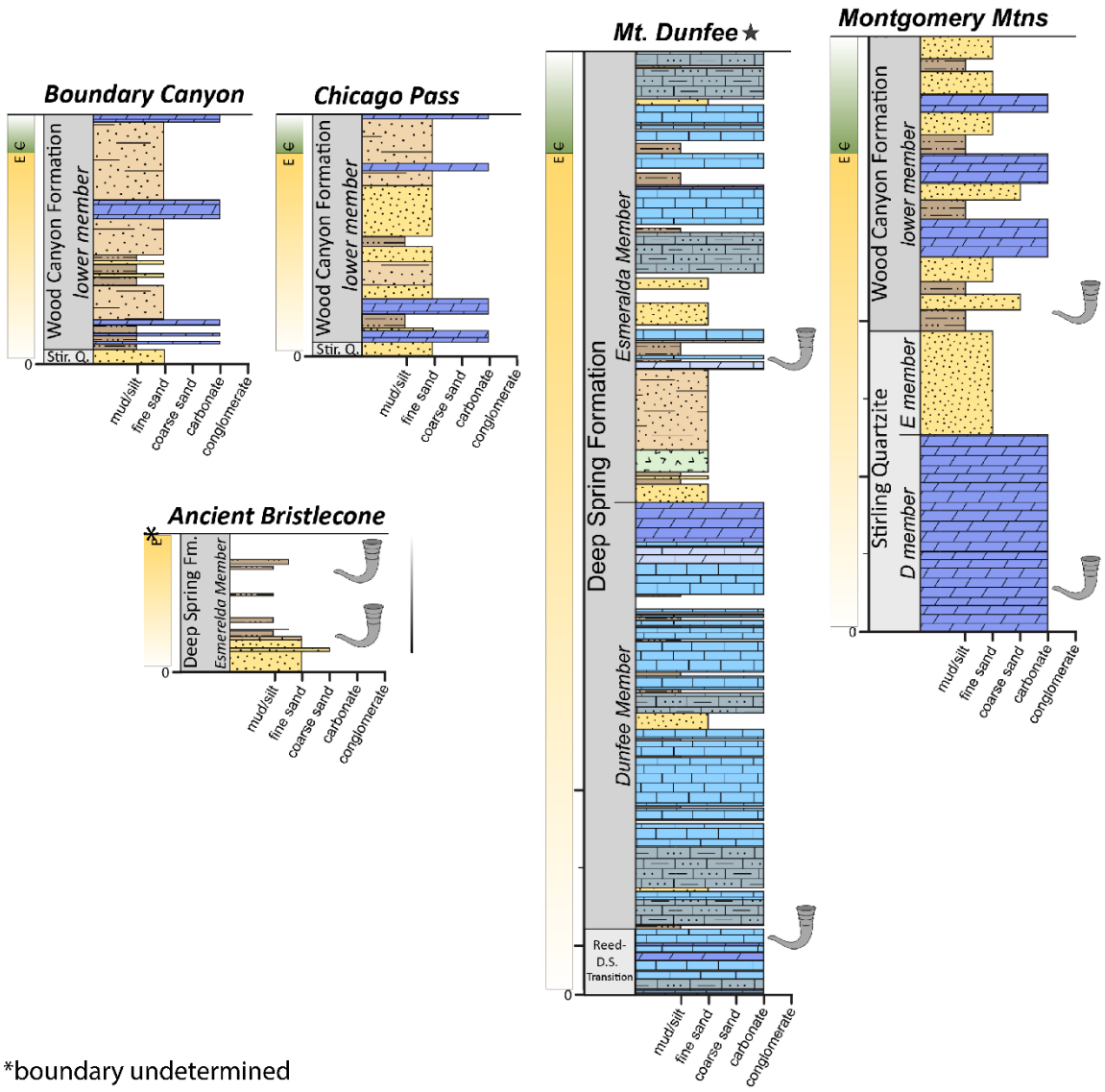

Figure 1.12. Stratigraphic columns from Ediacaran fossil containing sites from the Wood Canyon and Deep Spring formations of the western United States. Tubes represent known occurrences of tubicolous fossils.

(Stewart, 1970). The lower member is divided into three informal parasequences, each capped by a large, laterally extensive tan dolostone (Stewart, 1970; Hagadorn and Waggoner, 2000; Corsetti and Hagadorn, 2000). The third parasequence contains the Precambrian–Cambrian boundary denoted by the occurrence of *Treptichnus pedum*, the biostratigraphic marker for the base of the Cambrian (Hagadorn and Waggoner, 2000; Corsetti and Hagadorn, 2000). The middle and upper

members are rich in Cambrian fossils, including *Skolithos*, *Rusophycus*, *Zoophycos*, and trilobites (Sappenfield et al., 2012).

Prior to the appearance of *T. pedum* in third parasequence of the lower member, common fossils include simple horizontal traces, early mat mining traces, and occasional Ediacara biota fossils. Fossils have been collected from three sections of the lower member, (i) Montgomery Mountains, ~130 km northwest of Las Vegas, NV, (ii) Chicago Pass, near Pahrump, NV, and (iii) Boundary Canyon in the western half of the central portion of Death Valley National Park. Chicago Pass and Boundary Canyon are rich in trace fossils, while the Montgomery Mountains section contains few traces (Hagadorn and Waggoner, 2000; Corsetti and Hagadorn, 2000). The Montgomery Mountains section, however, contains the only non-biomineralized (and lightly biomineralized) tubicolous cloudinomorph fossils known from the Wood Canyon Formation (Selly et al., 2019; Schiffbauer et al., 2020).

1.5.1.1. Chicago Pass, Inyo County, California. The lower member of the Wood Canyon Formation at Chicago Pass contains late Precambrian–early Cambrian trace fossils. Chicago Pass is located just west of Pahrump, NV and contains the three diagnostic carbonate-capped parasequences, with the Precambrian–Cambrian boundary placed in the third parasequence based on the occurrence of *Treptichnus pedum* (Hagadorn and Waggoner, 2000; Corsetti and Hagadorn, 2000; O'Neil et al., *in review*). Traces are dominated by simple cylindrical horizontal burrows preserved in full relief. The microbially mat feeding trace, *Lamonte trevallis* has also been described, as well as cast/mold preservation of the Wormworld biomineralizer, *Cloudina* (Hagadorn and Waggoner, 2000; Corsetti and Hagadorn, 2000; O'Neil et al., 2020).

1.5.1.2. Boundary Canyon, Inyo County, California. Boundary Canyon is located along the California–Nevada border inside the boundary of Death Valley National Park. The thickest of the

Wood Canyon sections, Boundary Canyon contains a plethora of simple horizontal trace fossils and *Lamonte trevallis* (O'Neil et al., 2020). The Precambrian–Cambrian boundary is found in the third parasequence based on the appearance of *T. pedum*.

1.5.1.3. Montgomery Mountains, Nye County, Nevada. The Montgomery Mountains section is located approximately 3 km south-west of Johnnie, Nevada and contains the three diagnostic parasequences of the lower Wood Canyon Formation. The Ediacara biota body fossils, *Swartpuntia* and *Ernietta* have been described (Horodyski, 1991; Smith et al., 2017; Selly et al., 2019), as well as the tubular forms, *Saarina hagadorni*, *Archaeichnium*, *Cloudina*, *Corumbella,* and *Onuphionella* **(**Hagadorn and Waggoner, 2000; Selly et al., 2019). *T. pedum* appears in the third parasequence, marking the Precambrian–Cambrian boundary (Selly et al., 2019).

1.5.2. The Deep Spring Formation

The Deep Spring Formation is located along the California–Nevada border and is the lower Member of the Wood Canyon Formation, with the lower Wood Canyon parasequences being equivalent to the lower, middle, and upper members of the Deep Spring Formation. The Deep Spring is a mixed siliciclastic–carbonate system bounded by the Precambrian Reed Dolomite and the Cambrian Campito Formation (Stewart, 1970). Two fossiliferous sections, Mt. Dunfee in eastern Nevada, and Ancient Bristlecone Pine Forest north of Death Valley National Park in California, contain traces, Ediacara biota fossils, and cloudinomorphs.

1.5.2.1. Mount Dunfee, Nye County, Nevada. The section of the Deep Spring Formation at Mount Dunfee is dominated by thin shaley units and large microbial structures (stromatolites). Within the shales, a variety of well-preserved, detailed cloudinomorph fossils are preserved, as well as a number of poorly preserved tubes similar to those found at Ancient Bristlecone Pine Forest (Smith et al., 2016; Selly et al., 2019). The exceptional preservation of these fossils may be

attributed to the fine-grain sizes and low-energy environment in which they were buried. The sediments and fossils resemble those of the Montgomery Mountains section of the Wood Canyon Formation near Johnnie, Nevada.

1.5.2.2. Ancient Bristlecone Pine Forest, Inyo County, California. The Ancient Bristlecone Pine Forest in Inyo County, California contains three distinct fossil assemblages within the outcrops of the late Ediacaran–early Cambrian Deep Spring Formation (~555–541 Ma). The oldest of the three contains later representatives of the classic Ediacaran taxa, dominated by holdfast structures and erniettomorphs. Just above this outcrop, the erniettomorphs are lost and holdfast structures become much more rare. Members of a tubular vermiform fauna begin to appear, as well as early simple burrowing traces. The third and youngest of the assemblages is characteristically Cambrian, with large bilaterian burrowing and crawling traces and the disappearance of all diagnostically Ediacaran body fossils.

1.6. Conclusion

The western United States Precambrian–Cambrian fossiliferous units present a unique, diverse fossil assemblage that is becoming increasingly more competitive with the well-known global Lagerstätte. The fossils show a range of taphonomy that includes the oldest known preserved soft-tissue (cloudinomorph gut tracts) in the fossil record. Through use of new analytical approaches, the diversity of the western United States Ediacaran fauna is more advanced and "Cambrian" in nature than the typical Ediacaran assemblages. The Ancient Bristlecone Pine Forest section of the Deep Spring Formation, in particular, presents a unique opportunity to utilize technology and test new analytical approaches, as the unit contains a number of poorly preserved fossils that lack the characteristics needed for classification, but are generally identifiable when compared to known fossils from the surrounding localities. Further, investigations into trace fossil

assemblages provides us with information about the complete paleocommunities that thrived in the terminal Ediacaran and how the presence of bioturbation affects preservation and the faunal makeup prior to the Cambrian Explosion.

1.7. References

Bailey, J., Corsetti, F., Bottjer, D., and K. Marenco. 2006. "Microbially-Mediated Environmental Influences on Metazoan Colonization of Matground Ecosystems: Evidence from the Lower Cambrian Harkless Formation." PALAIOS 21(3):215-226.

Becker-Kerber, B., Pacheco, M.L.A.F., Rudnitzki, I.D., Galante, D., Rodrigues, F., and J. de Moraes Leme. 2017. "Ecological interactions in Cloudina from the Ediacaran of Brazil: implications for the rise of animal biomineralization." Scientific Reports 7:5482. Doi:10.1038/s41598-017-05753-8.

Bengtson, S., and Y. Zhao. 1992. "Predatorial borings in late Precambrian mineralized exoskeletons." Science 257, 367-369. doi:10.1126/science.257.5068.367

Benus, A.P. 1988. "Sedimentological context of a deep-water Ediacaran fauna (mistaken point formation Avalon Zone, Eastern Newfoundland." *New York State Mus. Bull* 463:8–9.

Bobrovskiy, I., Krasnova, A., Ivantsov, A, Luzhnaya Serezhnikova, E., and J. Brocks. 2019. "Simple sediment rheology explains the Ediacara biota preservation." *Nature Ecology and Evolution* 582–589. Doi:10.1038/s41559-019-0820-7.

Bottjer, D. and M. Clapham. 2006. "Evolutionary Paleoecology of Ediacaran Benthic Marine Animals." *Neoproterozoic Geobiology and Paleobiology.* Doi:10.1007/1-4020-5202-2_4.

Buatois, L.A., Narbonne, G.M., Mángano, M.G., Carmona, N.B., and P. Myrow. 2014. "Ediacaran matground ecology persisted into the earliest Cambrian." *Nature Communications* 5(1). doi:10.1038/ncomms4544

Buatois, L.A., Almond, J., Mángano, M.G., Jensen, S., and G.J.B. Germs. 2018. "Sediment disturbance by Ediacaran bulldozers and the roots of the Cambrian explosion." *Scientific Reports* 8:4514. Doi:10.1038/s41598-018-22859-9

Cai, Y. and H. Hua. 2007. "Pyritization in the Gaojiashan Biota." *Chinese Science Bulletin* 52(5):645–650. doi:10.1007/s11434-007-0080-9

Cai, Y., Hua, H., Xiao, S., Schiffbauer, J.D., and P. Li. 2010. "Biostratinomy of the late Ediacaran pyritized Gaojiashan Lagerstatte from Southern Shaanxi, South China: Importance of event deposits." *PALAIOS* 25(8):487–506. doi:10.2110/palo.2009.p09-133r

Cai, Y., Schiffbauer, J. D., Hua, H., and Xiao, S. 2012. "Preservational modes in the Ediacaran Gaojiashan Lagerstätte: Pyritization, aluminosilicification, and carbonaceous compression." *Palaeogeography, Palaeoclimatology, Palaeoecology* 326-328:109–117. doi:10.1016/j.palaeo.2012.02.009

Chen, J.,-Y., Bottjer, D.J., Li, G., Hadfield, M.G., Gao, F., Cameron, A.R., Zhanga, C.,-Y., Xianc, D.,-C., Tafforeauf, P., Liao, X. and Z.,-J. 2009. "Complex embryos displaying bilaterian characters from Precambrian Doushantuo phosphate deposits, Weng'an, Guizhou, China." *Proceedings of the National Academy of Sciences* 106(45):19056–19060. doi:10.1073/pnas.0904805106

Chen, Z., Zhou, C., Meyer, M., Xiang, K., Schiffbauer, J.D., Yuan, X., and S. Xiao. 2013. "Trace fossil evidence for Ediacaran bilaterian animals with complex behaviors." *Precambrian Research* 224:690-701. Doi: 10.1016/j.precamres.2012.11.004

Corsetti, F.A., and J.W. Hagadorn. 2000. “Precambrian–Cambrian transition: Death Valley, United States.” *Geology* 28:299–302, doi: 10.1130/0091-7613(2000)28<299:PTDVUS>2.0.CO;2

Coutts, F.J., Bradshaw, C.J.A., García-Bellido, D.C., and J.G. Gehling. 2018. “Evidence of sensory-driven behavior in the Ediacaran organism *Parvancorina*: Implications and autecological interpretations.” *Gondwana Research* 55:21–29. doi:10.1016/j.gr.2017.10.009

Cribb, A.T., Kenchington, C.G., Koester, B., Gibson, B.M., Boag, T.H., Racicot, R.A., Mocke, H., Laflamme, M., and S.A.F. Darroch. 2019. “Increase in metazoan ecosystem engineering prior to the Ediacaran–Cambrian boundary in the Nama Group, Namibia.” *Royal Society Open Science* 6(9):190548. doi:10.1098/rsos.190548

Darroch, S.A.F., Sperling, E.A., Boag, T., Racicot, R., Mason, S.J., Morgan, A.S., Tweedt, S., Myrow, P., Johnston, D., Erwin, D., and M. Laflamme. 2015. “Biotic replacement and mass extinction of the Ediacara biota.” *Proceedings of The Royal Society B* 282. doi: 10.1098/rspb.2015.1003

Darroch, S.A.F., Smith, E.F., Laflamme, M., and D.H. Erwin. 2018. “Ediacaran extinction and Cambrian explosion.” *Trends in Ecology and Evolution* 33:653–663. doi: 10.1016/j.tree.2018.06.003

Darroch, S.A.F., Cribb, A., Buatois, L., Germs, G., Kenchington, C., Smith, E., Mocke, H., O'Neil, G.R., Schiffbauer, J.D., Maloney, K., Racicot, R.A., Turk, K., Gibson, B., Koester, B., Almond, J., Boag, T., Tweedt, S., M. 2020. “The trace fossil record of the Nama Group, Namibia: exploring the terminal Ediacaran roots of the Cambrian explosion.” *Earth Science Reviews* 103435. Doi: 10.1016/j.earscirev.2020.103435.

Dornbos, S., Oji, T., Kanayama, A., and G. Sersmaa. 2016. “A new Burgess Shale-type deposit from the Ediacaran of western Mongolia.” *Scientific Reports* 6:23438. Doi: 10.1038/srep23438.

Droser, M.L. and J.G. Gehling. 2015. “The advent of animals: View from the Ediacaran.” *Proceedings of the National Academy of Sciences* 112(16):4865-4870. Doi:10.1073/pnas.1403669112

Dzik, Z. 2003. “Anatomical Information Content in the Ediacaran Fossils and Their Possible Zoological Affinities.” *Integrative and Comparative Biology* 43(1):114–126. Doi:10.1093/icb/43.1.114

Elliott, D. A., Trusler, P. W., Narbonne, G. M., Vickers-Rich, P., Morton, N., Hall, M., Hoffmann, K. H., and G. I. C. Schneider. 2016. "Ernietta from the late Edicaran Nama Group, Namibia." *Journal of Paleontology* 90(6), 1017-1026.

Erwin, D.H., Laflamme, M., Tweedt, S.M., Sperling, E.A., Pisani, D., and K.J. Peterson. 2011. “The Cambrian Conundrum: Early Divergence and Later Ecological Success in the Early History of Animals.” *Science* 334(6059):1091–1097. doi:10.1126/science.1206375

Ford, T.D. 1958. “Pre-cambrian fossils from Charnwood Forest.” *Proceedings of the Yorkshire Geological Society* 31(3):211–217. doi:10.1144/pygs.31.3.211

Gaines, R.R., Hammarlund, E.U., Hou, X., Qi, C., Gabbott, S.E., Zhao, Y., Peng, J., and D.E. Canfield. 2012. “Mechanism for Burgess Shale-type preservation.” *Proceedings of the National Academy of Sciences* 109(14):5180–5184. doi:10.1073/pnas.1111784109

Gehling, J. G. 1999. “Microbial Mats in Terminal Proterozoic Siliciclastics: Ediacaran Death Masks.” *PALAIOS* 14(1):40. doi:10.2307/3515360

Gehling, J.G., Narbonne, G.M., and M.M. Anderson. 2000. “The first named Ediacaran body fossil, *Aspidella terranovica*.” *Palaeontology* 43:427-456.

Gehling, J.G. and M.L. Droser. 2009. “Textured organic surfaces associated with the Ediacara biota in South Australia.” *Earth-Science Reviews* 96(3):196–206. doi:10.1016/j.earscirev.2009.03.002

Gehling, J.G., Runnegar, B.N., and M.L. Droser. 2014. “Scratch Traces of Large Ediacara Bilaterian Animals.” *Journal of Paleontology* 88(02):284–298. doi:10.1666/13-054

Grant, S. W. F. 1990. “Shell structure and distribution of Cloudina, a potential index fossil for the terminal Proterozoic.” *American Journal of Science* 290-A:261–294.

Hagadorn, J.W. and D.J. Bottjer. 1997. “Wrinkle structures: microbially mediated sedimentary structures common in subtidal siliciclastic settings at the Proterozoic–Phanerozoic transition.” *Geology* 25:1047–1050.

Hagadorn, J.W. and B. Waggoner. 2000. “Ediacaran fossils from the southwestern Great Basin, United States.” *Journal of Paleontology* 74:349–359, doi: 10.1666/0022-3360(2000)074<0349:EFFTSG>2.0.CO;2

Hoekzema, R.S., Brasier, M.D., Dunn, F.S., and A.G. Liu. 2017. “Quantitative study of developmental biology confirms *Dickinsonia* as a metazoan.” *Proceedings of the Royal Society B: Biological Sciences* 284(1862):20171348. doi:10.1098/rspb.2017.1348

Hong, H., Zhe, C., and Y. Xunlai. 2007. “The advent of mineralized skeletons in Neoproterozoic Metazoanew fossil evidence from the Gaojiashan Fauna.” *Geological Journal* 42(3-4):263–279. doi:10.1002/gj.1077

Horodyski, R.J. 1991. “Late Proterozoic megafossils from southern Nevada.” *Geological Society of America Abstracts with Programs* 23:163.

Hua, H., Pratt, B., and L. Zhang. 2003. “Borings in *Cloudina* Shells: Complex Predator-Prey Dynamics in the Terminal Neoproterozoic.” *PALAIOS* 18(4/5):454-459. Doi:

Laflamme, M., Flude, L.I., and G.M. Narbonne. 2012. “Ecological tiering and the evolution of a stem: the oldest stemmed frond from the Ediacaran of Newfoundland, Canada.” *Journal of Paleontology* 86(02):193–200. doi:10.1666/11-044.1

Laflamme, M., Darroch, S.A.F., Tweedt, S.M., Peterson, K.J., and D.H. Erwin. 2013. “The end of the Ediacara biota: Extinction, biotic replacement, or Cheshire Cat?” *Gondwana Research* 23(2):558–573. doi:10.1016/j.gr.2012.11.004

Langille, G. B. 1974. “Earliest Cambrian–latest Proterozoic ichnofossils and problematic fossils from Inyo County, California.” *[Ph.D. thesis]: Binghamton, State University of New York* 194.

Lin, J.-P., Gon, S.M., Gehling, J.G., Babcock, L.E., Zhao, Y.-L., Zhang, X.-L., Hu, S.-X., Yuan, J,-L., Yu, M.,-Y., and J. Peng. 2006. “A *Parvancorina*-like arthropod from the Cambrian of South China.” *Historical Biology* 18(1):33–45. doi:10.1080/08912960500508689

Liu, A.G., McIlroy, D., Antcliffe, J.B., and Brasier, M.D. 2011. “Effaced preservation in the Ediacara biota and its implications for the early macrofossil record.” *Palaeontology* 54(3):607–630. doi:10.1111/j.1475-4983.2010.01024.x

Liu, A.G., McIlroy, D., Matthews, J.J., and M.D. Brasier. 2012. “A new assemblage of juvenile Ediacaran fronds from the Drook Formation, Newfoundland.” *Journal of the Geological Society* 169(4):395–403. doi:10.1144/0016-76492011-094

Long, J., Zhang, S., and K. Luo. 2019. “Cryogenian magmatic activity and early life evolution.” *Scientific Reports* 9:6586. Doi:10.1038/s41598-019-43177-8

Martin, M.W. 2000. “Age of Neoproterozoic Bilatarian Body and Trace Fossils, White Sea, Russia: Implications for Metazoan Evolution.” *Science* 288(5467):841–845. doi:10.1126/science.288.5467.841

Mehra, A. and A. Maloof. 2018. “Multiscale study of *Cloudina* aggregates.” *Proceedings of the National Academy of Sciences* 115(11):E2519-E2527. DOI: 10.1073/pnas.1719911115

Meyer, M. 2010. “How plastic is Vendobionta morphology?: A geometric morphometric study of two groups of *Pteridinium* from the latest Neoproterozoic.” M.S. Thesis

Meyer, M., Xiao, S., Gill, B.C., Schiffbauer, J.D., Chen, Z., Zhou, C., and X. Yuan. 2014. “Interactions between Ediacaran animals and microbial mats: Insights from *Lamonte trevalli*s, a new trace fossil from the Dengying Formation of South China.” *Palaeogeography, Palaeoclimatology, Palaeoecology* 396:62–74. doi:10.1016/j.palaeo.2013.12.026

Muscente, A.D., Hawkins, A.D., and S. Xiao. 2015. “Fossil preservation through phosphatization and silicification in the Ediacaran Doushantuo Formation (South China): a comparative synthesis.” *Palaeogeography, Palaeoclimatology, Palaeoecology* 434:46–62. doi:10.1016/j.palaeo.2014.10.013

O’Neil, G.R., Tackett, L.S., and M. Meyer. 2020. “Petrographic evidence for Ediacaran microbial mat-targeted behaviors from the great basin, United States.” *Precambrian Research* 345:105768. doi:10.1016/j.precamres.2020.105768

Penny, A.M., Wood, R., Curtis, A., Bowyer, F., Tostevin, R., and K.-H. Hoffman. 2014. “Ediacaran metazoan reefs from the Nama Group, Namibia.” *Science* 344(6191):1504–1506. doi:10.1126/science.1253393

Reid, L.M., Payne, J.L., García-Bellido, D.C., and J.B. Jago. 2019. “The Ediacara Member, South Australia: lithofacies and palaeoenvironments of the Ediacara biota.” *Gondwana Research*. doi:10.1016/j.gr.2019.09.017

Sappenfield, A., Droser, M., Kennedy, M., and R McKenzie. 2012. “The oldest *Zoophycos* and implications for Early Cambrian deposit feeding.” *Geological Magazine* 149. Doi:10.1017/S0016756812000313.

Schiffbauer, J.D., Xiao, S., Sharma, K.S., and G. Wang. 2012. “The origin of intracellular structures in Ediacaran metazoan embryos.” *Geology* 40(3):223–226. doi:10.1130/g32546.1

Schiffbauer, J., Xiao, S., Cai, Y., Wallace, A. F., Hua, H., Hunter, J. Xu, H. Peng, Y., and Kaufman, A. J. 2014. “A unifying model for Neoproterozoic–Palaeozoic exceptional fossil preservation through pyritization and carbonaceous compression.” *Nature Communications* 5(5754). Doi:10.1038/ncomms6754

Schiffbauer, J.D., Huntley, J.W., O'Neil, G.R., Darroch, S.A.F., Laflamme, M., and Y. 2016. “The latest Ediacaran Wormworld fauna: setting the ecological stage for the Cambrian Explosion.” *GSA Today* 26:4–11. Doi:10.1130/GSATG265A.1

Schiffbauer, J. D., Selly, T., Jacquet, S. M., Merz, R. A., Nelson, L. L., Strange, M. A., Cai, Y., and E. F. Smith. 2020. “Discovery of bilaterian-type through-guts in cloudinomorphs from the terminal Ediacaran Period.” *Nature Communications* 11(205). Doi:10.1038/s41467-019-13882-z

Schopf, J.W. 2000. “Solution to Darwin’s dilemma: Discovery of the missing Precambrian record of life.” *Proceedings of the National Academy of Sciences* 97(13):6947–6953. doi:10.1073/pnas.97.13.6947

Selly, T., Schiffbauer, J.D., Jacquet, S.M., Smith, E.F., Nelson, L.L., Andreasen, B.D., Huntley, J.W., Strange, M.A., O'Neil, G.R., Thater, C.A., Bykova, N., Steiner, M., Yang, B., and Y. Cai. 2020. "A new cloudinid fossil assemblage from the terminal Ediacaran of Nevada, USA." *Journal of Systematic Palaeontology* 18(4):357-379. doi: 10.1080/14772019.2019.1623333

Smith, E. F., Nelson, L. L., Strange, M. A., Eyster, A. E., Rowland, S. M., Schrag, D. P., and Macdonald, F A. 2016. "The end of the Ediacaran: Two new exceptionally preserved body fossil assemblages from Mount Dunfee, Nevada, USA." *Geology* 44(11):911–914. doi:10.1130/G38157.1

Smith, E. F., Nelson, L. L., Tweedt, S. M., Zeng, H., and Workman, J. B. 2017. "A cosmopolitan late Ediacaran biotic assemblage: new fossils from Nevada and Namibia support a global biostratigraphic link." *Proceedings of the Royal Society B: Biological Sciences* 284(1858):20170934. doi:10.1098/rspb.2017.0934

Stewart, J. H. 1970. "Upper Precambrian and Lower Cambrian strata in the southern Great Basin, California and Nevada." *U.S. Geological Survey Professional Paper* 620(206).

Taylor, M. 1966. "Precambrian Mollusc-like Fossils from Inyo County, California." *Science*, 153(3732), 198-201.

Ye, Q., Tong, J., An, Z., Hu, J., Tian, L., Guan, K., and S. Xiao. 2017. "A systematic description of new macrofossil material from the upper Ediacaran Miaohe Member in South China." *Journal of Systematic Palaeontology* doi:10.1080/14772019.2017.1404499

Zakrevskaya, M. 2014. "Paleoecological reconstruction of the Ediacaran benthic macroscopic communities of the White Sea (Russia)." *Palaeogeography, Palaeoclimatology, Palaeoecology* 410:27–38. doi:10.1016/j.palaeo.2014.05.021

Zhu, M., Gehling, J.G., Xiao, S., Zhao, Y., and M.L. Droser. 2008. “Eight-armed Ediacara fossil preserved in contrasting taphonomic windows from China and Australia.” *Geology* 36(11):867. doi:10.1130/g25203a.1

CHAPTER 2: TAPHONOMIC VARIANTS OF TUBULAR FOSSILS FROM THE WHITE-INYO LATE EDIACARAN DEEP SPRING FORMATION, INYO COUNTY, CA

2.1. Introduction

Terminal Ediacaran marine faunal assemblages are dominated by small, abundant tube-shaped fossils representing potential early polychaetes (Schiffbauer et al., 2020), often only preserved under exceptional taphonomic conditions. Tubicolous (tube-dwelling worm) fossils from late Ediacaran outcrops of the western United States Death Valley and Great Basin regions exhibit a wide range of taphonomic quality, locally biasing the known taxonomic diversity of the area. In the western United States, well-preserved tubicolous fossils have been described from the Deep Spring Formation at Mount Dunfee near Gold Point, Nevada, and at the correlative Wood Canyon Formation in the Montgomery Mountains near Johnnie, Nevada (Fig. 2.1, Smith et al., 2017; Selly et al., 2019). Selly et al. (2019) classified well-preserved fossils from the two sites as "cloudinomorphs", a group of fossils bearing morphologies similar in form to the early biomineralizer, *Cloudina*. Unfortunately, classification of tubicolous organisms is difficult in instances of poor preservation, as cloudinomorph characteristics are not readily preserved and the general "tube-shape" of the fossils is also present in Ediacaran algal fossils. As is such, in the Deep Spring Formation at Ancient Bristlecone Pine Forest (ABPF) in Inyo County, California (Fig, 2.1).

Poorly-preserved, unclassified tube-shaped fossils occur in abundance in the late Ediacaran fossil beds within Ancient Bristlecone Pine Forest, but the tubes lack morphological characteristics seen in the exceptional specimens from Mt. Dunfee and Montgomery Mountains. Some of the ABPF tube-shaped fossils exhibit morphological characteristics that are used to define the Wormworld fauna, including cloudinomorph fossils (Selly et al., 2019), and other fossils that resemble macroalgae. Preservation of the fossils is not limited to the surface of the sedimentary

deposits, and include remnants of three-dimensional definitive tubicolous cloudinomorph body fossils preserved within the beds. Sedimentological conditions control many aspects of preservation and can affect the apparent diversity of a palaeocommunity.

Pyritization is the most commonly occurring mode of preservation in the Wormworld fauna, and is the mode of preservation observed for many tube-shaped fossils at ABPF. Pyritized fossils from Wormworld-containing localities are often preserved in three-dimensions and with a high level of detail, especially within specimens from the Wormworld fossils of the Gaojiashan Lagerstätte, where rapid initial burial promoted the precipitation of pyrite within the bacterial sulfate reduction zone. Following initial burial, slow sedimentation and a thick bacterial sulfate reduction zone allowed for continued precipitation of pyrite and full preservation of the three-dimensional fossils through pervasive pyritization. The process of pyritization may be halted in the event that the organism leaves the sulfate reduction zone (due to ongoing sedimentation), the amount of sulfate is exhausted, the amount of reduced iron is exhausted, or if all of the organic matter is consumed (Cai et al., 2012; Schiffbauer et al., 2014; Schiffbauer et al., 2020). The poor preservation of the ABPF tubes represent an undesirable outcome of the pyritization process, which may be caused by a number of factors, including pre-pyritization degradation and excessive time in the bacterial sulfate reduction zone.

Characterizing the preservation of tubicolous fossils over a broad geographic extent that contains a variety of fossil taxa (and ichnotaxa) and taphonomic modes clarifies the conditions limiting the occurrence of certain fossils, whether be it environmental restriction or taphonomic overprint. The presence of well-preserved tubicolous fossils in both the Deep Spring and Wood Canyon formations increases the likelihood of finding tubicolous fossils within the terminal Ediacaran at ABPF. Through taphonomic, morphological, and sedimentological comparisons

between the Deep Spring and Wood Canyon sites, the ABPF tubes can illustrate the preservational restrictions of the Wormworld fauna and the geographic extent of these important predecessors to the Cambrian Explosion.

2.2. Geological and Paleogeographical Context

Two synchronous formations, the Deep Spring and Wood Canyon, represent deposition along a shallow marine-offshore depth transect and contain Ediacaran fossils. The Deep Spring Formation is a mixed carbonate-siliciclastic system that covers several environments. The northwest sections are carbonate-dominated, with the amount of carbonate decreasing to the southeast until transitioning into the Wood Canyon Formation (Mount and Signor, 1991). Ancient Bristlecone Pine Forest is located on White Mountain, within Inyo County and the Inyo National Forest in California. North of Death Valley National Park. The Deep Spring Formation within ABPF appears as sporadic outcrops, including Ediacaran and biomineralized tubicolous fossils, and Cambrian trace fossils (Corsetti and Hagadorn, 2003). The Cambrian fossils from the ABPF area have been well-documented (McKee and Gangloff, 1969; Alpert, 1973; Firby and Durham, 1974; Alpert, 1975; Droser and Bottjer, 1998; Durham, 1993; Dornbos and Bottjer, 2001), while the Ediacaran fossils have been largely overlooked. The exceptional preservation and the abundance of Cambrian fossils allows a general demarcation between Precambrian and Cambrian-aged deposits.

2.3. Materials and Methods

2.3.1. Stratigraphy

Two transects were measured from a 0.6 km^2 survey area within Ancient Bristlecone Pine Forest (Fig. 2.2), using strike and dip to correlate outcrops, and combined to create a generalized stratigraphic column (Fig. 2.3).

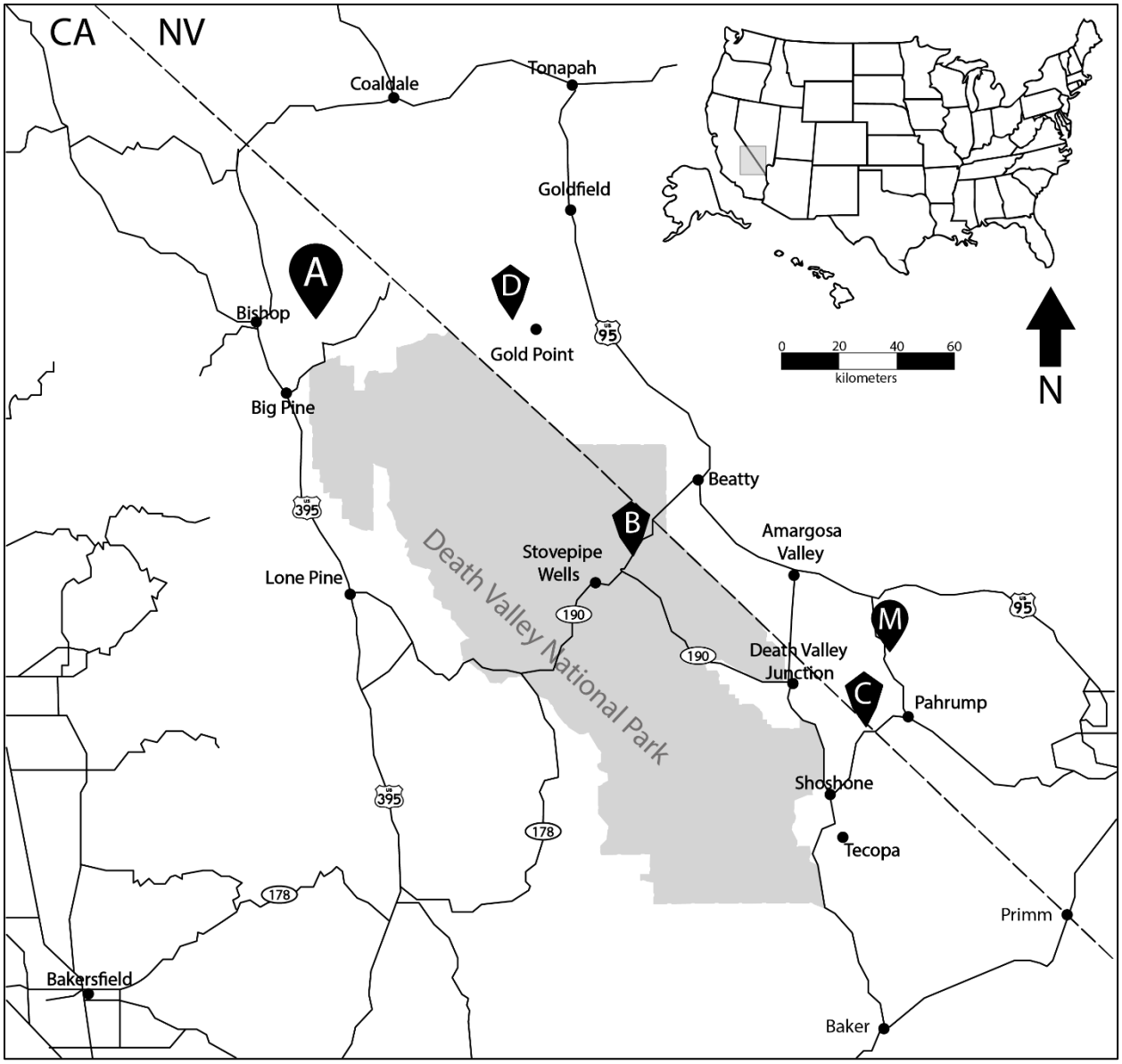

Figure 2.1. Map of Ediacaran fossil containing units of the Deep Spring (circle marker) and Wood Canyon (diamond marker) formations. A = Ancient Bristlecone Pine Forest, M = Montgomery Mountains, M = Mt. Dunfee, C = Chicago Pass, B = Boundary Canyon. Grey area represents Death Valley National Park.

2.3.2. Fossil collections

Trace and body fossils were collected from bedding planes and in float from identifiable autochthonous sources, where available. Fossils were also collected from talus deposits if the specimen appeared to be of interest.

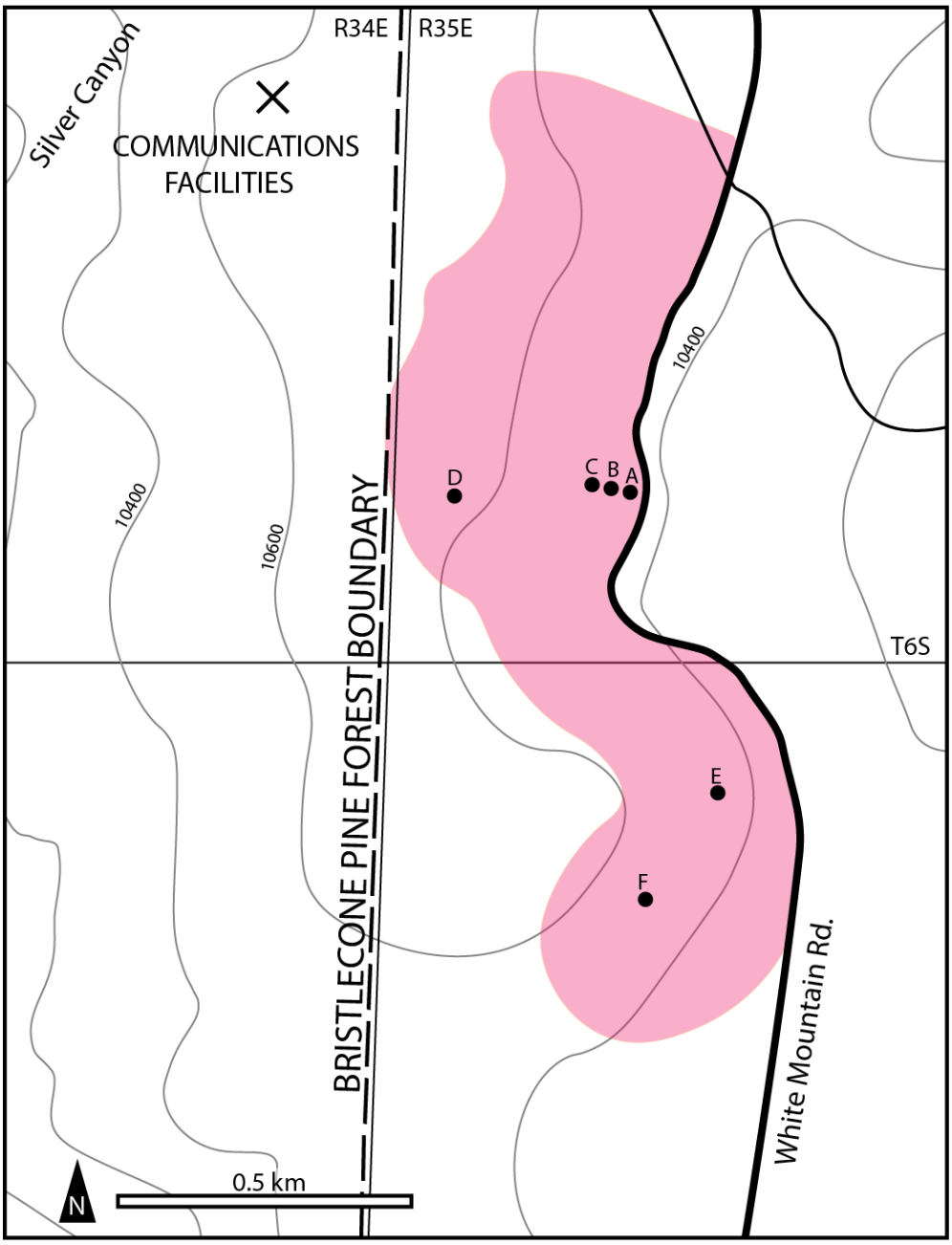

Figure 2.2. Map of the total investigated area (pink) within Ancient Bristlecone Pine Forest, Mt. Bancroft Quadrangle, California. A–D and E–F correspond to stratigraphic divisions in figure 2.3. Outcrop E corresponds to A, B, and C, and F corresponds with D based on sedimentology and fossil occurrences.

2.3.3. Lab analysis

All identifiable and potential fossils were photographed for image processing and analyses were conducted using Fiji freeware. Tube-shaped fossils were identified when possible. Samples

containing tube-shaped fossils were grouped according to macroscopic sedimentological similarities of the host rock and a subset were examined petrographically. Additional samples were imaged using a GE v|tome|x s microCT scanner in order to identify density anomalies and energy-dispersive X-ray spectroscopy (EDS) was conducted on a JEOL JSM-7600F scanning electron microscope (SEM).

2.4. Results

Approximately 40 m above the lowest Deep Spring bed of the measured section, are the lowest occurences of tube-shaped, potential tubicolous vermiform (worm-like) fauna begin to appear, above the first occurrences of early simple burrowing traces. Above the tube-containing outcrops are beds of characteristic Cambrian trace fossils, including large bilaterian burrowing and crawling traces, and the disappearance of all Ediacaran tubular fossils.

2.4.1. Sedimentology

Outcrops of the Deep Spring Formation at Ancient Bristlecone Pine Forest are dominated by quartz-rich siliciclastic siltstones and fine-grained sandstones (Fig. 2.4). Microbial mat textures are common, including wrinkle structures. Thin (<0.5mm) microbial mat laminae are evident in petrographic thin section (Fig. 2.4A, 2.5A). Iron-rich (pyrite) nodules (<1 mm) and pyrite clusters are common and are in the same size range as the corresponding host sediment (Fig. 2.4A, C–D, Fig. 2.5A–D). Tube-shaped fossils have been found to most commonly occur in eight sediment types:

2.4.1.1. Microbial mat-rich siltstones (Fig. 2.4A). Mottled light grey siltstones containing filamentous layers representing microbial mat laminae. Fluid escape structures and pyrite grains are common, especially within the thinner microbial mat laminae. Pyrite clusters are present, but

are not directly associated with the microbial mats. Filamentous microbial mat texture is evident on the sediment surface. Beds are light grey and typically ~5–10 mm in thickness.

2.4.1.2. Thick dark sandstones (Fig. 2.4B). Very fine-grained, quartz-rich sandstones with occasional low-angle cross-beds and euhedral pyrite grains. Grains are subangular and moderately sorted.Sediments are dark grey/greenish with bedding thicknesses of ~20–40 mm.

2.4.1.3. Siltstone with sandy lenses (Fig. 2.4C). Light grey siltstone with some muds and lenses of coarse silts and sands. Iron oxides are abundant. Silt grains are subangular and moderately sorted. Some of the finer, elongate grains have a tilted orientation within sand lenses, likely a remnant of cross-laminations. Bedding tends to be ~10–15 mm in thickness.

2.4.1.4. Organic-rich sandstones with pyrite clusters (Fig. 2.4D). Quartz-dominated sandstones with green and red accessory grains. Grains are subangular, with occasional rounded elongate grains. Evidence of filamentous microbial mat laminae and micas constrained to thin, discontinuous layers. Individual euhedral pyrite grains and clusters are present. There are no burrows or obvious sedimentary structures. Bedding tends to be ~10 mm in thickness.

2.4.1.5. Fine sandstones with euhedral pyrite (Fig. 2.4E). Fine sandstones, with some thin intra-bed laminations containing finer, darker grains, likely representing parting lineations. Grains are dominantly subangular with euhedral pyrite grains. Bedding is ~10–15 mm in thickness.

2.4.1.6. Red sandstones (Fig 2.4F). Sandstones with a surface exposure that is a reddish-maroon to reddish-tan hue. Grains are dominantly quartz with iron oxides. Filimentous-like textures are found in some layers, but are thin and discontinuous.

2.4.1.7. Platy sandstones (Fig. 2.4G). Fine quartz sandstone with subangular, moderately well-sorted grains. Matrix is dominated by iron oxides. There are no obvious sedimentary structures. Beds are comprised of ~5–10 mm laminae.

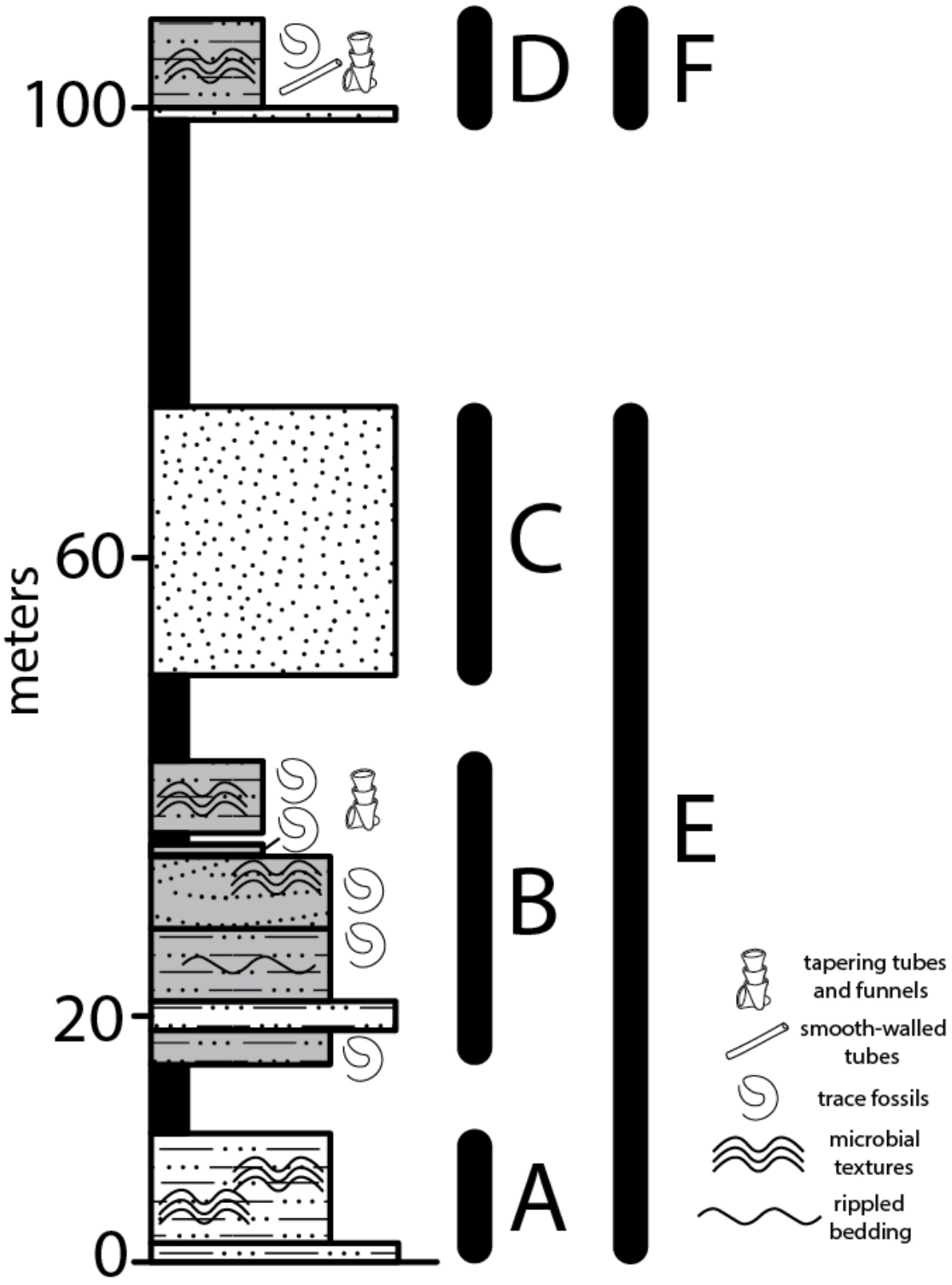

Figure 2.3. Stratigraphic column of the Ediacaran section of the Deep Spring Formation at Ancient Bristlecone Pine Forest, Inyo County, CA

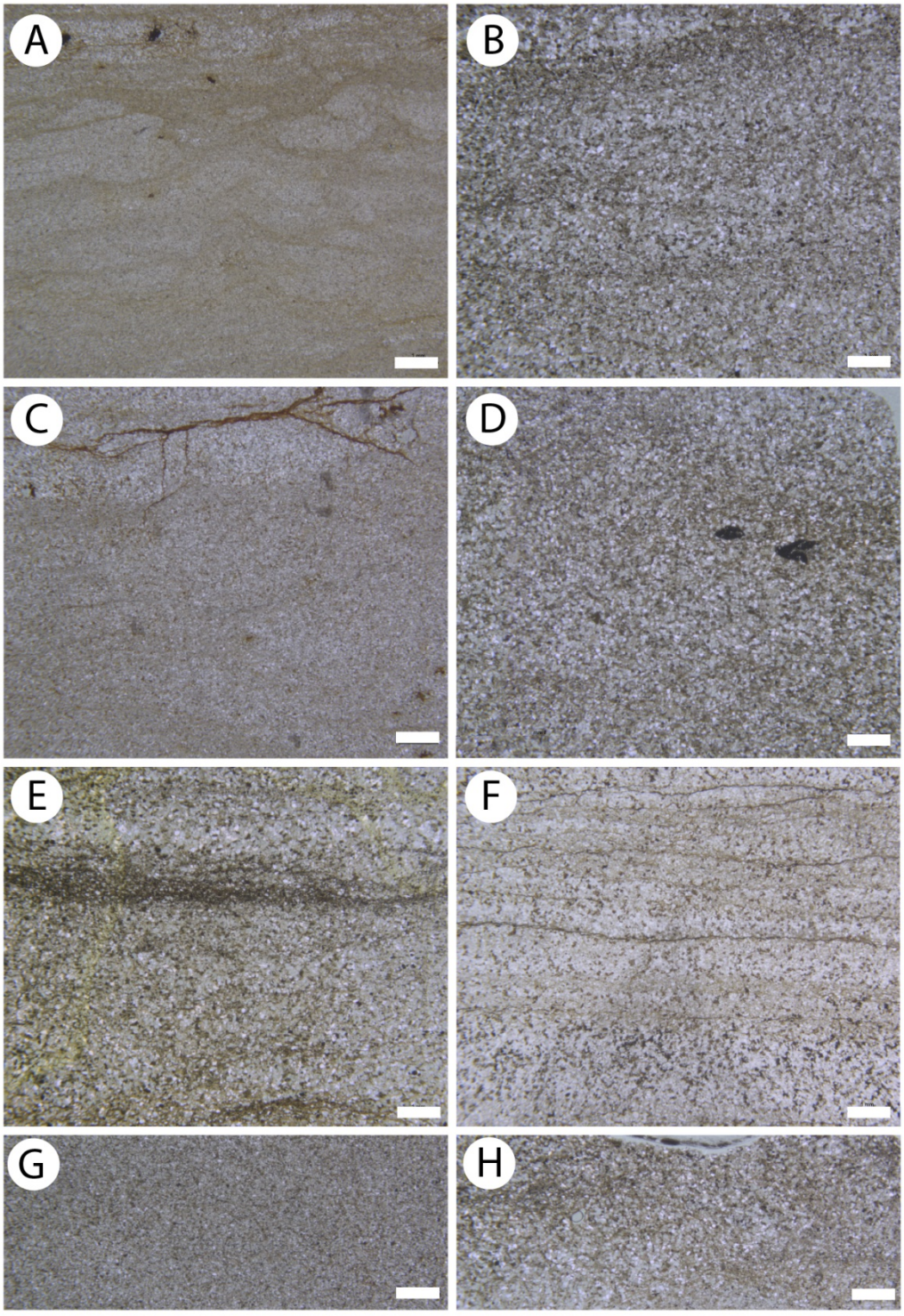

Figure 2.4. Petrographic thin-sections of fossil-bearing sediments. A) microbial mat-rich siltstone, arrows denote areas of obvious fluid escape “teepees”; B) thick dark siltstone; C) siltstone with sandy lenses; D) organic-rich siltstones with black pyrite clusters; E) Fine sandstone with euhedral pyrites; F) red sandstones G) **C** found as platy siltstones; H) **D** found as platy coarse siltstones to medium sandstones. Scale bar = 1 mm.

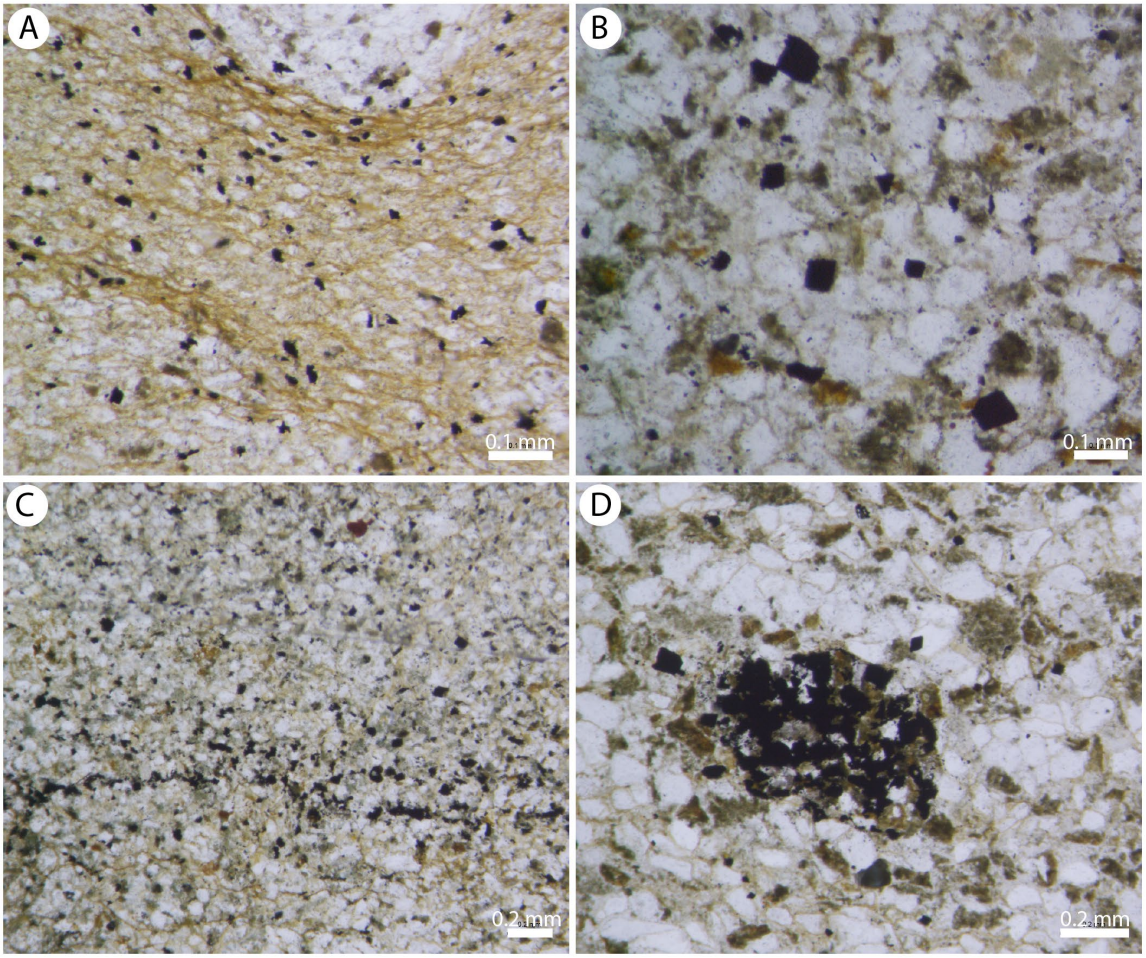

Figure 2.5. Petrographic thin sections of pyrite grains. A) pyrite grains within filamentous microbial mat microlaminae of Fig. 2.4A; B) individual cubic pyrite grains; C) layer of cubic pyrite grains; D) cluster of pyrite from Fig. 2.4D.

2.4.1.8. Platy siltstones (Fig. 2.4H). Medium-to-coarse grained quartz siltstones with rounded, moderately well-sorted grains. Matrix is dominated by iron oxides. There are no obvious sedimentary structures. Beds are comprised of ~5–10 mm laminae.

2.4.2. Preservation

2.4.2.1. Three-dimensional walled tubes. Pyritized, tube-shaped fossils are preserved with few morphological characteristics beyond distinct fossil walls (Fig. 2.6) and occasional evidence of stacked units (Fig. 2.6B–C). The walled tubes are mostly millimeter-scale and fall into three morphological groups. First, (type *i*) stacked and unstacked funnels encased within the host

sediment (Fig. 2.6A–B), (type *ii*) large (8–22 mm in length, 1–3 mm) tapering tubes with variable presence of diagnostic cloudinomorph characteristics on bedding planes (Fig, 2.6C), and (type *iii*) slightly smaller, "mid-sized" (5–8 mm in length, 0.4–0.8 mm in width) pyritized tapering tubes with distinct walls and no additional morphological characteristics (Fig. 2.6D–F), also on bedding planes.

While three-dimensionally preserved tubes are found in most of the siltstone and sandstone facies, morphological features are differentially distributed among the facies. Three-dimensionally preserved nanometer-scale individual funnels (Fig. 2.6A) and millimeter-scale stacked funnel tube-shaped fossils (Fig. 2.6B) are found in the thicker dark grey micaceous coarse siltstones and sandstones (Fig. 2.4B), as well as the dark grey/green thinly bedded (<1 cm) platy siltstones (Fig. 2.4G–H). The larger (type *ii*) tapering tubes were found in reddish-tan siltstones (Fig. 2.4F). One specimen shows evidence of stacked funnels (Fig. 2.6C), though this is not observed in other specimens. The mid-sized (type *iii*), tapering, pyritized-walled tubes are commonly found on the bedding planes of the thin (<1 cm) dark grey coarse-grained platy siltstones (Fig. 2.4G–H), as well as the light grey siltstones and sandstones (Fig. 2.4A, C–D). EDS analyses confirm that the three-dimensional tubular fossils are preserved through pyritization, indicated by the presence of the second iron (Fe) peak (Fig. 2.7A–B). This iron peak is also evident on the tube walls of cloudinomorph fossils from the Deep Spring Formation at Mt. Dunfee (Fig. 2.7C).

2.4.2.2. Two-dimensional "stains". Red-to-maroon elongated "smears" occur on the bedding planes of thin (<1 cm) dark grey coarse-grained platy siltstones (Fig. 2.4G–H). The "stains" are found on the same surfaces as the *iii*-type three-dimensional pyritized tubes. There are no morphological characteristics of the stains apparent beyond the potentially tapering tubular, shape. The "stains" are generally larger in length and width than the other pyritized tubular fossils

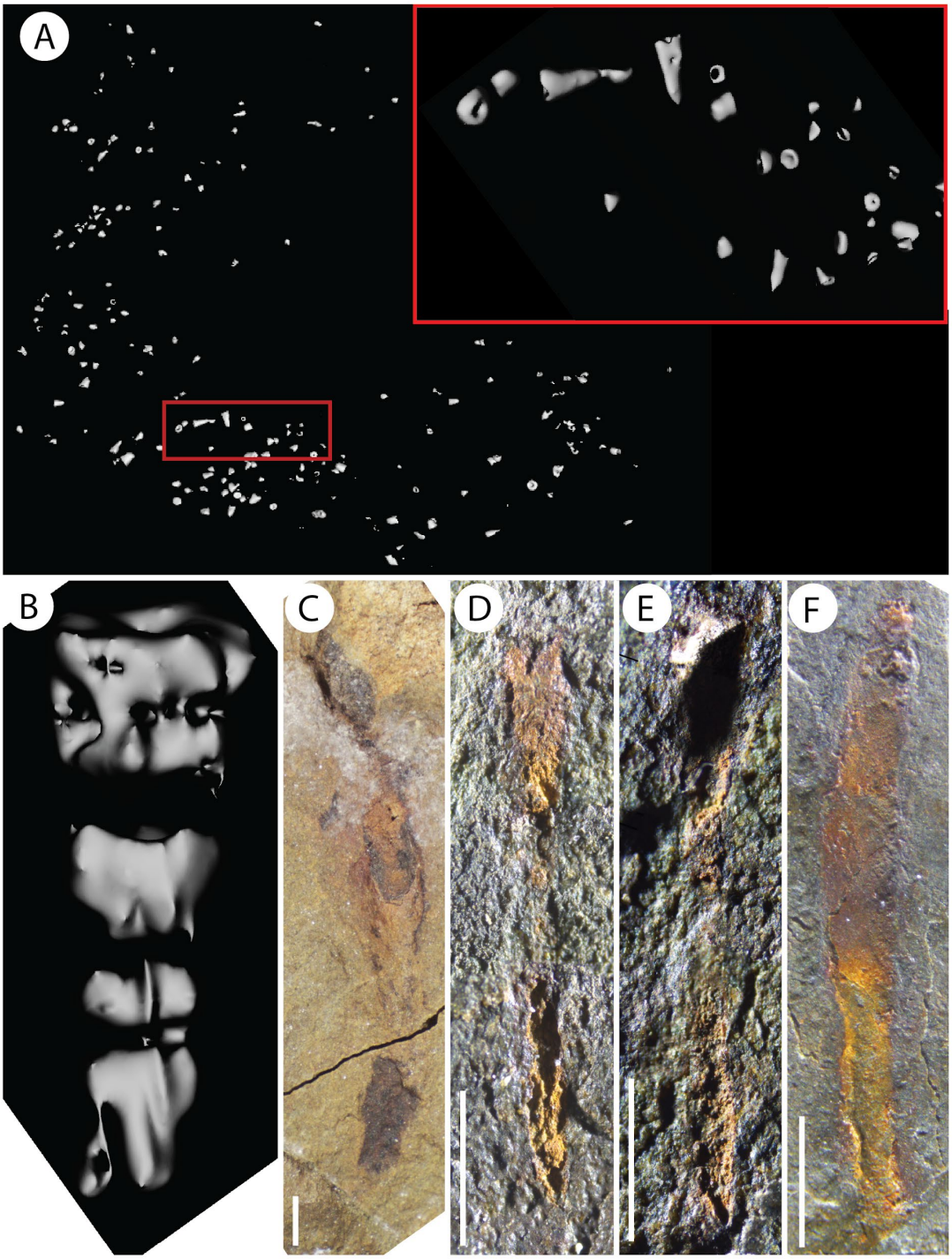

Figure 2.6. Three-dimensionally pyritized tubes. A) disarticulated funnels and cloudinomorph debris in micro-CT; B) stacked funnel cloudinomorph (i-type) in micro-CT; C) large, pyritized tube (ii-type) with evidence of stacked funnel structure; D–F) mid-sized pyritized tubes (iii-type). Scale = 2 mm.

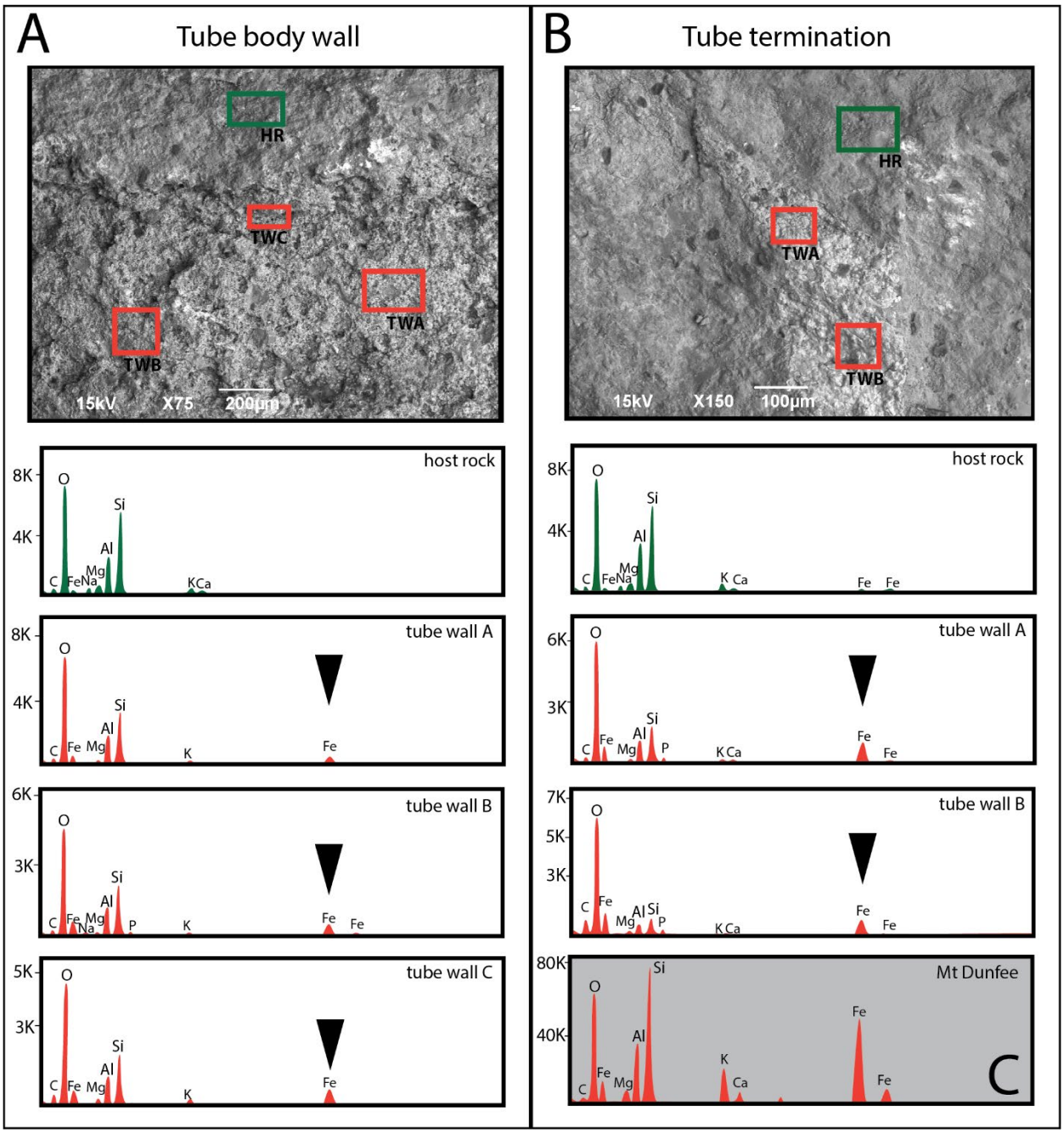

Figure 2.7. Energy-dispersive X-ray spectroscopy (EDS) spectra of a pyritized fossil. EDS analysis of (A) a termination of a pyritized tube-shaped fossil and (B) the fossil wall of a pyritized tube-shaped fossil from Ancient Bristlecone Pine Forest. Orange arrows indicate the second iron (Fe) peak common in instances of pyrite preservation. (C) EDS soectral from the tube wall of a pyritized Deep Spring cloudinomorph from Mt. Dunfee, NV. **A–B** were conducted on a JEOL JSM-7600F scanning electron microscope (SEM). **C** was conducted on a FEI Quanta 600 FEG Environmental Scanning Electron Microscope (ESEM) at 20kV and a 10.5 mm WD.

from the section, but the precise size cannot be confirmed due to a lack of fossil wall structures. Sizes are estimated at 12–30 mm in length and 0.5–1.0 mm in width.

2.4.2.3. Definitively non-cloudinomorph tubular macrofossils. Other tube-shaped fossils are present in the Ediacaran beds at Ancient Bristlecone Pine Forest that do not fit within the common size ranges and morphologies of described Wormworld tubular taxa. Three types of tube fossils that exhibit ambiguous morphologies include: (type *a*) filamentous (5–10 mm length, 0.1–0.5 mm width, based on individual "branches"), pyritized, non-tapering tubes with occasional branching (Fig. 2.9A–B), (type *b*) large (12–30 mm in length, 2.5–3 mm in width) non-tapering tubes with rounded terminations, preserved through carbonaceous compression and aluminosilicate replication (Fig. 2.9C–D), and type (*c*) mid-sized (~11–15 mm in length, 0.3–1.0 mm in width) pyritized, smooth-walled tubes with tapering terminations (Fig. 2.9E–F).

2.4.2.4. Algal fossils. The small, filamentous tubes are found in the light grey silts and sandstones (Fig. 2.4A and C). These tubes (type *a*) are typically found as individual "filaments", but branching specimens are also present (Fig. 2.9A–B).

2.4.2.5. Smooth-walled tubes. The large tubes with rounded terminations (type *b*) are preserved in light grey siltstones and sandstones, occasionally associated with large pyrite nodules (Fig. 2.4A, C–D). The three-dimensional cylindrical smooth-walled tubes with two tapering ends (type *c*) are preserved only within the dark grey/green micaceous siltstones (Fig. 2.4B).

2.5. Discussion

The Ancient Bristlecone Pine Forest outcrops of the late Ediacaran–early Cambrian Deep Spring Formation (~555–541 Ma) contains a taxonomic, taphonomic, and temporally significant range of fossils. The shallow marine facies observed in these deposits do not contain abundant fossils of exceptional preservation like those in Gaojiashan, Mt. Dunfee, or Johnnie, but

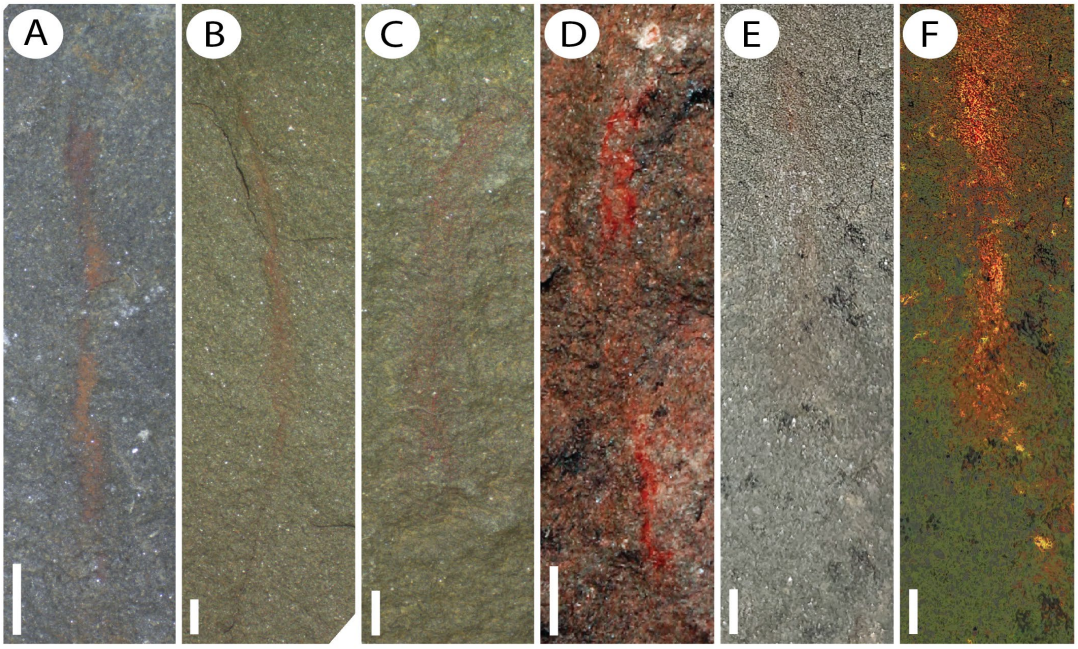

Figure 2.8. A–E) Two-dimensionally preserved tube-shaped fossils. F) High-contrast modified image of "E". Fossils do not have clear, well-formed fossil walls and are dominantly preserved as red stain-like smears of pyrite. Scale = 2 mm.

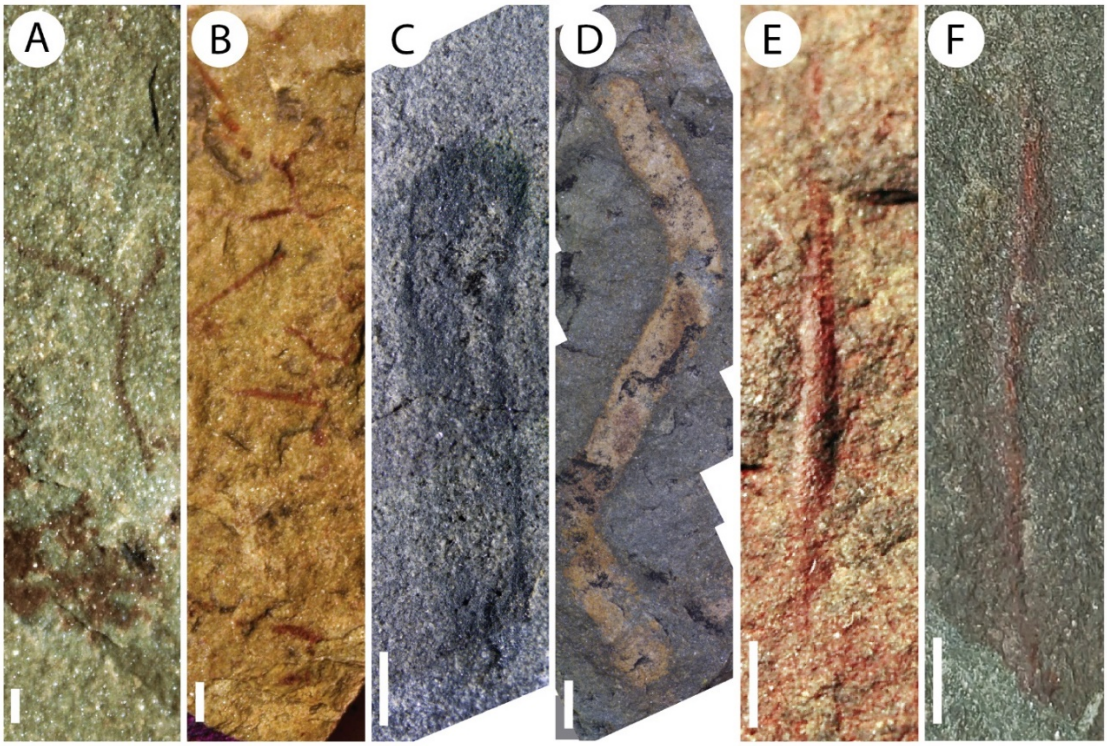

Figure 2.9. Definitively non-cloudinomorph tubular macrofossils from Ancient Bristlecone Pine Forest. A) Filamentous algae showing evidence of branching; B) Filamentous algae as individual filaments, with possible branching; C) Tube-shaped carbonaceous compression; D) Tube-shaped fossil with aluminosilicate replication; E–F) Pyritized, smooth-walled tube-shaped fossils. Scale = 2 mm.

rather exemplify what are likely to be more typical and widespread preservation modes, and therefore can illustrate primary controlling factors of preservation for these enigmatic fossil taxa.

2.5.1. Faunal interpretations

2.5.1.1. Three-dimensional pyritized tubes: Cloudinomorph interpretation. Selly et al. (2019) defined the Ediacaran cloudinomorphs as "typically millimetric tubular fossils constructed by nested, repeating, collared cylindrical units – commonly referred to as 'funnel-in-funnel' structures or 'collars'", based on specimens from the Gaojiashan Lagerstätte, Montgomery Mountains, Mt. Dunfee, and other areas of exceptional preservation. Of the ABPF tube-shaped fossils type *i*, only the disarticulated and articulated (stacked) funnels observed with microCT can be definitively classified as "cloudinomorphs" (Fig. 2.6A–B). Three-dimensional pyritized tubes on bedding planes (worm types *ii* and *iii*) lack the morphological information necessary for potential classification (Fig. 2.6D–F). While worm types *ii* and *iii* are not definitively cloudinomorphs, the possibility cannot be ruled out.

2.5.1.2. Two-dimensional preservation. The presence of the "stains" on the same surfaces as the three-dimensional pyritized tube-shaped fossils indicates that they are likely remnants of tube-shaped body plans that were degraded during or subsequent to burial. While these stains may represent very poorly preserved tube worms, the size of the stains (12–30 mm in length, 0.5–1.0 mm in width) is also consistent with the smooth-walled tubes (non-worm type *c*) (~11–15 mm in length, 0.3–1.0 mm in width), which are interpreted as probable algal origin (Fig. 2.8, 2.9E–F). Therefore, a definitive classification is not possible.

2.5.1.3. Additional three-dimensional tubes: Algal interpretation. The size and branching nature of the small, branching pyritized tubes (type *a*) provide strong evidence for an algal interpretation. Branching is a common feature of algae and is rare in the defined cloudinomorph

taxa, with the exception of the biomineralized *Cloudina* in cases of preserved asexual reproduction (Hua et al., 2005). The ABPF type *a* tubes are unlikely to represent asexually reproducing *Cloudina*, however, as the former exhibit multiple branch points and do not feature any evidence of biomineralization. The branching tubes from ABPF most closely resemble the algal fossil genus, *Doushantuophyton* of the South China Miaohe biota (Ye et al., 2017), but are not complete enough for definite classification.

2.5.1.4. Smooth-walled tubes. Low taphonomic quality of the larger tubes (type *b*) precludes classification, but the large size and rounded terminations are not consistent with cloudinomorph morphology. Overgrowth of aluminosilicate minerals on the fossil specimen surface destroyed diagnostic features, leaving only the general fossil shape. The larger tubes are similar in size and shape to currently unclassified smooth-walled tubes from the Deep Spring Fm. at Mt. Dunfee, NV, and the Wood Canyon Fm. at Johnnie, NV (Ye et al., 2017). The ABPF tubes are found as both two-dimensional compressions and as flattened, but three-dimensional tubes, often with an aluminosilicate coating, similar to Miaohe preservation (Ye et al., 2017). Compaction may have deformed the originally cylindrical tubes resulting in fossils appearing to be wider than the living body, leaving the length largely unaffected.

The three-dimensional cylindrical smooth-walled tubes with tapering ends (type *c*) are also morphologically similar to the Deep Spring and Wood Canyon tubes, but also resemble the Ediacaran alga, *Sinocylindra linearis*, known from the Sanlihuang section of the Miaohe biota units of South China (Ye et al., 2017). *S. linearis* are nearly straight, cylindrical ribbon-like fossils. The Miaohe specimen diameters range from 0.3–2.0 mm and the length from 5.0–50 mm (Ye et al., 2017), and the fossils also lack evidence of branching. The smooth-walled tubes at ABPF (type *c*) are generally smaller, at 0.3–1.0 mm in diameter and 11–15 mm in length, 0.3–1.0 mm.

Table 2.1. Preservational, morphological, size, and sedimentological comparisons between the ABPF tubes, known cloudinomorphs, and similar algae fossils from the Miaohe biota.

ID/taxa	Preservation			Morphology				size (SA based on median width)			Sedimentology		
	pyriti-zation	kerogen-ization/ aluminosi-licification	biomineral-ization	distinct walls	tapering	repeating units (i.e. funnels)	branching	large (median width >1.2 mm)	mid-size (0.6-1.2 mm)	small (0-0.5 mm)	silt-stone	sand-stone	pyrite
i	X			X	X	X		?	?	?	X	X	X
ii	X			X	X	X		X			X		
iii	X			X	X				X		X	X	X
a	X			X			X			X	X	X	X
b		X		X				X			X	X	X
c	X			X					X		X		X
"stains"	X				?				X		X		
cloudinomorphs	X	X	X	X	X	X		X	X	X			
Sinocylindra yunnanensis		X		X					X				
Sinocylindra linearis		X		X					X				
Doushantuophyton lineare	X			X			X			X			

The Dengying Formation sections containing the Miaohe biota were deposited in a low-energy. subtidal environment in a restricted basin (Xiao et al., 2002). Fossils are found in siliceous shales with dolostone interbeds, as well as thin-bedded argillaceous limestone (Ye et al., 2017). The difference in sedimentology between Miaohe and ABPF likely contributes to the higher number of fossils with identifiable characteristics in the Miaohe fauna fossils. Additionally, the Miaohe biota is extremely abundant in comparison to the ABPF tubes and may represent more habitable environmental conditions for the algal taxa.

2.5.2. Preservation and taphonomy of tube-shaped fossils

Pyritization is the most common preservation mode in the ABPF potential cloudinomorph tubes (Fig. 2.7). The pyrite replication of the ABPF specimens exhibits both pyrite overgrowths and pyrite clusters (Fig. 2.10). The resulting tubes are preserved with little to no morphological characteristics (Fig. 10A–B). Individual sedimentary pyrite nodules are common (Fig. 2.5), indicating high amounts of available iron in the sediment; an artefact that is also present in the Gaojiashan fossil beds (Cai and Hua, 2007). Additionally, pyrite framboids can be recognized in SEM imaging (Fig. 2.10C). Further, iron (Fe) concentration tends to be higher near the fossil walls (Fig. 2.7) reflecting the increased amount of organic matter present along the edges of the compressed tubes (Cai et al., 2007). The elemental concentrations may also be altered by precipitation of authigenic silica-rich clays. The pyritization process can be halted by the exhaustion of available sulfate and iron, and if burial conditions at ABPF were not lacking in either, pyrite growth continued unabated (Schiffbauer et al., 2020), destroying features that were initially preserved.

The variety of preservation types found at ABPF are also present in Lagerstätte deposits of tube-shaped fossils elsewhere. Although the corresponding Deep Spring Formation section at Mt.

Dunfee is known for its exceptionally preserved cloudinomorph fossils, poorly preserved tubes that mirror the preservation of the ABPF tubes are also present, including "pitted" textures, pyrite overgrowth, and residual "stains" (Fig. 2.10D–F, H). Differences in pyrite preservation quality are not uncommon in the Wormworld assemblages, for example, with two notably distinct pyritization taphonomic pathways present in the Gaojiashan fauna, with variations hypothesized to relate to the time of initiation of pyritization (Cai and Hua, 2007).

In addition to well-preserved tubes and poorly-preserved tubes in the Montgomery Mountains, a subset of the pyritized cloudinomorphs from the Wood Canyon Formation were found to contain pyritized gut-tracts, a body element with highly labile tissue that would typically not be preserved (Schiffbauer et al., 2020). In this instance, pyritization was halted by early exhaustion of sulfate and/or reduced iron early enough to prevent the destruction of the tissues, while also leading to a preserved outer tube with few morphological characteristics (Schiffbauer et al., 2020). The gut-tract containing tubes are also found with tubes with exceptionally preserved tube morphologies, but no internal replication of soft-tissues, indicating that preservation differences may be patchy due to available resources during the preservation process. The documented variability in preservation quality within singular fossil assemblages, including cloudinomorph tubes from Mt. Dunfee (and Gaojiashan) suggests a similar origin for the ABPF tubes. Further, the consideration of the poorly preserved Mt. Dunfee (and Gaojiashan) tubes as possible cloudinomorphs based on the occurrences of the more rare exceptional fossils warrants a similar consideration for the ABPF tubes.

The similarities and differences in preservation between the ABPF and Mt. Dunfee tubes may also clarify the driving force behind the major taphonomic issues observed at ABPF. While the tubes at ABPF are preserved in siltstones and fine sandstones, the Mt. Dunfee tubes are

preserved in low-energy dark shales. The exceptional quality of some tube-shaped fossils from Mt. Dunfee is attributed to the restricted dysoxic environment and fine sediments; however, poorly preserved tubes are fairly common at this locality and closely resemble the tube-shaped fossils from ABPF (Fig. 2.10). Type *i* tubes are interpreted as cloudinomorphs (evidenced by the encased stacked funnel tubes), suggesting that similar preservation pathways are present in both areas despite the different depositional environments, representing an enormous expansion of sedimentary deposits "likely" to contain tube-shaped fossils of the terminal Ediacaran.

The preservation quality within the Deep Spring Formation is likely to have been controlled by the size of the sulfate reduction zone, amount of available sulfate and/or the amount of reduced iron availability, and pre-burial taphonomy of the tubes, rather than the sedimentology. The commonality of pyrite grains in the sediment is interpreted as evidence for abundant iron, so it is not likely that iron played any limiting factor. The abundant pyrite framboids also indicate that there was likely also abundant sulfate, as the preservation process did not appear to be readily extinguished. The poor preservation of ABPF tubes may also be a remnant of early, pre-pyritization breakdown of the organic tube occurring at the sediment surface in a relatively shallow marine environment. No evidence for obrution deposits are observed at ABPF, a process that is likely to have been critical to rapidly place fossils into the anoxic zone, allowing for the breakdown of organic tissues (Cai et al., 2007). In the event that some degradation had taken place before the onset of pyritization, the tubes are more likely to be lacking in morphological characteristics, as well as only rarely producing articulated, fully replicated three-dimensional specimens. Further, the degraded tissues expand the available surface area for pyrite growth, leading to abundant pyrite framboids, as seen in SEM (Fig. 2.10C and F).

2.5.3. Sedimentological and environmental controls over taphonomy of tube-shaped fossils

The variation in taphonomy of the ABPF tubular fossils is consistent with a taphonomic model for a continuous preservational gradient among kerogenization, pyritization and aluminosilicification (Schiffbauer et al., 2014). The model proposes that the resulting taphonomy of soft-bodied, organic-walled organisms in the Ediacaran is based on the sedimentation rate, the size of the bacterial-sulfate reduction zone in which the organism passes through, and the availability of sulfate, iron, and organic matter. In this model, the final preserved fossil is either fully replicated in pyrite, incompletely pyritized with a calcite infill, a two-dimensional carbonaceous compression (kerogenization), replicated by clay minerals, or fall in between the pyritization, kerogenization, and aluminosilicification preservation modes (Schiffbauer et al., 2014).

In conditions with rapid post-burial sedimentation and a limited bacterial sulfate reduction zone, non-biomineralized organic-walled fossils are preserved through kerogenization, or carbonaceous compression. Only one specimen from the ABPF tubes is preserved in complete kerogenization, without a visible presence of pyrite or aluminosilicate coating. Although the tube cannot be definitively classified, it is out of the expected size range of the cloudinomorph organisms and may be algal in origin. During kerogenization, fossil preservation occurs dominantly in the methanogenesis zone of the sediment, spending a short time in the bacterial sulfate reduction zone, resulting in minimal pyrite growth, if any. Individual fossils preserved in both partial pyritization and partial kerogenization are also found within the Gaojiashan Wormworld fauna, occurring when rapid sedimentation shifts the bacterial sulfate reduction zone towards the surface and into the methanogenesis zone during the preservation process, and away from the buried organism (Schiffbauer et al., 2014).

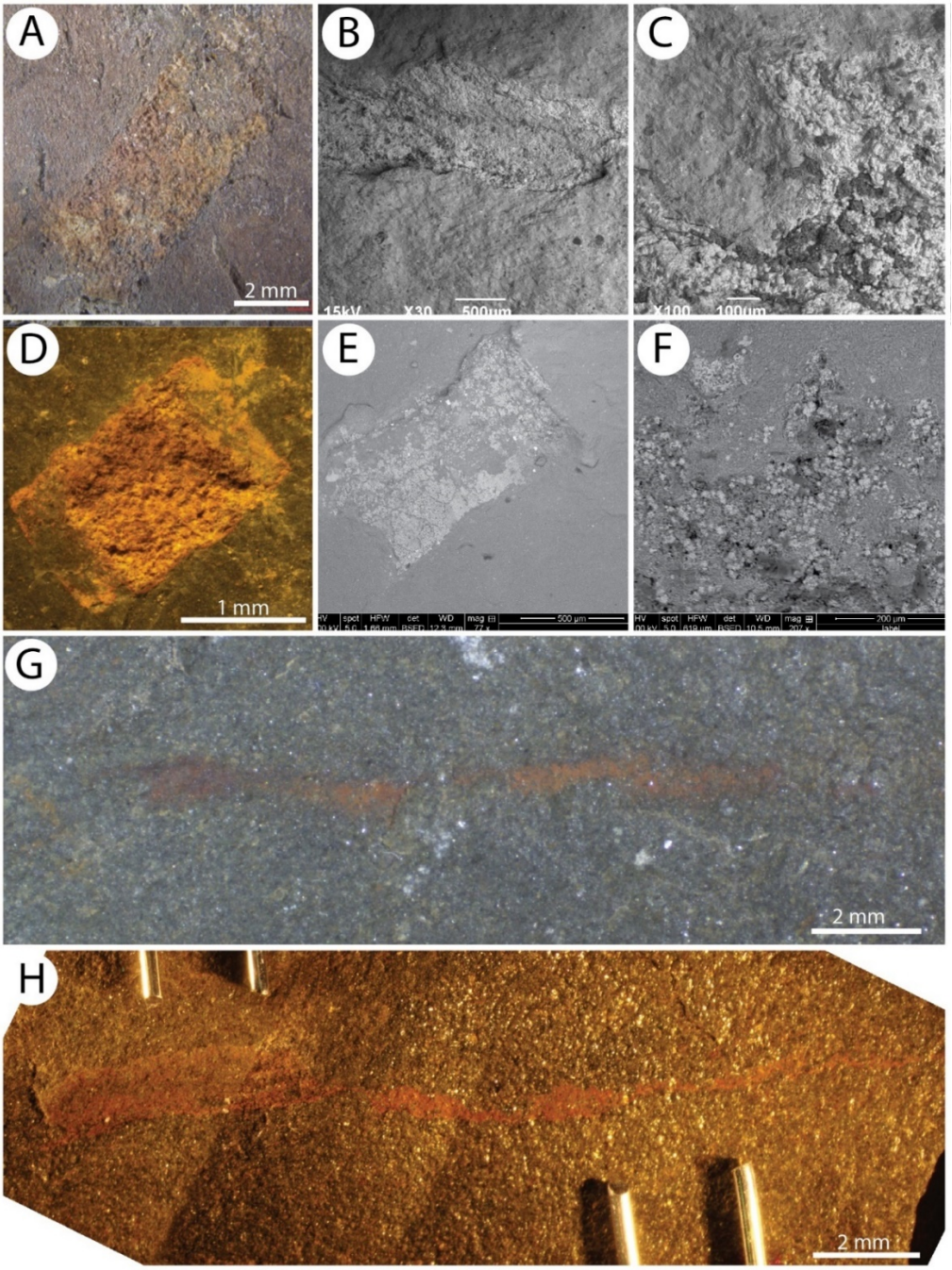

Figure 2.10. Comparisons of Deep Spring pyritized tube-shaped fossils from Ancient Bristlecone Pine Forest, CA and Mt. Dunfee, NV. A) Section of an ABPF pyritized tube; B) SEM image of a portion of an ABPF tube; C) SEM image of pyrite framboids and clusters along the termination of an ABPF tube; D) Section of a Mt. Dunfee pyritized tube; E) SEM image of a portion of a Mt. Dunfee tube; F) SEM image of pyrite framboids and clusters along the termination of a Mt. Dunfee tube; G) reddish "stain" from ABPF; H) reddish "stain" from Mt. Dunfee.

During the process of kerogenization, authigenic clay minerals may precipitate on the fossil surface, creating an aluminosilicate coating. A number of ABPF tubes interpreted as macroalgae show evidence of heavy aluminosilicate presence, eliminating any previously present morphological characteristics. Although present in exceptional fossil assemblages like the Gaojiashan Lagerstätte and the Burgess Shale, the driving force behind aluminosilicification is poorly constrained.

2.6. Conclusion

The paucity of biomineralization during much of the Ediacaran affects estimates for taxa outside rare preservational windows that produce Lagerstätten. This observation is not limited to the Ediacaran, however the metazoan lifemodes that appeared during the Cambrian diversification event frequently have modern analogues that facilitate paleoecological reconstructions. For example, fossilized hard parts, like jaws and claws, can be used to infer a food source based on modern morphologies even when that source is not readily preserved.

ABPF tube-shaped fossils provide examples of the pathway's preservational factors that resulted in poor quality fossils. The lack of evidence for rapid sedimentation events illustrate the results of a delay in the onset of pyritization, with compromised surfaces for pyrite nucleation before any sort of stabilization or replication in the majority of the ABPF fossils. There does, however, appear to be some sort of stabilization in the encased stacked funnel tubes, warranting further investigation. Pyrite overgrowth and the presence of framboids and clusters suggests high iron and sulfate availability, which prevented the termination of the pyritization process, destroying the fossils. These combined factors appear to have resulted in the tubes "self-destructing" in essence. The 'wormworld' tubicolous organisms (Fig. 2.11) have a taphonomic advantage over their Ediacara biota predecessors as the preserved tubes have higher stability than

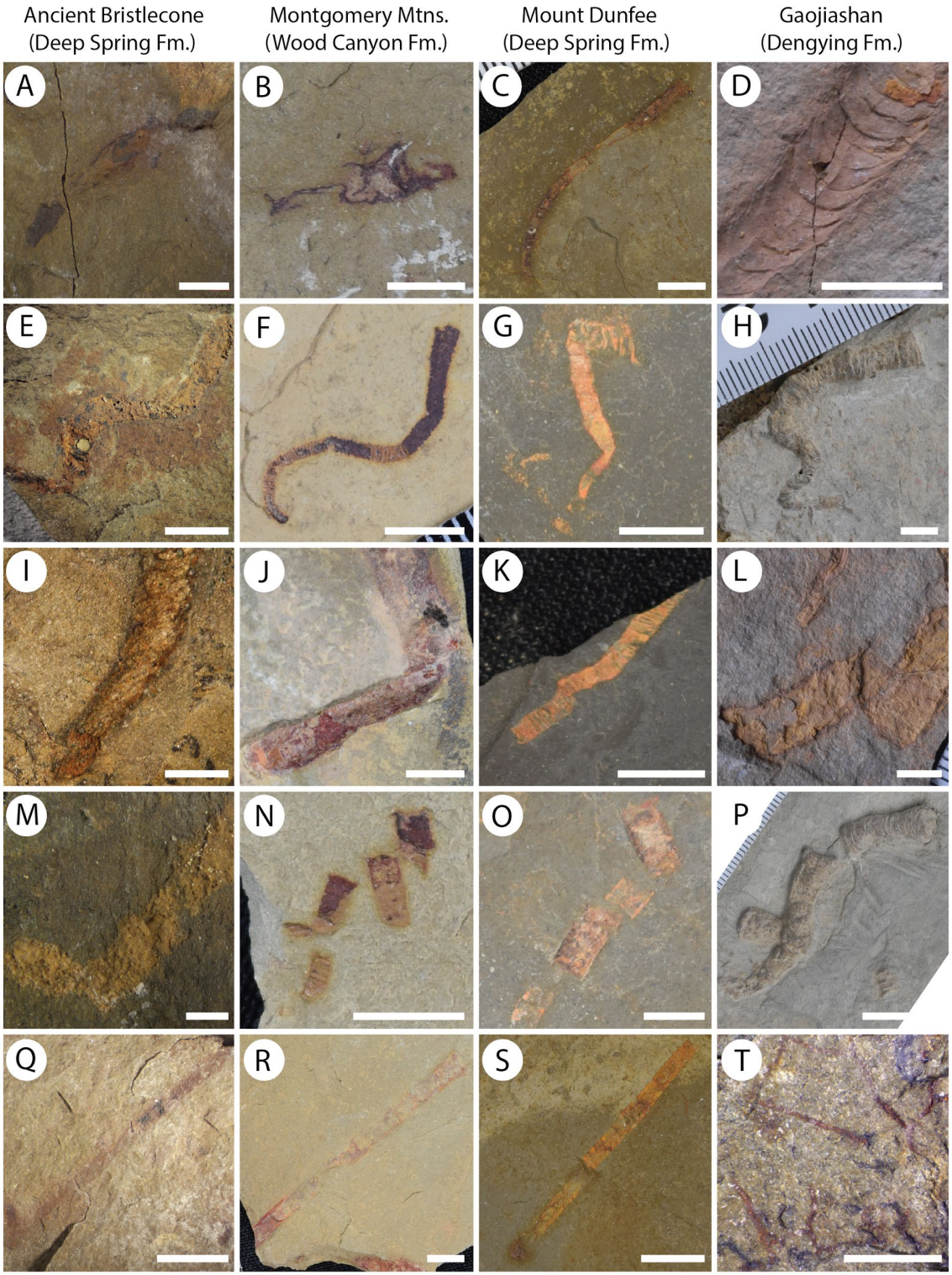

Figure 2.11. Examples of tube-shaped fossils from Ancient Bristlecone Pine Forest (Deep Spring Fm.), Montgomery Mountains (Wood Canyon Fm.), Mt. Dunfee (Deep Spring Fm.), and the Gaojiashan Lagerstätte (Dengying Fm.). A–D) Tubes with stacked funnels; E–H) Tubes with evidence of reorientation; I–L) Folded tubes; M–P) Disarticulated tubes; Q–S) Straight, smooth-walled tubes; T) Filamentous algae fossils from ABPF.

the “sand-filled organic sacs” (Hall et al., 2020). The taphonomic variants of the Wormworld fossils at ABPF and elsewhere illustrate the intricacies of the pyritization-kerogenization-aluminosilicification taphonomic pathway.

The Wormworld fauna became increasingly biomineralized leading up to the Ediacaran–Cambrian boundary, with the tubicolous *Costatubus bibendi* from Mt. Dunfee and Montgomery Mountains being lightly biomineralized preceding the global proliferation of what is considered to be one of the first macro-biomineralizers, *Cloudina* (Selly et al., 2020; Schiffbauer et al., 2020). The subtle transition from soft-bodied tubes to fully biomineralized tubes is constrained within the cloudinomorph morphoclade and has been largely accepted as occurring in the same or related lineages (Cai et al., 2011). The global extent and apparently sudden appearance of *Cloudina* indicates that the true geographic extent of the soft- bodied tubicolous organisms was much wider than what is known from the fossil record. Investigating the poor-preservation assemblages, like the Deep Spring fossils from Ancient Bristlecone Pine Forest, can help bridge the gap between the number of known soft-bodied tube and *Cloudina* sites. Thorough investigations into taphonomic varieties of oft-overlooked fossils can guide taxonomic identifications and reveal taphonomic conditions that can aid in the identification of a wider diversity of fossil localities.

2.7. References

Alpert S. P. 1973. *Bergaueria prantl* (Cambrian and Ordovician), a probable actinian trace fossil.” Journal of Paleontology 47(5):919–924.

Alpert, S. P. 1975. “*Planolites* and *Skolithos* from the upper Precambrian-lower Cambrian, White-Inyo Mountains, California.” Journal of Paleontology 49(3):508-521.

Cai, Y. and H. Hua. 2007. “Pyritization in the Gaojiashan Biota.” Chinese Science Bulletin 52:645-650. Doi: 10.1007/s11434-007-0080-9.

Cai, Y., Schiffbauer, J. D., Hua, H., and Xiao, S. 2012. “Preservational modes in the Ediacaran Gaojiashan Lagerstätte: Pyritization, aluminosilicification, and carbonaceous compression.” Palaeogeography, Palaeoclimatology, Palaeoecology 326-328:109–117. doi:10.1016/j.palaeo.2012.02.009

Dornbos, S. Q., and D. J. Bottjer. 2001. “Taphonomy and Environmental Distribution of Helicoplacoid Echinoderms.” PALAIOS 16(3):197–204. doi:10.1669/0883-1351(2001)016<0197:taedoh>2.0.co;2

Durham. J. W. 1993. “Observations on the Early Cambrian Helicoplacoid Echinoderms.” Journal of Paleontology 67(4):590-604. Doi:10.1017/S0022336000024938

Firby, J. B. and J. W. Durham. 1974. “Molluscan radula from earliest Cambrian.” Journal of Paleontology 48(6).

Hall, J. G., Smith, E. F., Tamura, N., Fakra, S. C., and T. Bosak. 2020. “Preservation of erniettomorph fossils in clay-rich siliciclastic deposits from the Ediacaran Wood Canyon Formation, Nevada.” Interface Focus 10:20200012. doi:10.1098/rsfs.2020.0012

Hua, H., Chen, Z., Yuan, X., Zhang, L., and S. Xiao. 2005. “Skeletogenesis and asexual reproduction in the earliest biomineralizing animal *Cloudina*.” Geology 33(4):277–280. Doi: 10.1130/G21198.1

McKee, E. H., and Gangloff, R. A. 1969. Stratigraphic distribution of archaeocyathids in the Silver Peak Range and the White and Inyo Mountains, western Nevada and eastern California.” Journal of Paleontology 43(3):716-726.

Mount, J. F., and Signor, P. W. 1991. “The Proterozoic-Cambrian transition of the White-Inyo Range, eastern California: Dawn of the Metazoa.” in Hall, C. A., Doyle-Jones, V., and

Widawski, B., eds., “Natural History of Eastern California High-Altitude Research”, White Mountain Research Station Symposium 3:455-488.

Schiffbauer, J., Xiao, S., Cai, Y., Wallace, A. F., Hua, H., Hunter, J. Xu, H. Peng, Y., and Kaufman, A. J. 2014. “A unifying model for Neoproterozoic–Palaeozoic exceptional fossil preservation through pyritization and carbonaceous compression.” Nature Communications 5(5754). Doi:10.1038/ncomms6754

Schiffbauer, J. D., Huntley, J. W., O'Neil, G. R., Darroch, S. A. F., Laflamme, M., and Y. Cai. 2016. “The latest Ediacaran Wormworld fauna: setting the ecological stage for the Cambrian Explosion.” GSA Today 26:4–11. Doi:10.1130/GSATG265A.1

Schiffbauer, J. D., Selly, T., Jacquet, S. M., Merz, R. A., Nelson, L. L., Strange, M. A., Cai, Y., and E. F. Smith. 2020. “Discovery of bilaterian-type through-guts in cloudinomorphs from the terminal Ediacaran Period.” Nature Communications 11(205). Doi:10.1038/s41467-019-13882-z

Selly, T., Schiffbauer, J. D., Jacquet, S. M., Smith, E. F., Nelson, L. L., Andreasen, B. D., Huntley, J. W., Strange, M. A., O’Neil, G. R., Thater, C. A., Bykova, N., Steiner, M., Yang, B., and Y. Cai. 2020. “A new cloudinid fossil assemblage from the terminal Ediacaran of Nevada, USA.” Journal of Systematic Palaeontology 18(4):357-379. doi: 10.1080/14772019.2019.1623333

Smith, E. F., Nelson, L. L., Tweedt, S. M., Zeng, H., and Workman, J. B. 2017. “A cosmopolitan late Ediacaran biotic assemblage: new fossils from Nevada and Namibia support a global biostratigraphic link.” Proceedings of the Royal Society B: Biological Sciences 284(1858):20170934. doi:10.1098/rspb.2017.0934

Xiao, S., Yuan, X., Steiner, M., and A. H., Knoll. 2002. “Macroscopic carbonaceous compressions in a terminal Proterozoic shale: a systematic reassessment of the Miaohe biota, South China.” Journal of Paleontology 76(2):347–376. doi:10.1666/0022-3360(2002)076<0347:mcciat>2.0.co;2

Ye, Q., Tong, J., An, Z., Hu, J., Tian, L., Guan, K., and S. Xiao. 2017. “A systematic description of new macrofossil material from the upper Ediacaran Miaohe Member in South China.” Journal of Systematic Palaeontology doi:10.1080/14772019.2017.1404499

CHAPTER 3: FLUCTUATIONS IN BIOTURBATION INTENSITY FROM THE EDIACARAN–CAMBRIAN BOUNDARY SECTION AT CHICAGO PASS, CA[1]

3.1. Introduction

In addition to the tubular body fossils, the Ediacaran Wormworld is represented in the trace fossil record, with simple horizonal burrows and grazing traces likely formed by worm-shaped bilaterians. The prevalence and diversity of burrowing behaviors steadily increased through the Ediacaran into the Phanerozoic (Bottjer, 2010; Buatois et al. 2018), resulting in fundamental changes in the nature of the seafloor that Seilacher and Pflüger (1994) termed the agronomic revolution. During the late Ediacaran and early Cambrian, bioturbation was generally limited to the shallow-marine realm (Gougeon et al. 2018). Late Ediacaran burrows were, for the most part, morphologically simple and were largely lacking in indicators of complex systematic mining behaviors prior to the appearance of *Treptichnus pedum* at the Ediacaran–Cambrian boundary (Herringshaw et al. 2017).

Although the disruptive impact of Ediacaran bioturbation on the seafloor sediment was low in comparison with later Cambrian and early Ordovician ecosystem engineering (Tarhan et al. 2015; Herringshaw et al. 2017; Tarhan, 2018), late Ediacaran shallow marine deposits often contain abundant mat-feeding traces (both supra-mat and intra-mat), a novel and potentially disruptive behavior at the water-mat interface (Herringshaw et al. 2017). Ichnofossil assemblages resulting from the earliest trace-making communities provide insight into the ecological impact of burrowing behaviors and the prevalence of these behaviors just prior to the Cambrian

---

[1] The material in this chapter was co-authored by Gretchen O'Neil, Lydia Tackett, and Michael Meyer. Gretchen O'Neil had primary responsibility for collecting samples in the field and identification of fossils and sediments from the collected material. Gretchen O'Neil was the primary developer of the conclusions that are advanced here. Gretchen O'Neil also drafted and revised all versions of this chapter. Lydia Tackett and Michael Meyer served as proofreaders and provided feedback on the analyses conducted by Gretchen O'Neil.

diversification event, commonly known by the more embellished term, the Cambrian Explosion (Mángano and Buatois, 2014). The Ediacaran provided excellent conditions for the preservation of individual traces due to the unique taphonomic window provided by both the ubiquitous matgrounds and few motile benthic organisms (Callow and Brasier, 2009; Laflamme et al. 2011). For example, Ediacaran–Cambrian trace fossils from the Nama Group in Namibia show a dramatic increase in trace diversity and burrowing intensity paired with a significant loss of Ediacara biota diversity during the very latest Ediacaran (Darroch et al. 2015; Darroch et al. 2018, Cribb et al. 2019). In the Death Valley region, sedimentary deposits also record the Ediacaran–Cambrian transition (Smith et al. 2017; Tarhan et al. 2020), but the ecological impact of increasing bioturbation created by shallow infaunal and surficial trace-making behaviors through this interval is poorly constrained.

Trace fossil distributions are commonly facies controlled, and a significant change in burrowing behavior across the Ediacaran–Cambrian boundary requires facies-specific characterization. Here, trace fossil occurrences and associated behaviors are documented along a vertical stratigraphic succession and between different marine facies of the lower Wood Canyon Formation at Chicago Pass, Death Valley region, California. Analyses of the trace fossils from Chicago Pass reflect the increasing bioturbation intensity seen in the Namibian boundary sections, indicating that biotically-driven ecosystem restructuring in the latest Ediacaran is not a localized event, but rather, a wide-spread, potentially global signal (Cribb et al. 2019).

3.2. Geologic Setting

The Wood Canyon Formation crops out at various localities of Inyo County in California and Nye and Clark Counties in Nevada (Fig. 3.1A). It is comprised of three members, the lower, middle, and upper, with the Ediacaran–Cambrian boundary biostratigraphically defined in the

lower member (Corsetti and Hagadorn, 2000; Sappenfield et al. 2012; Smith et al. 2017). The lower member of the Wood Canyon Formation sits stratigraphically above the Ediacaran Stirling Quartzite, a pink-grey coarse-grained quartzite unit, and below the middle member, a highly resistant conglomeratic and arkosic unit (Muhlbauer, 2020). The section of focus, Chicago Pass (Fig. 3.1B and C), in easternmost California across the Nevada-California border from Pahrump, NV preserves an offshore-to-shallow marine facies, shallower than corresponding sections to the west (Corsetti and Hagadorn, 2000). The section contains abundant trace fossils up to and across the Ediacaran–Cambrian boundary and analyses are limited to this unit.

3.3. Materials and Methods

Trace fossils were identified and divided into categories based on the behaviors that produced the trace. Classifications included simple feeding, grazing, and complex feeding burrows (based on ethological classifications from Seilacher [1964] and the most recent descriptions of the traces [Buatois and Mángano, 2016; Gougeon et al. 2018]). The parent sedimentary rock was classified by facies and relative age based on stratigraphic position. Depositional environments were characterized based on sedimentology and field observations in order to identify facies specific fossil occurrences and environmental preferences of trace makers. Most sedimentary units tended to be fissile and substantial exposed bedding planes were rare, but *in situ* slabs were collected from sedimentary units that contained trace fossils where possible. The surfaces of the extracted slabs were highly irregular in shape. Uncollectable fossiliferous bedding planes were photographed in the field, regardless of facies, and constituent trace fossils were identified.

The surface area analyzed for trace fossil coverage varied based on the amount of available material and only trace fossil bearing samples were included in the study. Fiji image processing freeware was used to measure the total surface area of each imaged slab, as well as the approximate

surface area coverage of the contained burrows (Schindelin et al. 2012; Meyer et al. 2014; Buatois et al. 2018; Miguez-Salas et al. 2019), with a minimum of 1,200 mm^2 and a maximum of 21,600 mm^2 (surface area analyzed). Approximate bioturbated surface area relative to total surface area

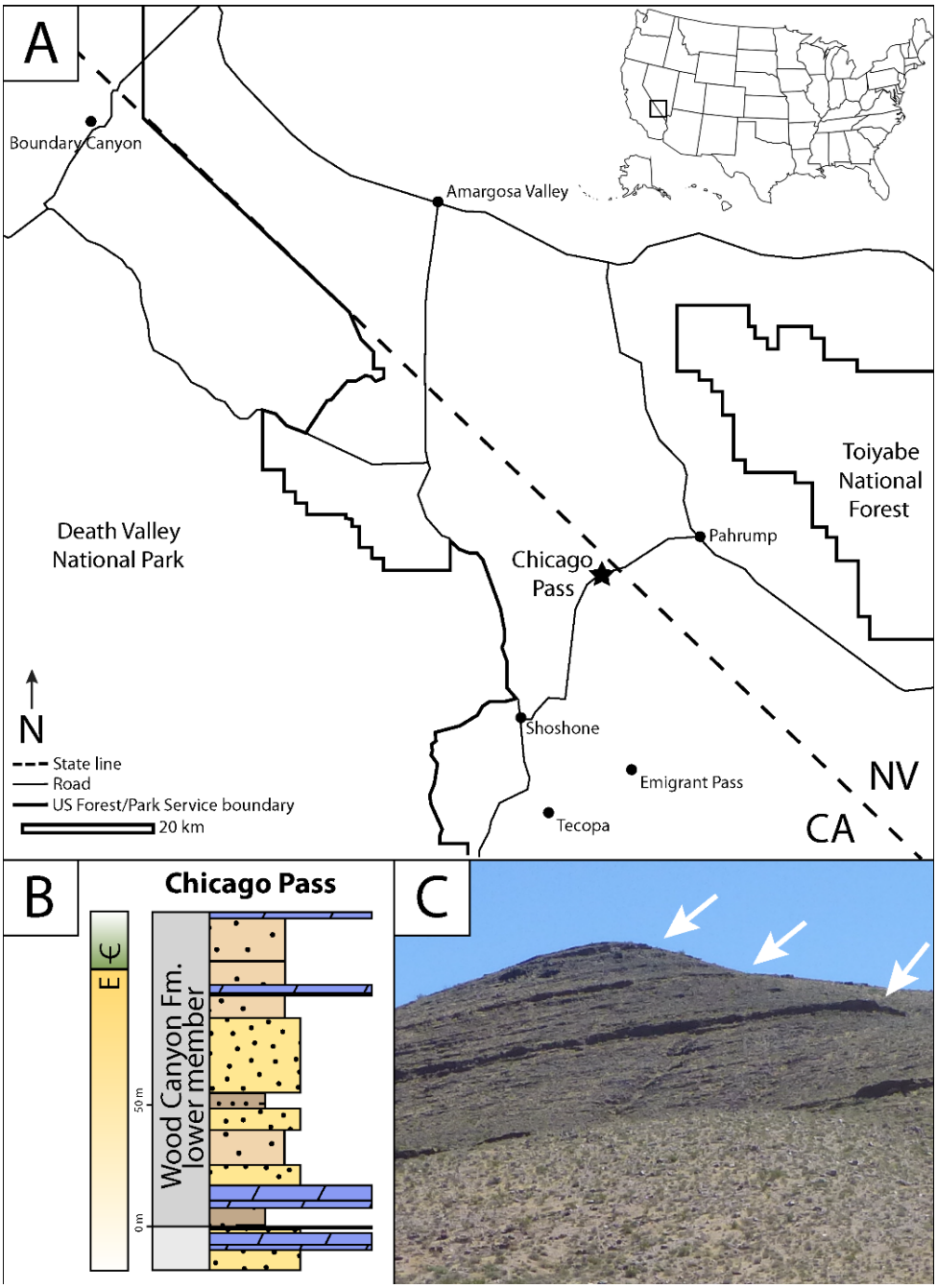

Figure 3.1. Chicago Pass, Inyo County, CA. (A) Map of Chicago Pass locality along the Nevada–California boundary; (B) Generalized stratigraphic column of the Chicago Pass section of the Wood Canyon Formation; (C) Outcrop from the road. White arrows indicate massive dolomite units capping the three parasequences.

of each slab was used to generate percent coverage by trace fossils per unit area for quantitative comparisons of bioturbation intensity between horizons (Meyer et al. 2014; Buatois et al. 2018). Comparable facies were identified in order to document both temporal and environmental trends in the ichnofossil assemblage across the Ediacaran–Cambrian boundary. Environmental engineering intensity (EEI) values were based on Herringshaw et al. (2017) and a value range was calculated for the newly described trace, *Lamonte trevallis* using the same parameters (O'Neil et al. 2020).

Samples containing *L. trevallis* were also analyzed via scanning electron microscopy (FEI Quanta 600F) with secondary (SE) and backscattered (BSE) electron imaging. Their elemental composition was determined using a Bruker AXS QUANTAX 400. SE imagery records only topographical surface information, whereas BSE is sensitive to the differences that arise due to the varying atomic numbers and densities of the constituent materials, also known as Z-contrast (Meyer et al. 2012).

3.4. Results

3.4.1. Chicago Pass stratigraphy

The lower member of the Wood Canyon Formation is dominated by shallow marine facies, transitioning into the braided-plain facies of the middle member (Hagadorn and Waggoner, 2000; Kennedy and Droser, 2011; Muhlbauer et al. 2020). The lower member was deposited during a highstand systems tract, characterized by three shallowing-upwards parasequences (Corsetti and Hagadorn, 2000; Smith et al. 2017), that overlie a carbonate unit capping the pink quartzite of the Sterling Quartzite. The section contains the three distinct, massively-bedded, laterally-extensive carbonate units, which cap the parasequences (Fig. 3.1C) (Corsetti and Hagadorn, 2000; Hogan et al. 2011; Smith et al. 2017).

The base of the first parasequence at Chicago Pass is placed just above a carbonate unit capping the pink quartzite of the Stirling Quartzite. Above the carbonate of the Stirling Quartzite, the first parasequence is approximately 17 meters thick dominated by friable green and red slope-forming fine-grained siltstones and an approximately 5-meter thick carbonate unit cap marker bed.

The second parasequence is approximately 75 meters thick. The lower half of the parasequence is largely masked by sedimentary cover, with occasional sandstone beds and siltstones with ripple bedforms. Thick (~10 m) packages of sandstones begin at ~36.5 m above the Stirling–Wood Canyon contact before transitioning into interbedded green and red siltstones and sandstones at ~75 m above contact. The top of the parasequence is capped by the second major carbonate unit of the member at ~92 m.

The third parasequence is approximately 32 m thick and is largely comprised of interbedded siltstone and rippled sandstone (1 cm to 1 m-thick beds) appearing green, red, pink, tan, and grey in section. Sedimentary structures are common at the top of sandstone beds above the *T. pedum* zone (Ediacaran–Cambrian boundary). The parasequence is capped by the third major carbonate unit of the member occupying the range of ~123–152 m above the Stirling Quartzite–Wood Canyon contact. The carbonate bed contains ripples, rip-up clasts, and mud clasts.

Temporal shifts in grain sizes are apparent through the vertical section, from very fine-grained silts present only in the first parasequence, to coarser siltstones in the lower portion of the second parasequence, and eventually to interbedded siltstones and sandstones in the upper portion of the second and sporadically within the third parasequence. The green and red siltstones and sandstones are common in the second and third parasequences and contain the majority of the trace fossils from this section, including the boundary marking fossil, *Treptichnus pedum* (Smith et al. 2017), and other shallow burrowing traces.

3.4.2. Facies descriptions

The lower member of the Wood Canyon Formation is primarily comprised of six facies, which may be discerned in the field (Fig. 3.2) and through petrographic features (Fig. 3.3). Facies A (Fig, 3.2A and 3.3A) is comprised of thinly laminated quartz-dominated siltstones devoid of trace fossils and lacking structural indicators of sediment reworking. Facies A presents variably as tan, pink, red or micaceous green sediments in hand sample, based on the amount of muscovite and iron oxide cementation. Quartz-dominated deposits with some iron oxide cements that lack muscovite appear tan to pink in color. Samples with high amounts of muscovite appear light blueish-green in hand sample, while high amounts of iron oxides present more red. The sediments were likely deposited in a low energy, deep environment, in the offshore-lower shoreface transition zone.

Facies B (Fig. 3.2B and 3.3B) exhibits normal grading in thin section and high variability in grain size from very fine silt to medium sand. The thickness of beds characterized as facies B varies throughout the section formed as a result of turbidites developing from storm deposition deeper in the ramp setting, below wave-base in the lower shoreface. Identifiable trace fossils are absent in facies B.

Facies C (Fig. 3.2C and 3.3C) is dominated by quartz siltstones to silty sandstones with sub-angular to sub-rounded grains and moderate sorting, which characterize the majority of the "red and green beds" that dominate the section. Colors of the units vary based on micaceous mineral and iron oxide content, similar to facies A. Bedding thickness is highly variable, with sporadic beds of less than 10 cm and large packages with thicknesses of up to 7 m. Fine cross-lamination is common in thin section and can also be observed occasionally in the unit itself.

Ripples are observed on bedding planes. Trace fossils are common. Facies C is likely to represent the middle shoreface, a medium energy environment.

Facies D (Fig. 3.2D and 3.3D) is comprised of coarse siltstones-to-sandstones, the latter of which exhibit cross-bedding. Grains are well-rounded and well-sorted. Beds are typically less than 0.5 m in thickness, averaging around 0.3 m. Trace fossils are present. The source of the sediments was most likely a high-energy environment, interpreted here as the upper shoreface.

Facies E (Fig. 3.2E and 3.3E) is comprised of highly resistant, microcrystalline dolostone. These large carbonate ledges first occur within the Wood Canyon at the top of the first parasequence, but are also found just below the alternating with the mudstones of facies A. The lower carbonate beds are believed to be part of the Stirling Quartzite and may indicate an unconformable surface at the base of the Wood Canyon. Facies E also makes up the massive, laterally extensive units that cap the second and third parasequences. The carbonate of these units was deposited in a shallow, lagoonal environment and does not preserve trace fossils.

Facies F (Fig. 3.2F and 3.3F) consists of dolomitized carbonate dominated by intraclasts. Intraclasts vary in size and include grapestones up to 3 mm in diameter. This facies occurs twice within our sampled section, in the dolomite unit just below the Stirling–Wood Canyon contact and above the thick micritic dolostone at the top of the first parasequence. The close proximity to the parasequence-capping dolomite beds of facies E of the Wood Canyon indicates that facies F may have been sourced from an unpreserved shoal. However, the occurrence of facies F below the contact does not support this interpretation, making the paleoenvironmental interpretation of facies F debatable. Facies F does not contain trace fossils.

3.4.3. Facies summary

The facies present within the lower member of the Wood Canyon Formation are indicative of a mixed siliciclastic-carbonate system, with shallow carbonate formation sourced from a lagoonal paleoenvironment with the possible presence of a seaward barrier island. Non-carbonate deposits are dominated by silts and fine sands, exhibiting sedimentary structures common to shallow marine shoreface deposits. The lower, middle, and upper shoreface facies transition abruptly into lagoonal deposits at the top of each parasequence. Facies A comprises the siliciclastic portion of the first parasequence and is present just below the carbonate unit that caps the parasequence. Facies B exhibits thin graded layers, resultant of deeper storm events. The storm

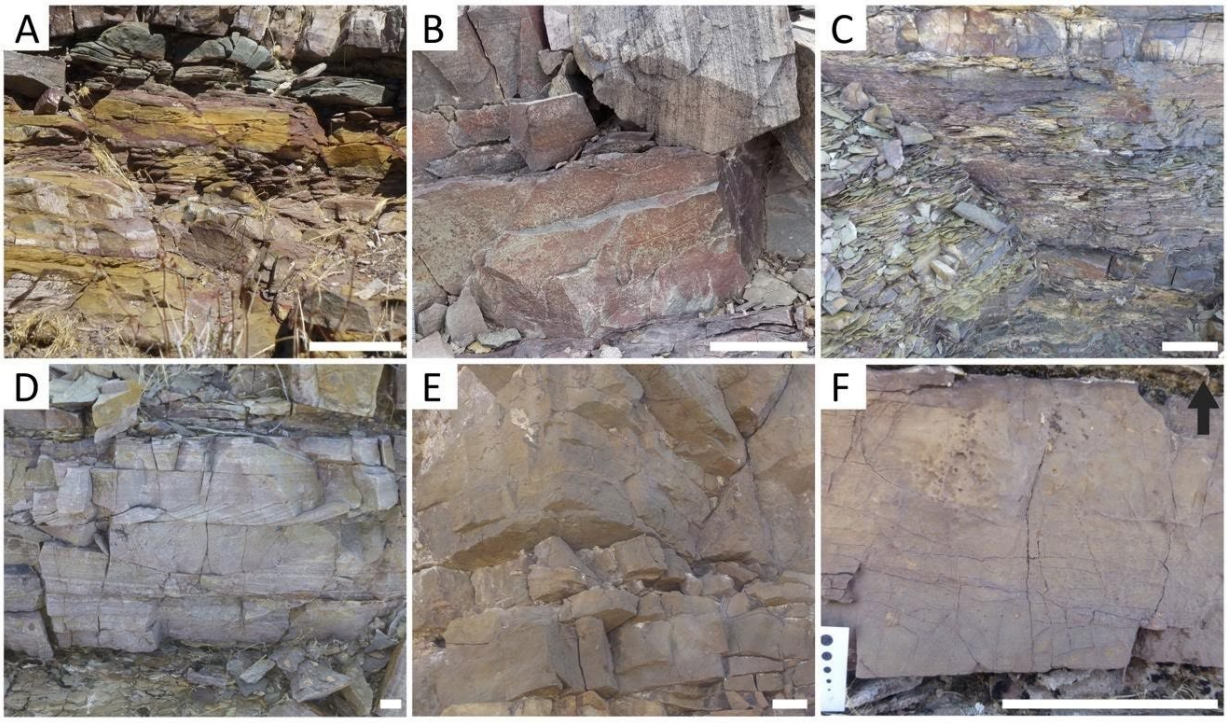

Figure 3.2. Facies A–F in outcrop exposures. (A) Fine siltstones of facies A; (B) Silt-to-fine sandstones of faces B; (C) Micaceous green and red siltstones from facies C; (D) Cross-bedded coarser siltstones and sandstones of facies D; (E) Massive carbonate capping a parasequence; (F) Carbonate material containing facies F.

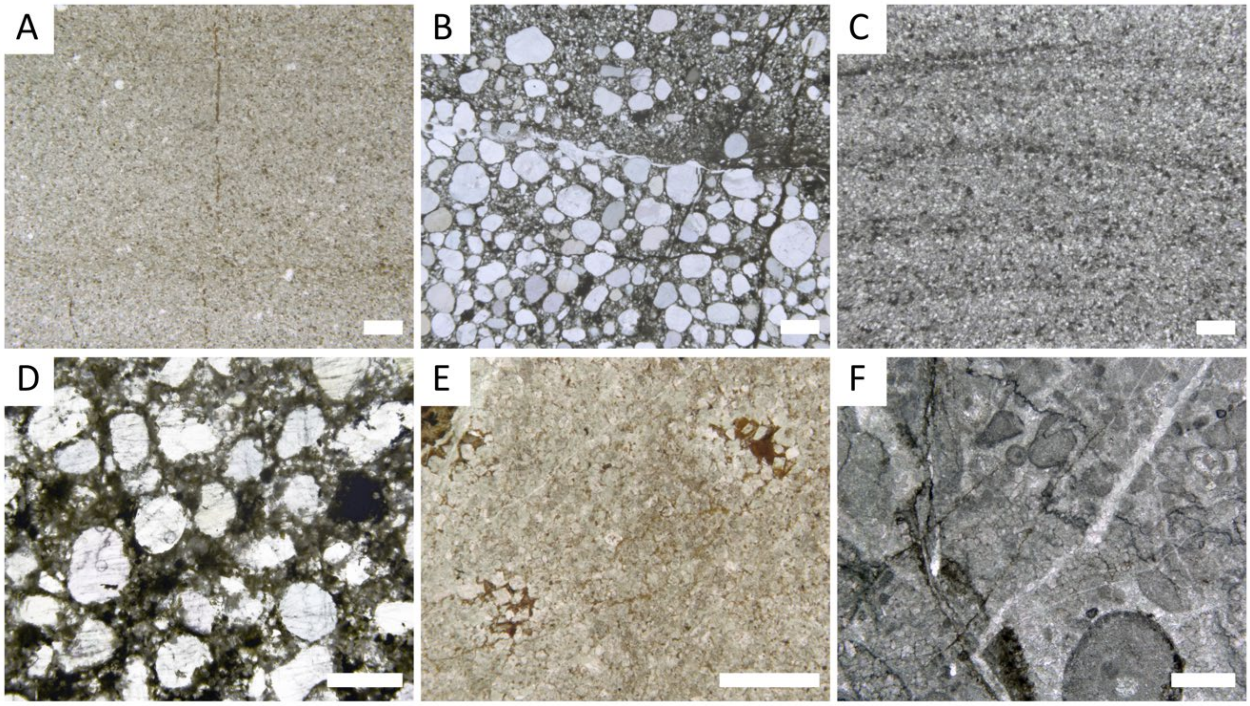

Figure 3.3. Thin-sections of facies A–F corresponding Figure 3.2A–F.

event deposits are preserved as turbidites, which range in thicknesses and were deposited in a deeper environment. Facies B occurs intermittently, reminiscent of the irregularity and varying depths of the turbidites. Facies C is present in the second and third parasequences and varies greatly in color based on the amount of iron oxide cement and the occasional presence of muscovite flakes. Packages of facies C siltstones and sandstones are common in the upper portion of the second parasequence and are sporadic throughout the third parasequence. Facies D is sourced from an upper shoreface environment. The higher energy environment resulted in large grain sizes, good sorting, and cross-bedding. Facies E is highly crystallized and likely formed in place, within the lagoonal environment.

The three parasequences of the lower member of the Wood Canyon Formation show a progressively shallowing marine system (Fig. 3.4A). The deepest facies, facies A, dominates the first parasequence. A transgressive event following the occurrence of facies E at the top of the parasequence begins the second parasequence with facies C. The second parasequence contains

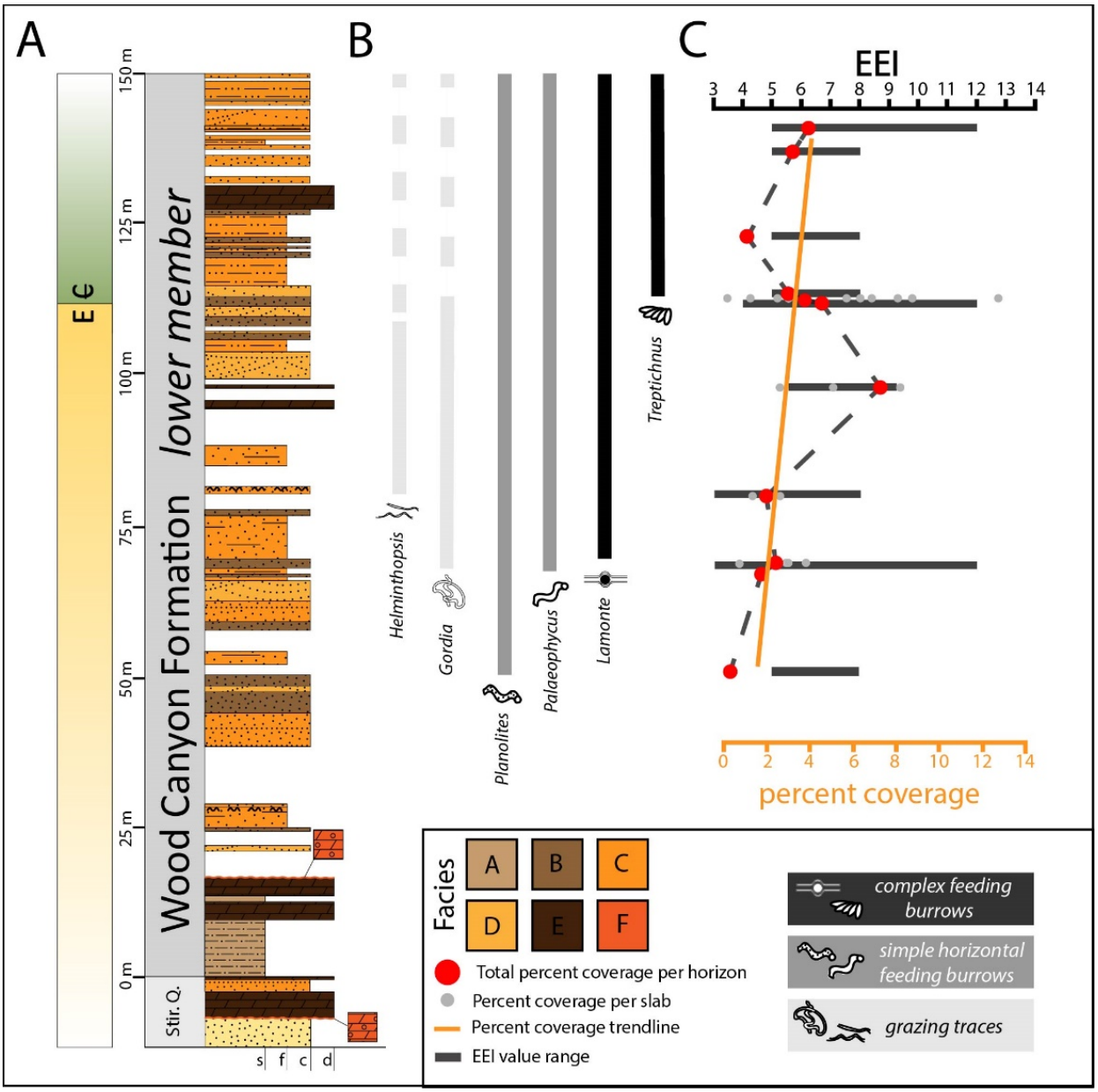

Figure 3.4. Trends and EEI values of trace fossils. (A) Stratigraphic column of the Chicago Pass section; (B) Ranges of trace fossil occurrences, dashed lines indicate the level at which some traces could not be found but are likely present. Light grey indicates grazing traces, dark grey indicates simple horizontal feeding burrows, and black indicates complex feeding burrows; (C) Calculated percent coverage values per horizon (red dot) and per slab within each horizon (grey dot). Black bars indicate the range of EEI values for each horizon based on Herringshaw et al. 2017.

larger grain size, sedimentary structures, and trace fossils, especially dominant in the upper portion, as the environment became shallower. Again, facies E is followed by a transgressive event, leading to the overlying facies D of the third parasequence. The third and final parasequence

is dominated by the shallower facies, with frequent cross-bedded sandstones and trace fossils throughout the section.

3.4.4. Trace fossil assemblages

The Ediacaran and Cambrian ichnofossil assemblages at Chicago Pass are dominated by surficial to shallow burrowing (Fig. 3.5) and grazing traces (Fig. 3.6A–C). No trace fossils were observed within the first parasequence, although *Planolites* has been reported by others in a quartzite unit at the base of the section (Hagadorn and Waggoner, 2000; Corsetti and Hagadorn, 2000; Sappenfield et al. 2012). The second and third parasequences contain abundant trace fossils, particularly in facies C, which tended to be restricted to the upper, shallower portion of the second parasequence and spread throughout the entirety of the third. The present ichnofossils ranged from low-impact surficial grazing to higher-impact more robust, complex microbial mat mining traces, based on calculated EEI values (Fig. 3.4B and C). Grazing traces and simple feeding burrows were associated with ripples and microbially induced sedimentary structures indicative of the presence of microbial mat-like organics (Fig. 3.6D). Imprints of holdfasts from Ediacaran organisms frequently occur throughout the section but have a low bioturbation impact and are taxonomically problematic (Fig. 3.6E–F).

The suite of ichnofossils in the third parasequence at Chicago Pass includes *Treptichnus pedum*, as well as an unidentified treptichnid and *T. bifurcus* (Fig. 3.7A–D, Buatois and Mángano, 1993). *T. pedum* was identified approximately 19 m above the second carbonate unit and 10 m below the base of the third unit. Three *T. pedum* specimens were collected *in situ* from one outcropping of red and green siltstones, allowing for confident placement of the Ediacaran–Cambrian boundary interval. An additional complex microbial mat mining trace, *Lamonte trevallis* occurred stratigraphically below and up into the Ediacaran–Cambrian boundary interval (Fig.

3.7E–G). Elemental composition analyses indicated the presence of abundant organic material associated with *L. trevallis* that was significantly different then surrounding sedimentary facies (Fig. 3.7H–J). The entire third parasequence was abundant in trace fossils, and specimens were collected from multiple bedding planes above and below the *T. pedum* horizon.

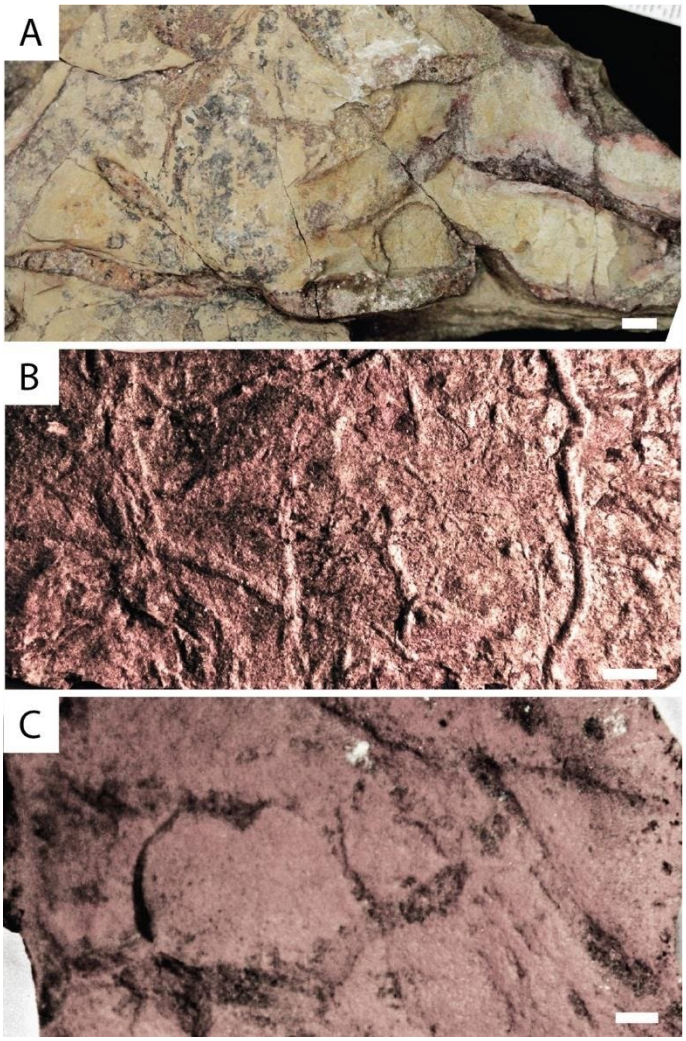

Figure 3.5. Simple horizontal burrows . (A–B) *Planolites*; (C) *Palaeophycus*. Scale = 5 mm

In addition to *T. pedum* and *L. trevallis*, the Ediacaran beds at Chicago Pass are awash with simple horizontal traces, including the shallow infaunal *Planolites* and *Palaeophycus* (Fig. 3.5A–B and C, respectively) and surficial grazing *Gordia marina* and *Helminthopsis* (Fig. 3.6A–C) feeding modes. These ichnotaxa represent distinct trace-making behaviors with differential impact

on sedimentary surface conditions, and the temporal and stratigraphic distribution of such behavioral characterizations are described below.

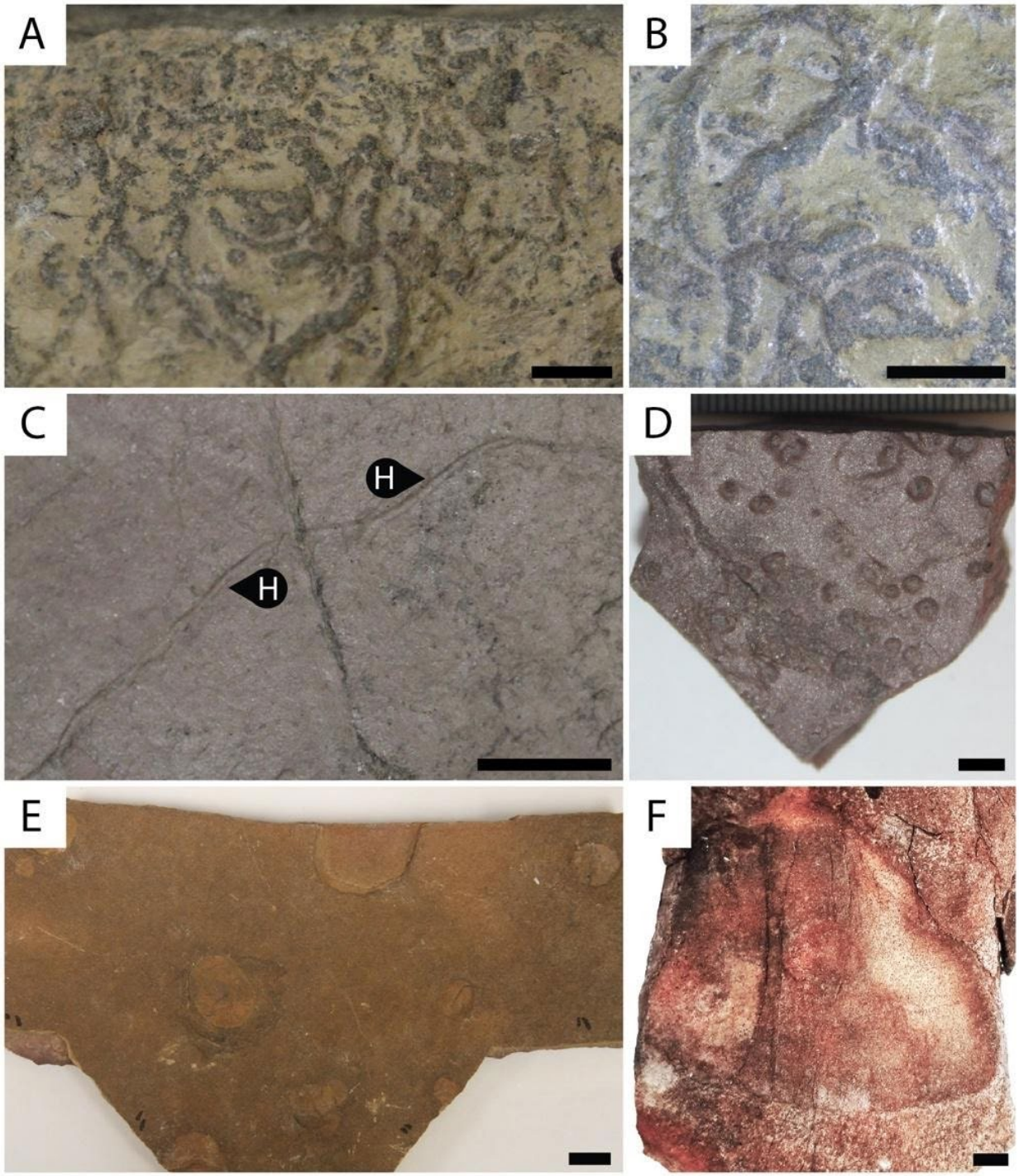

Figure 3.6. Grazing traces, microbially induced sedimentary structures, and holdfasts. (A) *Gordia marina*; (B) Winding trails of *Gordia marina* from **A**; (C) *Helminthopsis isp.*; (D) Microbially induced sedimentary structures, *Intrites*; (E–F) Ediacaran holdfasts. Scale = 1 cm.

3.4.4.1. Simple horizontal feeding burrows. Traces identified as simple horizontal feeding burrows represent opportunistic shallow mining behaviors, lacking evidence of complex or systematic targeted feeding (Fig. 3.7, Macnaughton and Narbonne, 1999; Liu and McIlroy, 2015). Two simple feeding burrows were identified at Chicago Pass. The most common, *Planolites*, occurs most frequently in facies C beginning approximately 42 m above the top of the first massive carbonate bed (Fig. 3.5A–B). *Planolites* is an unlined, straight-to-curved shallow infaunal burrow, which lacks external and internal structure, and commonly has an internal fill that is distinct from the host rock (Pemberton and Frey, 1982). The simple feeding trace, *Palaeophycus*, also occurs throughout the section (Fig. 3.5C). Chicago Pass *Palaeophycus* are similar in size to (and are commonly associated with) *Planolites*, rendering them to be surficially indistinguishable in densely burrowed horizons. The two ichnotaxa share many characteristics, however, *Palaeophycus*, is lined and consistently contains infill that is identical to the host rock (Fernández and Pazos, 2012). All but one specimen was collected from facies C. The first definitive occurrence of *Palaeophycus* is ~33 m above the first occurrence of *Planolites* (Fig. 3.4B).

3.4.4.2. Grazing traces. Traces classified as those representing grazing behaviors include shallow meandering-to-winding traces that lightly penetrate the surface of the substrate (Han and Pickerill, 1995). Two ichnotaxa at Chicago Pass were classified as simple grazing traces, *Gordia* and *Helminthopsis* (Fig. 3.6A–B and 5C, respectively). This is the first documented occurrence of *Helminthopsis* at Chicago Pass, but the similar looped trace, *Helminthoidichnites* has been described (Hagadorn and Waggoner, 2000; Corsetti and Hagadorn, 2000). Our specimens do not show indication of branching or looping but do show irregular meandering (Fig. 3.6C) known to be exhibited by *Helminthopsis* (Cribb et al. 2019). Specimens of *Gordia marina* were present at 65 m and in the boundary interval at ~112 m. *Gordia* is a small, tightly looping unlined

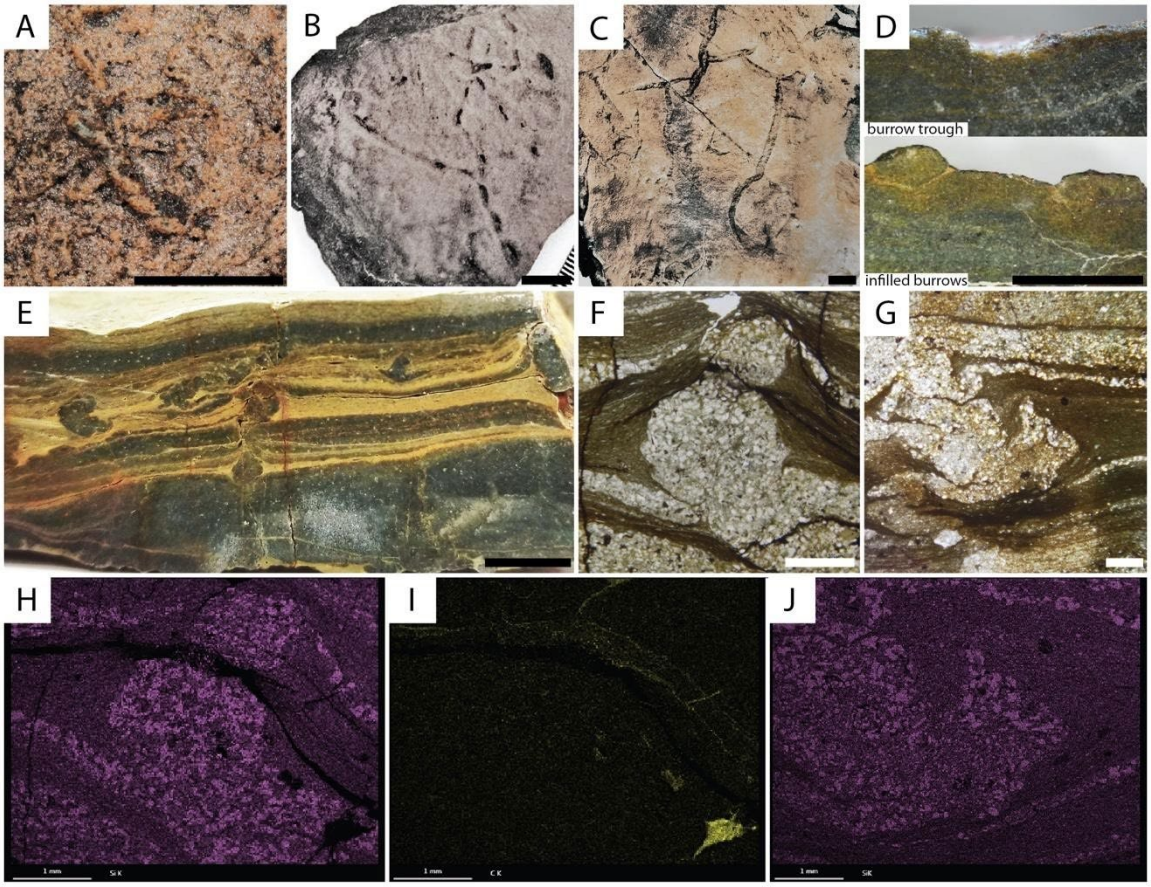

Figure 3.7. Complex trace fossils from Chicago Pass. (A) *Treptichnus pedum* (B) unidentified treptichnid (C) *Treptichnus bifurcus* (D) Cross-section view of **C** showing burrow troughs and infilled burrows (E) Cross-section of *Lamonte trevallis* containing specimen; (F) Thin-section of stacked *L. trevallis*; (G) *L. trevallis* showing subsequent sediment collapse; (H) EDS map of **F** showing relative Si concentrations; (I) EDS map of **F** showing relative C concentrations; (H) EDS map of **G** showing relative Si concentrations. Black scale = 1 cm, white scale = 1 mm.

burrow (Hammersburg et al. 2018). Widths of individual traces are typically only 1 mm at maximum. Specimens were only observed in the green and red siltstones, and were associated with both *Helminthopsis* and *Planolites*. Grazing traces are visible on the surface of the rock and have low impact on the sediments in comparison to the more robust feeding traces, *Planolites* and *Palaeophycus* (EEI values, Fig. 3.4C). Both *Helminthopsis* and *Gordia* were rare and never exceeded 1% of surface area coverage and were not incorporated into the final total surface area coverage.

3.4.4.3. Complex feeding burrows. Two complex feeding trace genera were observed at Chicago Pass. Three specimens of the Ediacaran–Cambrian boundary marker, *Treptichnus pedum* were collected *in situ* (Fig. 3.6A). Specimens are curved with probe-like projections that appear on the surface at low angles to each other (Singh et al. 2017). The first occurrence of *T. pedum* is approximately 19 m above the top of the second carbonate unit, in which two of the three specimens occur and is found in facies C. *T. pedum* appears just above a strikingly green, non-fossiliferous bed. The fourth *in situ* specimen was collected above the third massive carbonate unit at 141 m and was found on the same bed as the additional treptichnids (Fig, 3.7B–D). An additional trace, the undermat mining trace, *Lamonte trevallis* appears in the second parasequence at ~67 m and continues through the Ediacaran–Cambrian boundary (Fig. 3.7E–G). Specimens were identified in petrographic thin-sectioning and show targeted feeding on microbial mat microlaminae (Fig. 3.7E–J, Meyer et al. 2014). Unlike grazing traces, complex feeding traces are robust, much like *Planolites* and *Palaeophycus*, record important escalations in complexities, and mark the Ediacaran–Cambrian boundary. The occurrences of complex feeding traces were used to calculate fossils ranges and the placement of the Ediacaran–Cambrian boundary. The surface area coverage of individual burrows was included in the total surface area coverage.

3.5.4.4. Trace fossils and facies relationships. Trace fossil assemblages in comparable, recurring facies exhibited stratigraphic trends through the lower member of the Wood Canyon Formation (Fig. 3.4A–B). Trace fossils of facies A in the first parasequence have been observed in previous studies in low abundance. Traces were also absent-to-rare in facies B, E, and F, but present and prevalent in facies C and D, within the lower and upper shoreface, and first appear in the upper portion of the second parasequence within facies C, below the Ediacaran–Cambrian boundary. The distribution of trace fossils and facies within the lower member of the Wood

Canyon Formation indicate an increasing intensity and diversity of burrowing through time with some facies restriction to the lower and upper shoreface, confirmed through petrographic analyses of burrowed and unburrowed material.

3.4.4.5. Ichnofossil surface area coverage. The percent trace fossil coverage of simple horizontal feeding burrows increases temporally in facies C and D (Fig. 3.4C). Microbial mat mining complex feeding traces appeared prior to the Ediacaran–Cambrian boundary, marked by the complex feeding trace *T. pedum*, but were difficult to identify without thin-sectioning of burrowed material (Fig. 3.7E–J).

Simple horizontal feedings burrows include the two most common ichnotaxa at Chicago Pass, *Planolites* and *Palaeophycus*, and thus drive the majority of the resulting data. Surface area coverage by simple horizontal feeding burrows presents with relatively high values from ~57 m above the base of the section to –87 m, before declining through ~97 m (Fig. 3.4C). Immediately prior to the Ediacaran–Cambrian boundary, simple horizontal feeding burrow surface coverage increases again, and then reaches its highest coverage of surface area in sedimentary horizons immediately above the Ediacaran–Cambrian boundary (5.4–5.7%). Moving into the Cambrian sediments, simple horizontal feeding burrow surface area coverage returned to and maintained slightly lower (~4.4%), but still high values in trace containing facies C and D. No significant change in the widths of simple horizontal feeding burrows through time was observed (R^2 = 0.00374), suggesting that burrow diameters are not contributing to the changes observed during this interval.

3.5. Discussion

3.5.1. Trace fossil distributions and facies

The Chicago Pass section preserves an offshore-to-shallow marine facies, shallower than corresponding sections to the west (Corsetti and Hagadorn, 2000). Trace fossils are rare in facies A of the first parasequence, where deposition may have preceded intense trace-making activities within the Wood Canyon, or the preserved environment may have been too far offshore for most early trace makers. In facies B, high-energy reworking and transport of sediments limited the preservation of antecedent traces and the sediment may have settled at a depth where trace makers are sparse. The conditions of formation for facies E hindered the potential for fossil preservation and is, thus, absent in trace fossil observations. The most abundant traces were observed in facies C and D, respectively representing lower and upper shoreface deposition. Although present in the second parasequence, facies C and D are sparse in traces until ~67 m, towards the middle of the second parasequence. Among the other facies containing fewer or no traces, controlling factors are not as well constrained. Overall, our results show the beginning of established burrowing behaviors in the upper part of the second parasequence at Chicago Pass and document the emergence of simple horizontal feeding traces in the lower and upper shoreface as ecologically important components of shallow marine ecosystems.

3.5.2. Surface area coverage trends

Simple horizontal feeding burrows had the most impact on the structure of the sediment in comparison to the low-impact grazing and the rare complex feeding traces based on environmental engineering intensity (EEI Fig. 3.4C, Herringshaw et al., 2017) values and relative abundances of the traces. The trend in surface area coverage within simple horizontal feeding traces suggests that significant ecological processes were underway during the interval leading up to the Ediacaran–

Cambrian boundary. The near absence of traces in the stratigraphically lowest part of the lower member of the Wood Canyon Formation is comparable to what is known of the majority of middle-to-late Ediacaran trace assemblages, excepting a few remarkable outliers (Pecoits et al. 2012).

The appearance and continued occurrences of simple feeding traces in the second parasequence at Chicago Pass marks the onset of prevalent shallow marine motility and bioturbation in the Death Valley region. The resulting ecosystem restructuring eased and promoted infaunal lifemodes, driving the increase in simple horizontal feeding traces in the terminal Ediacaran. The lack of significant changes in average trace width through time indicates that the increase in prevalence of simple feeding traces was due to an increase in bioturbating intensity rather than an increase in tracemaker size. By the Ediacaran–Cambrian boundary, simple horizontal feeding tracemakers were consistent components of the marine ecosystem preserved in the Death Valley region and potentially drove the active seeking of organic food sources through complex burrowing.

3.5.3. The Death Valley boundary sections

A multitude of trace and body fossil studies of the Wood Canyon Formation have been conducted in previous years. The middle and upper members of the Wood Canyon have yielded a variety of Cambrian fossils, including trilobites and archaeocyathids (Jensen et al. 2002; Corsetti and Hagadorn, 2000). The lower member is taxonomically and sedimentologically diverse, with fossil localities preserving body fossils of the classic Ediacaran taxa *Ernietta* and *Swartpuntia*, the 'Wormworld' fauna, including *Cloudina* and soft-bodied cloudinomorphs, as well as additional traces (Horodyski, 1991; Hagadorn and Waggoner, 2000; Schiffbauer et al. 2016; Smith et al. 2016; Selly et al. 2019). The diversity of the preserved fauna bolsters the potential that the trace

fossils at Chicago Pass were produced by motile organisms that likely interacted directly with, and altered the ecosystem of, the sessile benthic biota.

3.6. Conclusions

The lower member of the Wood Canyon Formation at Chicago Pass presents a suite of metazoan traces that increase in intensity, diversity, and complexity through the late Ediacaran and into the Cambrian. The traces are overwhelming dominated by simple horizontal burrows, but also have evidence of grazing and complex mat mining behaviors. The presence of the trace fossils is likely somewhat controlled by facies. However, the trace bearing facies are abundant and ubiquitous in section, allowing for general intensity changes to be tracked. The overall positive trajectory of trace fossil intensity through time, represented by the surface area coverage of individual burrows, is concurrent with an increase in diversity brought about by the introduction of complex feeding behaviors, like those of *Treptichnus pedum* and *Lamonte trevallis,* most recently described from Chicago Pass. The escalation of behaviors and intensity at Chicago Pass reflects the trend found in the Nama Group of Namibia, indicating that trace maker activity escalation was widespread and evident across the Ediacaran–Cambrian boundary.

3.7. References

Bottjer, D.J. 2010. "The Cambrian substrate revolution and early evolution of the phyla." Journal of Earth Sciences 21, 21–24. doi: 10.1007/s12583-010-0160-7

Buatois, L.A. and Mángano, M.G. 1993. "The ichnotaxonomic status of *Plangtichnus* and *Treptichnus*." ICHNOS 2, 217–224. doi: 10.1080/10420949309380095

Buatois, L.A., and Mángano, M.G. 2016. "Recurrent patterns and processes: The significance of ichnology in evolutionary paleoecology, in The Trace-Fossil Record of Major Evolutionary Events. Volume 1. Precambrian and Paleozoic", edited by Mángano, M.G.

and L.A. Buatois, 449–473. Amsterdam: Springer, Topics in Geobiology. doi: 10.1007/978-94-017-9600-2

Buatois, L.A., Almond, J., Mángano, M.G., Jensen, S., and Germs, G. 2018. "Sediment disturbance by Ediacaran bulldozers and the roots of the Cambrian explosion." Scientific Reports 8, 4514. doi: 10.1038/s41598-018-22859-9

Callow, R., and Brasier, M. 2009. "Remarkable preservation of microbial mats in Neoproterozoic siliciclastic settings: Implications for Ediacaran taphonomic models." Earth-Science Reviews 96, 207–219. doi: 10.1016/j.earscirev.2009.07.002

Corsetti, F.A., and Hagadorn, J.W. 2000. "Precambrian–Cambrian transition: Death Valley, United States." Geology 28, 299–302, doi: 10.1130/0091-7613(2000)28<29 9.PTDVUS>2.0.CO;2

Cribb, A., Kenchington, C., Koester, B., Gibson, B., Boag, T., Racicot, R., Mocke, H., Laflamme, M., and Darroch, S.A.F. 2019. "Increase in metazoan ecosystem engineering prior to the Ediacaran–Cambrian boundary in the Nama Group, Namibia." Royal Society Open Science 6, 190548. doi: 10.1098/rsos.190548.

Darroch, S.A.F., Sperling, E.A., Boag, T., Racicot, R., Mason, S.J., Morgan, A.S., Tweedt, S., Myrow, P., Johnston, D., Erwin, D., and Laflamme, M. 2015. "Biotic replacement and mass extinction of the Ediacara biota." Proceedings of the Royal Society B 282. doi: 10.1098/rspb.2015.1003

Darroch, S.A.F., Smith, E.F., Laflamme, M., and Erwin, D.H. 2018. "Ediacaran extinction and Cambrian explosion." Trends in Ecology and Evolution 33, 653–663. doi: 10.1016/j.tree.2018.06.003

Fernández, D.E., and Pazos, P.J. 2012. “Ichnology of Marginal Marine Facies of the Agrio Formation (Lower Cretaceous, Neuquén Basin, Argentina) at its Type Locality.” Ameghiniana 49, 505–524. doi:10.5710/amgh.27.2012.439

Gougeon, R.C., Mángano, M.G., Buatois, L.A., Narbonne, G.M., and Laing, B.A. 2018. “Early Cambrian origin of the shelf sediment mixed layer.” Nature Communications 9, 1909. doi: 10.1038/s41467-018-04311-8

Hagadorn, J.W. and Waggoner, B. 2000. “Ediacaran fossils from the southwestern Great Basin, United States.” Journal of Paleontology 74, 349–359, doi: 10.1666/0022-3360(2000)074<034 9.EFFTSG>2.0.CO;2

Hammersburg, S., Hasiotis, S., and Robison, R. 2018. “Ichnotaxonomy of the Cambrian Spence Shale Member of the Langston formation, Wellsville Mountains, Northern Utah, USA.” Paleontological Contributions 20, 1–66. doi: 10.17161/1808.26428

Han, Y., and Pickerill, R.K. 1995. “Taxonomic review of the ichnogenus *Helminthopsis* Heer 1877 with a statistical analysis of selected ichnospecies.” ICHNOS 4, 83–118. doi: 10.1080/10420949509380118

Herringshaw, L.G., Callow, R.H.T., and McIlroy, D. 2017. “Engineering the Cambrian explosion: the earliest bioturbators as ecosystem engineers. in Earth System Evolution and Early Life”, edited by Brasier, A.T., D. McIlroy, D., and McLoughlin, N. 369–382. London: Geological Society, Special Publications. doi: 10.1144/sp448.18

Hogan, E., Fedo, C., and J. Cooper. 2011. “Reassessment of the Basal Sauk Supersequence Boundary across the Laurentian Craton-Margin Hinge Zone, Southeastern California.” Journal of Geology 119. doi: 10.1086/661990

Horodyski, R.J. 1991. “Late Proterozoic megafossils from southern Nevada.” Geological Society of America Abstracts with Programs 23, 163.

Jensen, S., Droser, M.L., and N.A. Heim. 2002. “Trace fossils and ichnofabrics of the lower Cambrian Wood Canyon Formation, southwest Death Valley area.” Field trip guide book, Society for Sedimentary Geology 93,123–135.

Kennedy, M.J., and Droser, M.L. 2011. “Early Cambrian metazoans in fluvial environments, evidence of the non-marine Cambrian radiation.” Geology 39, 583–586. doi: 10.1130/G32002.1

Laflamme, M., Schiffbauer, J.D., Narbonne, G.M., and Briggs, D.E.G. 2011. “Microbial biofilms and the preservation of the Ediacara biota.” Lethaia 44, 203–213. doi: 10.1111/j.1502-3931.2010.00235.x

Liu, A., and McIlroy, D. 2015. “Horizontal surface traces from the Fermeuse Formation, Ferryland (Newfoundland, Canada), and their place within the Late Ediacaran ichnological revolution.” Geological Association of Canada Special Paper 9.

Macnaughton, R.B., and Narbonne, G.M. 1999. “Evolution and Ecology of Neoproterozoic-Lower Cambrian Trace Fossils, NW Canada.” PALAIOS 1 4.97–115. doi: 10.2307/3515367

Mángano M.G. and Buatois, L.A. 2014. “Decoupling of body-plan diversification and ecological structuring during the Ediacaran–Cambrian transition: evolutionary and geobiological feedbacks.” Proceedings of the Royal Society B 281. doi: 10.1098/rspb.2014.0038

Meyer, M., Xiao, S., Gill, B.C., Schiffbauer, J.D., Chen, Z., Zhou C., and Yuan, X. 2014. “Interactions between Ediacaran animals and microbial mats: Insights from *Lamonte trevallis*, a new trace fossil from the Dengying Formation of South China.”

Palaeogeography, Palaeoclimatology, Palaeoecology 396, 62–74. doi: /10.1016/j.palaeo.20112.026

Miguez-Salas, O., Dorador, J., and Rodríguez-Tovar, F.J. 2019. “Introducing Fiji and ICY image processing techniques in ichnological research as a tool for sedimentary basin analysis.” Marine Geology 413, 1–9.

Muhlbauer, J.G., Fedo, C.M., and Moersch, J.E. 2019. “Architecture of a distal pre-vegetation braidplain: Cambrian middle member of the Wood Canyon Formation, southern Marble Mountains, California, USA.” Sedimentology. doi: 10.1111/sed.12677

O’Neil, G.R., Tackett, L.S., and Meyer, M.B. 2020. “Petrographic evidence for Ediacaran microbial mat-targeted behaviors from the Great Basin, United States.” Precambrian Research 345. doi: 10.1016/j.precamres.2020.105768

Pecoits, E., Konhauser, K., Aubet, N.R., Heaman, L.M., Veroslavsky, G., Stern R.A., and Gingras, M. 2012. “Bilaterian burrows and grazing behavior at >585 million years ago.” Science 336,1693–1696. doi: 10.1126/science.1216295

Pemberton, S.G., and Frey, R.W. 1982. “Trace Fossil Nomenclature and the *Planolites*-*Palaeophycus* Dilemma.” Journal of Paleontology 56, 56843-56881.

Sappenfield, A., Droser, M.L., Kennedy, M.J., and McKenzie, R. 2012. “The oldest Zoophycos and implications for Early Cambrian deposit feeding.” Geological Magazine 149, 1–6. doi: 10.1017/S0016756812000313.

Schindelin, J., Arganda-Carreras, I., Frise, E., Kaynig, V., Longair, M., Pietzsch, T., Preibisch, S., Rueden, C., Saalfeld, S., Schmid, B., Tinevez, J.Y., White, D.J., Hartenstein, V., Eliceiri, K., Tomancak, P., and Cardona, A. 2012. “Fiji: an open-source platform for biological-image analysis.” Nature Methods 9, 676-82. doi: 10.1038/nmeth.2019.

Schiffbauer, J.D., Huntley, J.W., O'Neil, G.R., Darroch, S.A.F., Laflamme, M., and Cai, Y. 2016. "The Latest Ediacaran Wormworld Fauna: Setting the Ecological Stage for the Cambrian Explosion." GSA Today 26, 4-11. doi: 10.1130/GSATG265A.1.

Seilacher, A. 1964. "Sedimentological classification and nomenclature of trace fossils." Sedimentology 3, 253–256. doi: 10.1111/j.1365-3091.1964.tb00464.x.

Seilacher, A., and Pflüger, F. 1994. "From biomats to benthic agriculture: a biohistoric revolution." in Biostabilization of Sediments, edited by Krumbein, W.E., Peterson, D.M., and Stal, L.J. 97–105. Odenburg: Bibliotheksund Informationssystem der Carl von Ossietzky Universität.

Selly, T., Schiffbauer, J.D., Jacquet, S.M., Smith, E.F., Nelson, L.L., andreasen, B.D., Huntley, J.W., Strange, M.A., O'Neil, G.R., Thater, C.A., Bykova, N., Steiner, M., Yang, B., and Cai, Y. 2020. "A new cloudinid fossil assemblage from the terminal Ediacaran of Nevada, USA." Journal of Systematic Palaeontology 18, 357-379. doi:10.1080/14772019.2019.1623333

Singh, B.P., Bhargava, O.N., Mikuláš, R., Prasad, S.K., Singla, G., and Kaur, R. 2017. "*Asteriacites* and other trace fossils from the Po Formation (Visean–Serpukhovian), Ganmachidam Hill, Spiti Valley (Himalaya) and its paleoenvironmental significance." Geologica Carpathica 68, 464–478. doi: /10.1515/geoca-2017-0030

Smith, E.F., Nelson, L.L., Strange, M., Eyster, A.E., Rowland, S., Schrag, D.P., and Macdonald, F.A. 2016. "The end of the Ediacaran: Two new exceptionally preserved body fossil assemblages from Mount Dunfee, Nevada, USA." Geology 44, 911–914. doi: 10.1130/G38157.1

Smith, E.F., Nelson, L.L., Tweedt, S.M., Zeng, H., and Workman, J.B. 2017. “A cosmopolitan late Ediacaran biotic assemblage: new fossils from Nevada and Namibia support a global biostratigraphic link.” Proceedings of the Royal Society B: Biological Sciences 284. doi: 10.1098/rspb.2017.0934

Tarhan, L.G. 2018. “Phanerozoic shallow marine sole marks and substrate evolution.” Geology 46, 755–758. doi: 10.1130/G45055.1

Tarhan, L.G., Droser, M., Planavsky, N.J., and Johnston, D. 2015. “Protracted development of bioturbation through the early Palaeozoic Era.” Nature Geoscience 8, 865–869. doi: 10.1038/ngeo2537

Tarhan, L.G., Myrow, P.M., Smith, E.F., Nelson, L.L., and Sadler, P.M. 2020. “Infaunal augurs of the Cambrian explosion: An Ediacaran trace fossil assemblage from Nevada, USA.” Geobiology 00, 1–11. doi: 10.1111/gbi.12387

CHAPTER 4: PETROGRAPHIC EVIDENCE FOR EDIACARAN MICROBIAL MAT-TARGETED BEHAVIORS FROM THE DEATH VALLEY REGION, UNITED STATES[1]

4.1. Introduction

Ediacaran trace fossil assemblages like those of the Wood Canyon Formation at Chicago Pass, CA, were dominated by simple, horizontal burrows, reflecting a quiescent, non-antagonistic ecosystem just prior to the onset of the Cambrian Explosion (Droser et al., 1999). Traces representing complex behaviors, like targeted feeding and systematic mining are largely tied to the Cambrian substrate revolution, beginning with the boundary-marking trace *Treptichnus pedum* (Brasier et al., 1994; Landing, 1994; Bottjer, 2010). However, increasing research and utilization of more extensive analyses on terminal Ediacaran (555–542 Ma) traces has led to the recognition of ichnofossils that, although rare, support the appearance of complex, systematic bioturbating behaviors much earlier than previously thought (Jensen et al., 2000; Chen et al., 2013; Meyer et al., 2014; Cribb et al., 2019). One such trace, *Lamonte trevallis*, thus far only described from the Dengying Formation in South China, bears a similarity on the bedding planes to common Precambrian traces, such as *Planolites* and *Palaeophycus* **(**Pemberton and Frey, 1982; Meyer et al., 2014). When subjected to petrographic sectioning, *L. trevallis* exhibits morphological features that are better interpreted as complex behaviors, exhibiting strong evidence for targeted microbial mat penetration (Meyer et al., 2014). Complex undermat mining behaviors, like *Lamonte trevallis*,

---

[1] The material in this chapter was co-authored by Gretchen O'Neil, Lydia Tackett, and Michael Meyer and is part of a published manuscript in Precambrian Research. The publisher, Elsevier, allows the use of this material by the author for non-commercial purposes. Gretchen O'Neil had primary responsibility for collecting samples in the field and identification of fossils and sediments from the collected material. Gretchen O'Neil was the primary developer of the conclusions that are advanced here. Gretchen O'Neil also drafted and revised all versions of this chapter. Lydia Tackett and Michael Meyer served as proofreaders and provided feedback on the analyses conducted by Gretchen O'Neil. Michael Meyer also provided the scanning electron analyses.

indicate that the terminal Ediacaran fauna compares more closely to the Cambrian fauna than to the earlier classic Ediacara biota (Darroch et al., 2018).

Within the sedimentary beds of the Wood Canyon Formation at Chicago Pass and Boundary Canyon, CA, late Precambrian–early Cambrian trace fossils are dominated by simple cylindrical horizontal burrows preserved in full relief. The most common traces result from passive dwelling behaviors, lacking evidence of systematic movement and active feeding by the trace makers (Seilacher et al., 2005). However, preferential penetration of layers of organic material was identified approximately 54 m above the Wood Canyon–Stirling Quartzite contact and within the Precambrian–Cambrian boundary interval (112 m above contact based on the occurrence of *Treptichnus pedum*) at Chicago Pass and 63.7 m above the contact at Boundary Canyon.

Most early traces lack indicators of purposeful feeding and grazing behaviors, such as regular winding and looping, and instead appear to be opportunistic in nature with happenstance burrowing through abundant organic material. The identification of circular-to-oval burrow cross-sections restricted to microbial mat laminae is evidence of the advancement of complex behaviors from opportunistic to targeted in the late Ediacaran. This evidence is backed up by the presence of larger grain sizes on average within the burrow infill than in the sediment layers. The difference in grain size indicates that the sediment was not sourced directly from the surrounding material and instead was brought into the mat layer during targeted feeding. Through grain size analyses of burrow-containing thin-sections from the Ediacaran–Cambrian Wood Canyon Formation, the stratigraphic and temporal intervals in which these complex behaviors appeared can be discerned even within heavily horizontally bioturbated material.

4.2. Geologic Setting

The lower Member of the Wood Canyon Formation is a Precambrian–Cambrian boundary-spanning shallow-marine siliciclastic unit comprised of three shallowing-upwards parasequences (Sappenfield et al., 2012; Jensen et al., 2002; Corsetti and Hagadorn, 2000; Hagadorn and Waggoner, 2000). Each parasequence is capped by a large, laterally-continuous, resistant carbonate bed. The first and oldest of the three parasequences contains few traces (Corsetti and Hagadorn, 2000). Consistent burrowing appears in the second parasequence and persists throughout the remainder of each section. The Precambrian–Cambrian boundary is placed in the third parasequence, based on the presence of *Treptichnus pedum* (Corsetti and Hagadorn, 2000; Hagadorn and Waggoner 2000).

The Chicago Pass section is located slightly west of the Nevada–California border, ~18 km from the town of Pahrump, Nevada (Fig. 4.1A and B). The stratigraphic section contains the Stirling Quartzite–Wood Canyon contact and is vertically continuous through the three diagnostic lower Wood Canyon parasequences (Mata, 2012). Chicago Pass is dominated by burrowing trace fossils (Fig. 4.2A–D) with the occasional resting traces (potentially cnidarian) and Ediacaran holdfasts (Fig. 4.2E). The Boundary Canyon section is located ~ 11 km west of the NV–CA border, near Hell's Gate, Death Valley National Park (Fig. 4.1A and B). Boundary Canyon represents a slightly more offshore environment than that of Chicago Pass and contains a similar suite of fossils, but with a lower occurrence of microbial mat facies.

4.3. Materials and Methods

Sedimentary rocks were collected every 2–4 m beginning at the Stirling Quartzite contact and continuing through the three parasequences of the lower Wood Canyon Formation at each locality. Hand samples were thin-sectioned and examined for microscopic morphological

structures resulting from environmental and biotic reworking. Thin-sections were not limited to known fossiliferous units in an attempt to avoid overlooking evidence of bioturbation, especially for burrows that are not visible on the bedding plane.

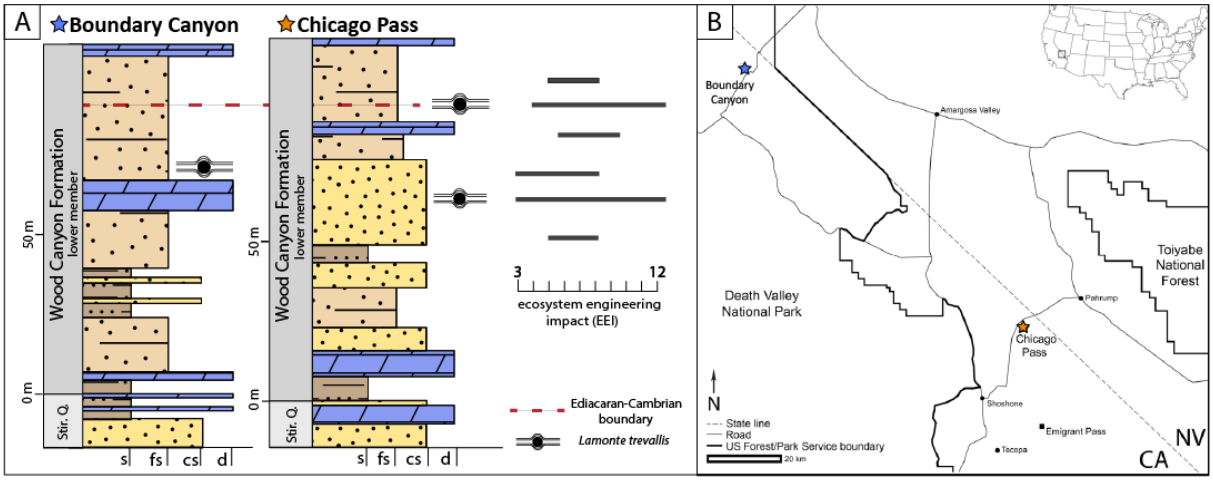

Figure 4.1. Stratigraphic columns of Chicago Pass and Boundary Canyon and map of area. (A) Generalized stratigraphic columns of the lower Member of the Wood Canyon Formation at Boundary Canyon and Chicago Pass. Stratigraphic levels at which Lamonte trevallis was found are indicated on the stratigraphic columns. Ecosystem engineering impact values are shown for the Chicago Pass section (calculations based on Herringshaw et al., 2017), (B) Locality map of the Boundary Canyon and Chicago Pass Wood Canyon localities along the Nevada–California border.

The most common trace within the lower Wood Canyon, *Planolites*, as well as the known *L.* trevallis from South China, contain infill that differs from the host rock, whether in grain size or composition (Meyer et al., 2014). This is a common feature resulting from the infilling of burrows penetrating into homogenized sediment. Microbial microlaminae were present within siltstones throughout the stratigraphic section. Microbial mat-penetrating burrows, with relatively coarser infill to that of the host rock, were found at approximately 35 m below the PC–C boundary and within the boundary interval at Chicago Pass and just above the second parasequence at Boundary Canyon (Fig. 4.3A–F). The shape of the burrows in cross-section varies, with some specimens appearing slightly ovoid due to compaction. The surrounding microbial microlaminae

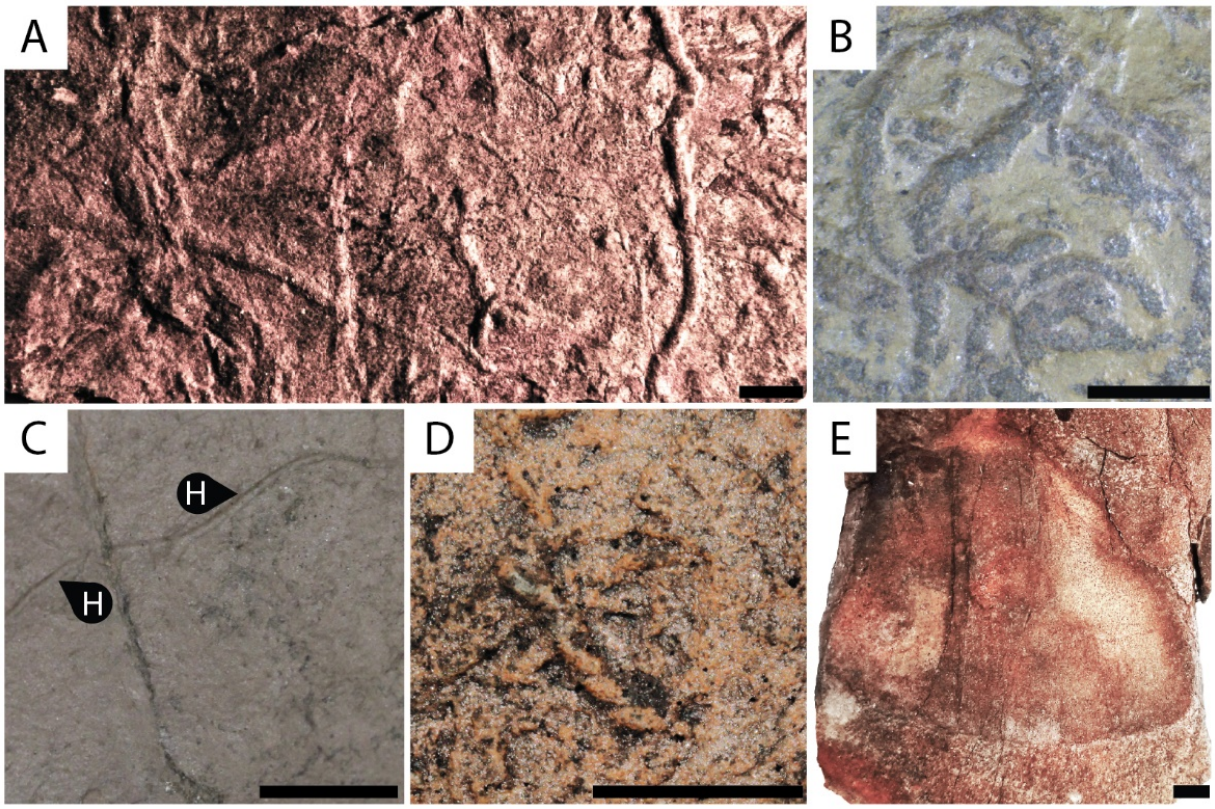

Figure 4.2. Common trace fossils from Chicago Pass and Boundary Canyon. (A) Simple horizontal dwelling burrows, *Planolites* isp., (B) looped grazing trace, Gordia marina, (C) grazing trace, *Helminthopsis* isp., (D) *Treptichnus pedum* from the Ediacaran–Cambrian boundary, (E) Ediacaran holdfast. Scale = 1 cm

thin on either side of the burrow cross-sections, indicating that the penetrative burrows were more structurally resistant post-burial than the organic material. Estimated pre-compaction microbial mat thicknesses were calculated based on the methods used in Meyer et al., (2014).

Thin-sections containing layers of organic matter within the host sediment were selected for transect box analysis, in order to compare grain sizes of the penetrative burrow infill to the host sediment. For the Chicago Pass thin-sections, multiple horizontal transects within each thin-section were divided into 1.5 mm^2 boxes with spacing of 0.5 mm (Fig. 4.4). Selected horizontal transects contain unbroken and/or burrow penetrated organic-rich microlaminae, as well as non-organic host sediment-filled layers. Layers interpreted as microbial mat microlaminae, or organic layers, appear dark, wavy, and filamentous in thin-section, unlike mud layers that lack the filamentous structure

(Fig. 4.5A–C). The microbial mat laminae are found alternating with the silts of the host rock within samples in mottled bedding (Fig. 4.5D). The number of transects was based on the size of the petrographic thin-section and occurrence of continuous laminae. Up to 50 maximum grain diameters were measured within each box using Fiji image processing (Fig. 4.4) (Schindelin et al., 2012). In cases where organic matter is dominant and measurable grains are limited, less than 50 measurements were taken. The same methods were applied to the Boundary Canyon sample, however the microbial microlaminae were thinner and sparser in comparison to the Chicago Pass counterparts. In order to confidently track differences between host rock and organic microlaminae, the mat-containing transect (transect 2) was divided further into three transects of 0.5 mm^2 boxes spaced every 0.5 mm.

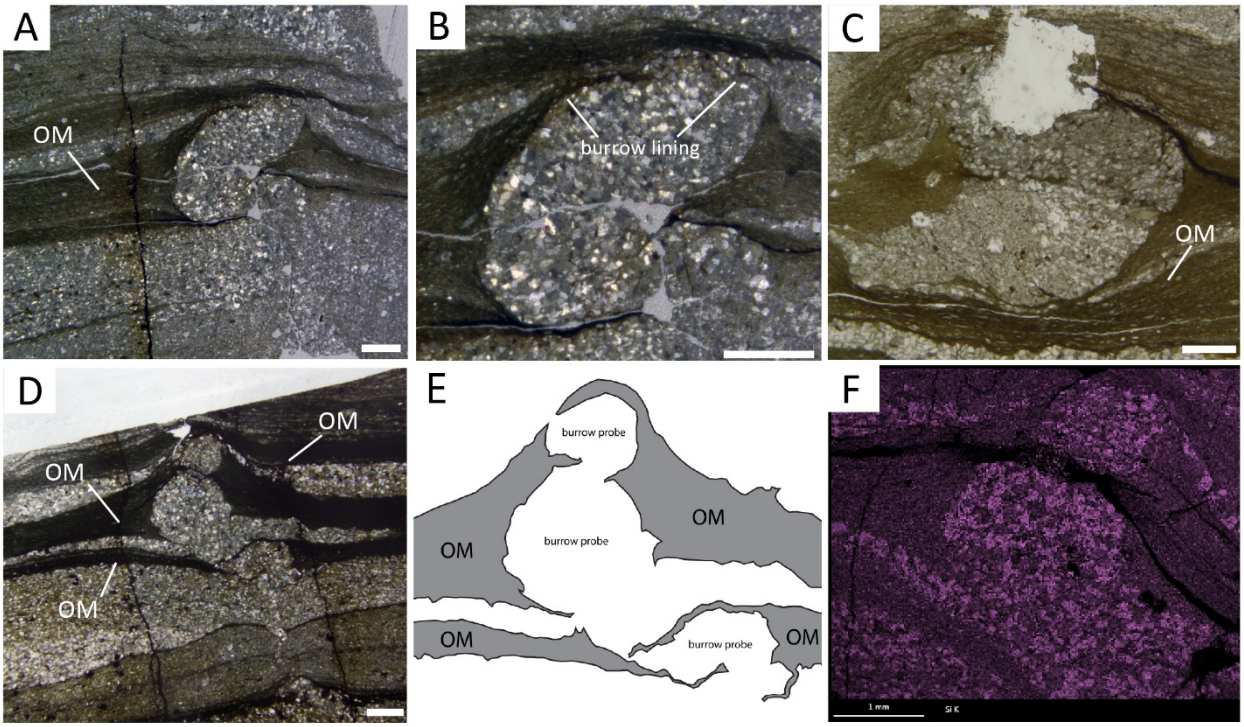

Figure 4.3. *Lamonte trevallis* in petrographic thin section. (A) *Lamonte trevallis* from the Wood Canyon Formation, (B) magnification of possible burrow lining from A, (C) *Lamonte trevallis* from the Wood Canyon Formation, (D) example of "stacked" *L. trevallis*, (E) diagram of targeted burrow penetration through microbial mat horizons (modeled after D), (F) map of D showing relative Si concentrations, OM = organic matter. Scale = 1 mm.

Burrow infill can often be distinguished from the host-sediment through differences in grain size and/or composition. To identify differences in grain sizes, minimum, maximum, and mean grain diameters were compared between the three transect categories (unburrowed organic, burrowed organic, and non-organic). Mann-Whitney pairwise tests were applied to the diameters of individual grains within each box. Bonferonni-corrected p-values were used to identify statistically significant grain size differences across and between transects.

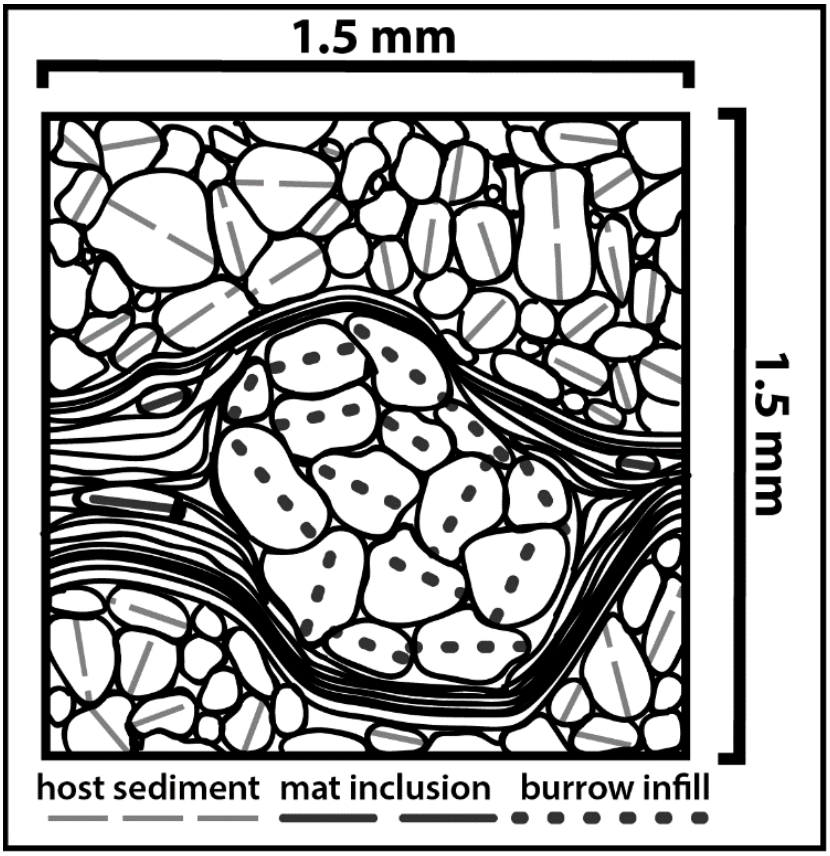

Figure 4.4. Example of burrow infill analysis. Boxes are 1.5 mm^2. Dotted and dashed lines represent the diameter measurement of an individual grain.

4.4. Systematic Paleoichnology

Ichnogenus *Lamonte* Meyer et al., 2014

Type species. *Lamonte trevallis* Meyer et al., 2014 (Dengying Formation, Wuhe, Hubei Province, South China)

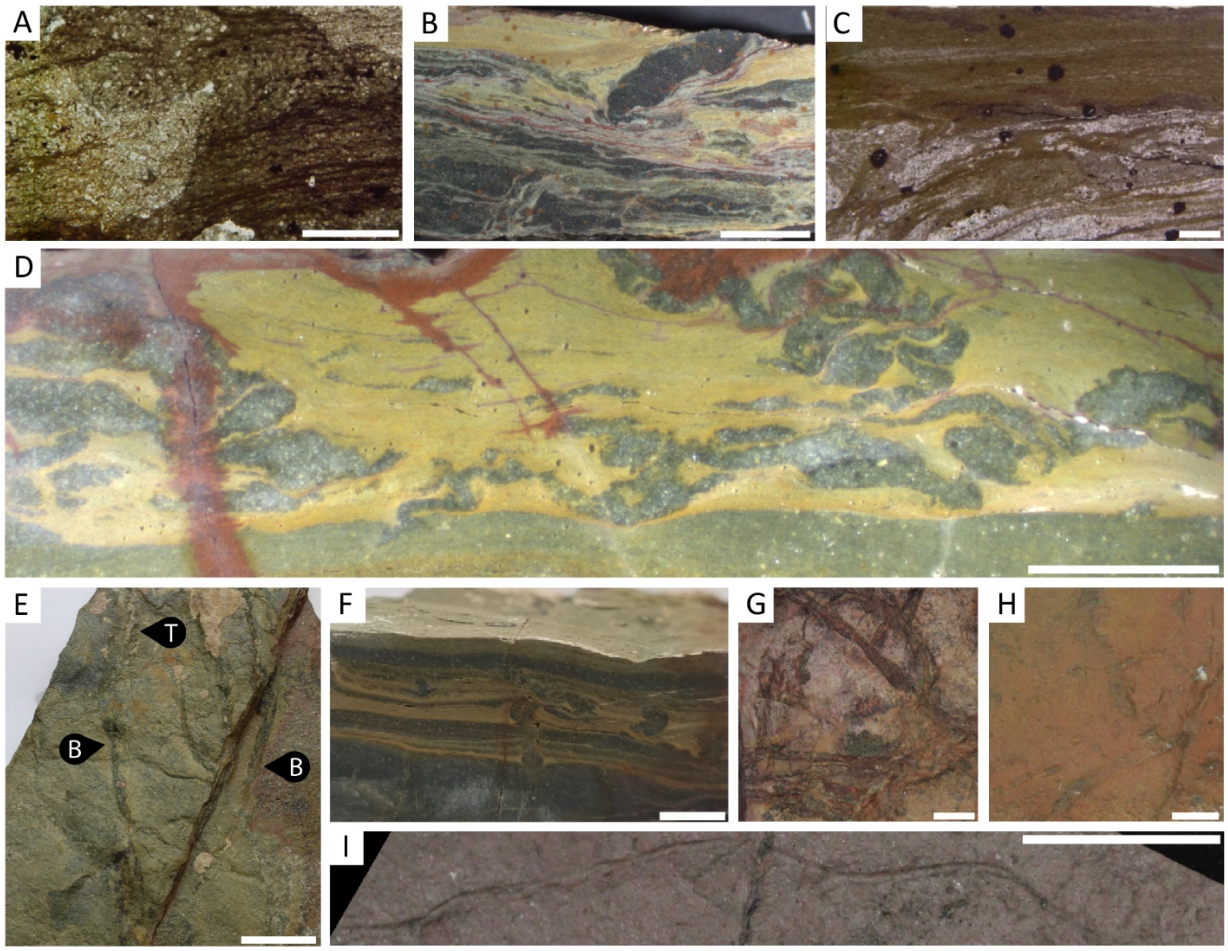

Figure 4.5. Microbial mat containing specimens in cross-section and surface traces. (A) Thin section of microbial mat microlaminae with filamentous structures (right) interacting with a collapsed burrow (left), scale = 1 mm, (B) cross-section of hand sample with mud laminae, scale = 1 cm, (C) mud layers overlying silty host sediment in thin section, scale = 1 mm, (D) cross-section of "mottled" hand sample, scale = 1 cm, (E) surface of penetrative burrow-containing hand sample with a dwelling burrow and trail characteristic of *Lamonte isp.* T = scratch marks or trails, B = horizontal burrows/tunnels in epirelief, scale = 1 cm, (F) cross-section of microbial mat laminae in E, scale = 1 cm, (G) *Planolites* from the Chicago Pass section, scale = 1 cm, (H) *Palaeophycus* from the Chicago Pass section, scale = 1 cm, (I) *Helminthopsis* from the Chicago Pass section, scale = 1 cm.

Diagnosis. After Meyer et al., (2014), small, scratch-like trails that transition into millimeter wide burrows or pits on the surface of the rocks, coupled with penetrative burrows within crinkled and microlaminated microbial layers.

Occurrence. Burrowed specimens from the lower member of the Wood Canyon Formation at Chicago Pass and Boundary Canyon, California, USA. (Specimen IDs: CP511-LT1, CP511-LT2, CP428-LT1, CP428-LT2, and BC464-LT1, reposited at The North Dakota Heritage Center and State Museum, GPS: 36.143382 N, −116.15109000 W and 36.749057 N, −116.96619700 W)

Description. Quartz-dominated siltstone containing crinkled, mottled layers of organic matter (Fig. 4.5D). Surface burrows are found in positive relief and are occasionally associated with *Planolites*. Burrows are 2–5 mm in width, curved-to-winding, and overlap when intersecting with another burrow. Tracks are visible on the surface in isolated traces (Fig. 4.5E). In thin-section, burrows are seen preferentially penetrating layers of organic material. Burrows are originally circular-to-oval in cross-section, with occasional secondary reworking of the filamentous organic layer into the burrow area. Burrow infill composition is mineralogically similar to the host rock but contains slightly larger grains on average. Possible burrow linings are associated with a subset of the burrows (Fig. 4.3B).

Burrow interactions with microbial mat layers perforate the previously intact mat, differing from penetration of malleable muddy sediments by a surface burrow (Buatois et al., 2005). The perforation permanently ruptures the mat layer, as it lacks the amorphous qualities of the fine non-organic sediments. Deformation of the underlying and overlying layers supports this interpretation. Evidence of burrow stacking can be seen in one (possibly two) specimen, where multiple burrows are found vertically stacked within the same microbial lamination (Fig. 4.2B and D).

Previous discussions of *L. trevallis* have questioned the validity of the ichnotaxon, arguing that individual parts of the trace assemblage (surface tracks/trails, dwelling structures, and mat-penetrating burrows) represent taphonomic variants of a simple undermat mining tunnel confined

to the mat layer (Mángano and Buatois, 2016). The three morphological components are not present in all specimens from other localities and the mat-penetrating cross-sections of *L. trevallis* from the Wood Canyon Formation are the result of dwelling burrows. Surface trails that are abundant in the Dengying Formation material are rare in the Wood Canyon specimens. A portion of the surficial traces from the Denying Formation are associated with parallel scratch-like markings or shallow pits, potentially resulting from the movement of a bilaterian organism with bristle-like appendages (Chen et al., 2019). The occurrence of the surface trails was not deemed necessary for the classification of the ichnofossils due to the low preservation potential of this component. Meyer et al., (2014) also described "pit-like" structures that may result from vertical burrowing behaviors. The pit structures are common in the Wood Canyon material, but are not associated directly with the burrows and could be interpreted as holdfast-like structures of a separate organism or microbially induced sedimentary structures. While the three components may be differentially interpreted, the association of the dwelling burrow exclusively with the microbial mat layer indicates purposeful mat mining behavior.

4.5. Results

4.5.1. Traces

The Chicago Pass PC–C boundary interval 1 sample contains a combination of the three trace morphologies characteristic of the late Ediacaran undermat mining trace, *Lamonte trevallis* (Fig. 4.5E and F) (Meyer et al., 2014). The surface traces consist of a combination of three-dimensional infilled horizontal burrows (reminiscent of *Planolites* and *Palaeophycus*; Fig. 4.5G and H) and surface traces (reminiscent of *Helminthopsis* and *Helminthoidichnites*; Fig. 4.5I). Cross-sections through the sample and in thin-section contain evidence of targeted mat feeding (Fig. 4.5F). Chicago Pass PC–C boundary interval 2 and Boundary Canyon samples, also contain

evidence of infaunal mat penetration. However, the two samples lack evidence of epibenthic locomotion in hand sample, but are abundant in three-dimensional infilled horizontal burrows. These traces are associated with *Planolites* and *Palaeophycus*, and are easily mistaken for the two common ichnotaxa from the Ediacaran of the Great Basin region (Fig. 4.5G and H).

4.5.2. Biotic interactions with microbial mat layers

When organic layers are present in the absence of penetrative burrows, the microbial laminae are continuous unless interrupted by sedimentary structures (Fig. 4.6A). When organic layers are absent, sediments tend to be highly laminated and contain distinct sedimentary microstructures, like cross-bedding (Fig. 4.6B and C, respectively). The undisturbed organic layers and laminated sediments do not contain evidence of penetrative burrows, even when sourced from hand samples containing horizontal burrows.

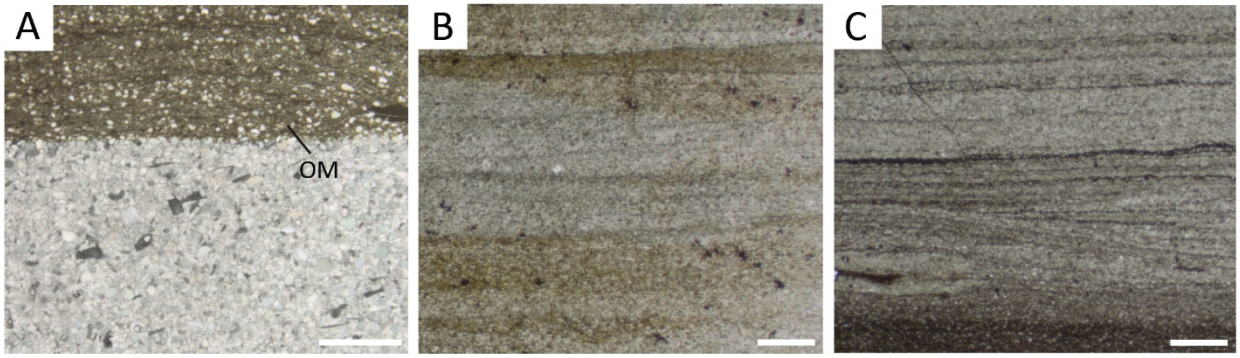

Figure 4.6. Sedimentary structures in thin section. (A) thin-section of thick microbial mat horizon from within the burrowed sediments of the second parasequence. (B) siltstone bed from just below the second massive carbonate unit. (C) cross-bedded siltstone from just below the second massive carbonate bed. Scale = 1 mm.

Table 4.1. Significance tests for grainsize differences between the burrow infill and the host sediment for two Chicago Pass specimens. Non-significant p-values are highlighted in black. P-values were calculated in PAST 4.02 software using Mann-Whitney pairwise tests with Bonferonni-corrections

Sample locality	Infill box	Average p-value	Minimum p-values	Maximum p-values	Individual box grainsize significance					
Chicago Pass Boundary Interval 2	2B	2.26E-12	6.28E-15	1.10E-11	1.10E-11	2.54E-13	6.28E-15	3.11E-14	8.97E-15	
	2C	5.26E-11	4.39E-14	2.59E-10	2.59E-10	3.23E-12	5.33E-14	5.04E-13	4.39E-14	
	3C	1.37E-08	3.51E-13	6.79E-08	6.79E-08	3.38E-10	1.08E-12	1.51E-11	3.51E-13	
	3D	7.25E-10	2.93E-14	3.61E-09	3.61E-09	1.50E-11	2.93E-14	3.52E-13	3.81E-14	
	3E	2.62E-06	1.01E-11	1.31E-05	1.31E-05	1.58E-08	1.30E-11	3.90E-10	1.01E-11	
	3F	1.56E-07	6.66E-13	7.78E-07	7.78E-07	1.89E-09	1.34E-12	3.48E-11	6.66E-13	
Chicago Pass Boundary Interval 1	3E	9.25E-06	4.82E-12	1.64E-04	1.60E-09	3.89E-11	5.69E-12	3.23E-11	2.26E-08	
					4.91E-11	3.36E-09	4.08E-10	8.06E-09	3.04E-09	
					2.77E-10	4.82E-12	1.36E-06	1.03E-07	8.37E-08	
					1.96E-05	3.70E-09	5.21E-09	3.98E-09	0.000164	9.43E-06
	4J	5.77E-06	9.26E-12	8.19E-05	8.19E-05	7.76E-06	1.24E-05	1.19E-06	4.81E-09	
					1.15E-08	3.22E-06	1.47E-05	1.81E-10	4.20E-11	
					7.10E-10	2.75E-10	1.05E-10	1.92E-11	5.18E-11	
					9.26E-12	6.23E-11	1.17E-10	4.41E-11	3.84E-10	1.01E-11
	4K	7.95E-03	3.24E-10	8.94E-02	2.23E-07	3.20E-09	3.24E-10	4.74E-09	3.63E-06	
					1.33E-08	9.39E-08	3.23E-08	4.65E-06	2.17E-05	
					2.33E-07	2.37E-08	0.00027	0.00054	5.38E-05	
					0.04738	9.05E-06	2.92E-05	1.06E-05	0.08939	0.02913

Thin-sections containing *L. trevallis* contain distinct ruptures of previously continuous organic microlaminae (Fig. 4.43A–D). Ruptures appear to be originally circular-to-oval in shape, with occasional disruption by reworked organic layers or intrastratal shrinkage cracks associated with microbial mats (Harazim et al., 2013). The amount of compaction varies between microlaminae. Estimated original microbial mat thicknesses from the Chicago Pass specimens range from 3 to 5.7 mm with compaction ratios of 1:1.3–1:3.6. The Boundary Canyon specimen showed the least amount of compaction with a ratio of 1:1.2, estimating a mat thickness of ~1 mm.

4.5.3. Grain size and burrow infill

When maximum grain sizes of each individual box were compared within the horizontal transects, the infill of mat-penetrating burrows was significantly larger than the host sediment-filled boxes in all but one instance at Chicago Pass (Fig. 4.7, Table 4.1). Mann-Whitney pairwise tests almost always resulted in significant p-values for burrow infill in relation to the corresponding unbroken microbial mat microlaminae. Further, significant p-values were nearly absent from the host rock containing transects and between boxes with unbroken microbial mat microlaminae. Maximum and minimum grain sizes had similar distributions, but were highly susceptible to outliers. In rows containing only the host rock or unbroken organic microlaminae without sedimentary disruption, there were no considerable divergences (> 0.002 mm2) from the mean. Distributions of individual diameters within the 1.5 mm2 boxes show a consistent pattern of infill grain sizes being larger on average than the corresponding host rock and unbroken mat layers in each of the Chicago Pass thin-sections (Fig. 4.8). The Boundary Canyon thin-section does not show any distinctive excursions within the 1.5 mm^2 boxes, but does show increased grain size in the infill within the 0.5 mm^2 boxes (Fig. 4.9).

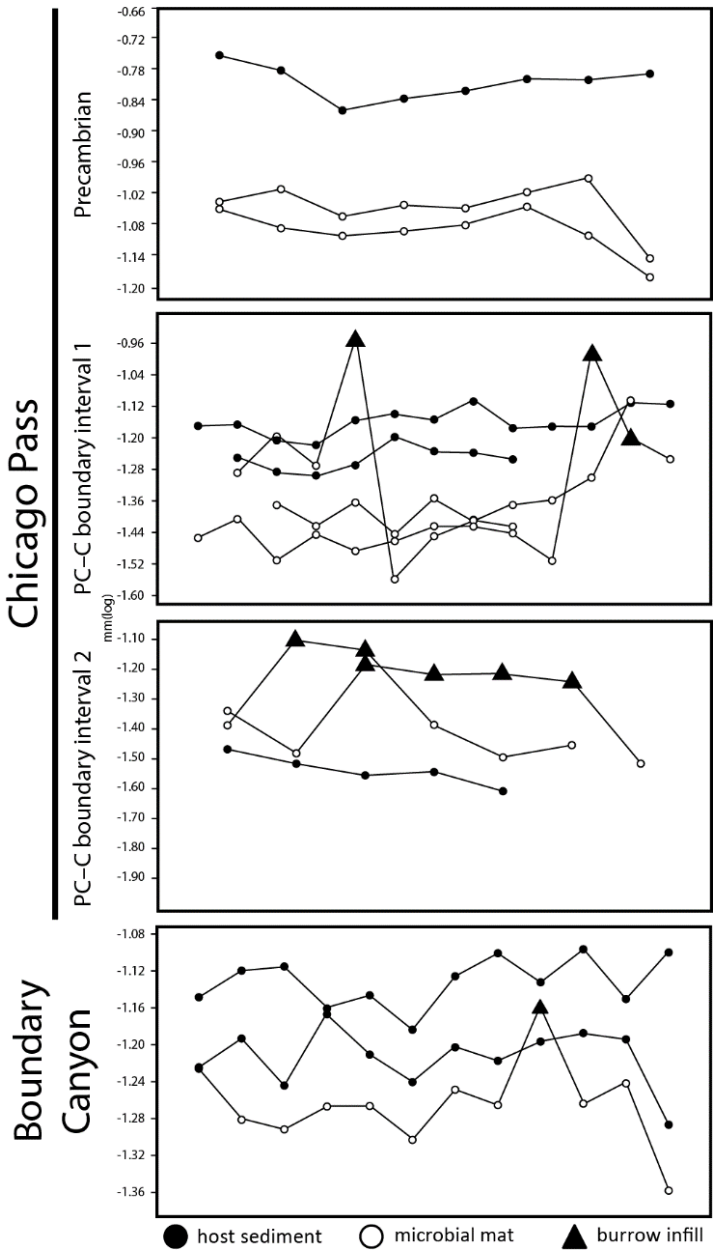

Figure 4.7. Mean grain size for individual boxes by row. Solid triangles indicate boxes that were dominantly comprised of burrow infill, empty circles indicate boxes dominated by unbroken microbial microlaminae, filled circles indicate boxes along a host-sediment transect.

4.6. Discussion

The preferential targeting of organic material is evidence of complex feeding behaviors absent from previous communities of Precambrian bioturbators from California. Mat feeding behaviors were dominantly surficial, simple, and opportunistic prior to the appearance of

Treptichnus pedum. *Planolites* and *Palaeophycus* comprised the majority of traces, but lack penetrative behaviors and are considered to be semi-infaunal at most.

The dark, filimentous microlaminae have been interpreted as microbial mat in origin based on previous studies of mat-containing units (Chakraborty et al., 2012, Chen et al., 2013, Gorin et al., 2008, Harazim et al., 2013, Loyd and Corsetti, 2010, Noffke et al., 2006, Noffke, 2000, Meyer et al., 2014) and also have been reproduced in modern environments (Noffke et al., 2006). Mud laminae are also found throughout the unit and closely resemble microbial mat microlaminae (Fig. 4.5B and C). However, the layers of mud can be differentiated from microbial mats based on the absence of the filamentous structures diagnostic of the mats (Fig. 4.4A), lack of distinct burrows, and increased susceptibility to disruption and collapse of layers from sedimentary reworking. Additionally, elemental mapping shows a distinct difference in the elemental makeup of the organic material and the sediment, especially in Si concentrations (Fig. 4.3F, EDS maps produced on an FEI Quanta 600F scanning electron microscope with a Bruker AXS QUANTAX 400 x-ray spectrometer). When burrows interact with nonmat mud layers, accumulation of the mud around the burrow leads to undeformed laminae, differing from the perforated nature of the microbial layers from the penetration of the burrows in this study (Harazim et al., 2013). Mats and mud layers occasionally co-occur, decreasing the stability and cohesion of the mat layers and deforming previously intact burrow cross-sections (Fig. 4.2F).

The mat-targeted nature of the burrow penetration, surface characteristics of the traces, and the sedimentary structures of the containing host rock lead us to classify this trace as *Lamonte trevallis*. *L. trevallis*, thus far only described from the carbonate facies of late Ediacaran portion of the Denying Formation, South China, is interpreted as an undermat mining trace that preferentially targets organicrich layers within crinkled microlaminae bearing rocks (Fig. 4.4D and F) (*L.*

trevallis, Meyer et al., 2014). The interpretation of targeted matpenetration is supported by the lack of significant grain size excursions from the mean within the host sediment layers. If the mining behavior was passive and opportunistic, it would be expected that burrows would also penetrate into the host-sediment layers, creating an increase in grain size from the burrow infill. Comparable traces have also been observed in sediments from the Swartpunt locality in southern Namibia (Meyer, personal communication). The presence of *L. trevallis* within carbonate and siliciclastic facies indicates that the trace was not limited to a singular environment and more likely represents an advance in behaviors within the Ediacaran bioturbating fauna.

The occurrence of *Lamonte trevallis* in Precambrian–Cambrian deposits of the Great Basin is not the only fossil similarity to the Denying Formation. Reports of late Precambrian soft-bodied tubicolous fossils, similar to *Conotubus*, *Gaojiashania*, *Wutubus*, and *Ningqiangella* of the Gaojiashan Lagerstätte (Denying Fm.), from the Wood Canyon Formation near Johnnie, NV and the Deep Spring Formation at Mount Dunfee, NV also relate the two localities (Selly et al., 2019, Smith et al., 2017, Schiffbauer 2016, Schiffbauer et al., 2016). The morphological parallels between the fossils of the Dengying Formation and the Great Basin units increase the likelihood that the two paleogeographically distinct regions represent similar paleoenvironments during the latest Ediacaran 'Wormworld' (Schiffbauer et al., 2016).

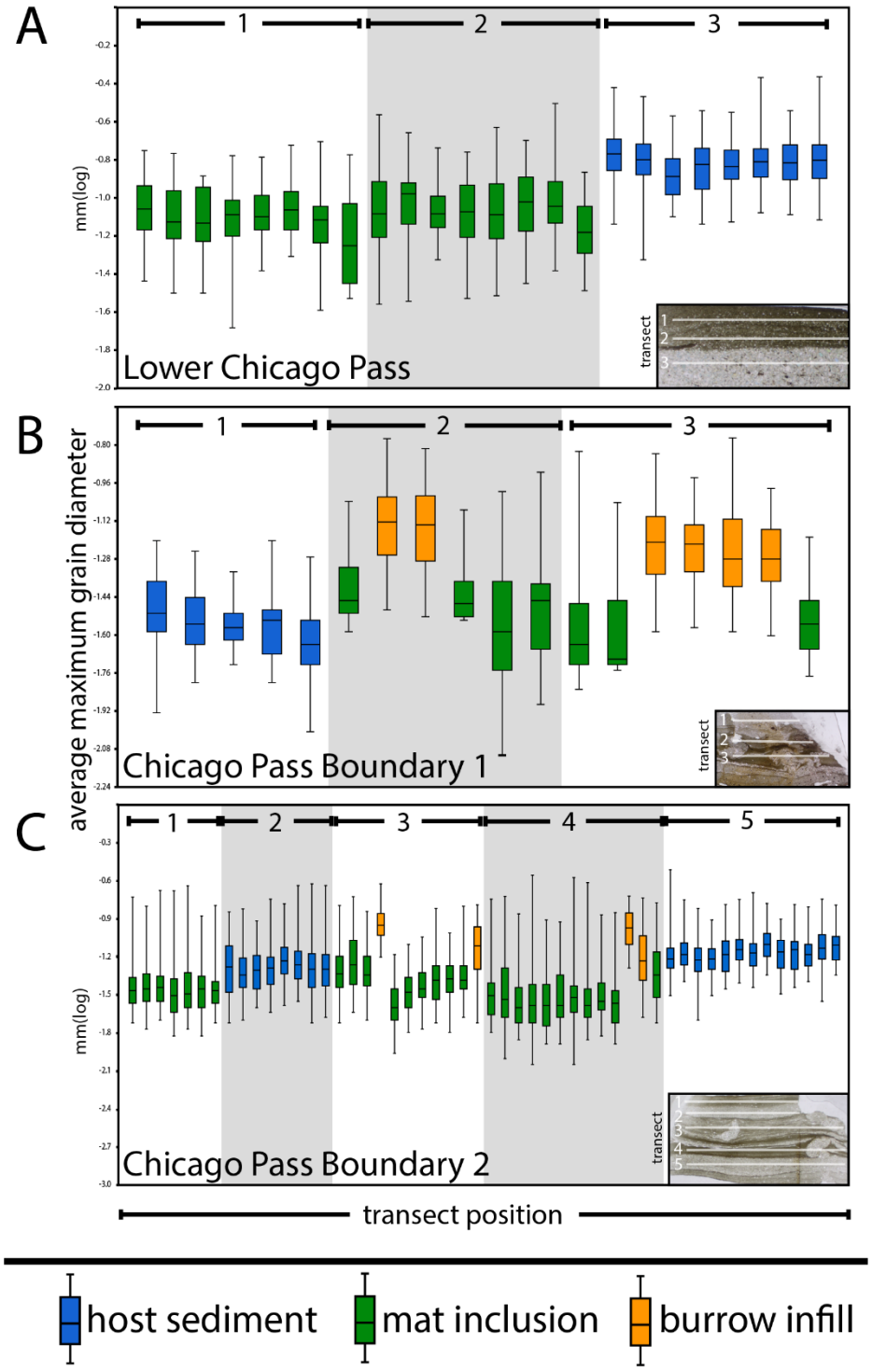

Figure 4.8. Boxplot analyses of grain size distributions within the Chicago Pass samples. Transect numbers are indicated below, with 1 being the uppermost transect. Green = microbial mat microlaminae, blue = host rock, orange = burrow infill. Images of the measured petrographic sections are inset. (A) Lower Chicago Pass thin-section containing unbroken microbial laminae and host rock, (B and C) Chicago Pass boundary interval thin-sections containing host rock, unburrowed microbial laminae, and burrowed microbial laminae.

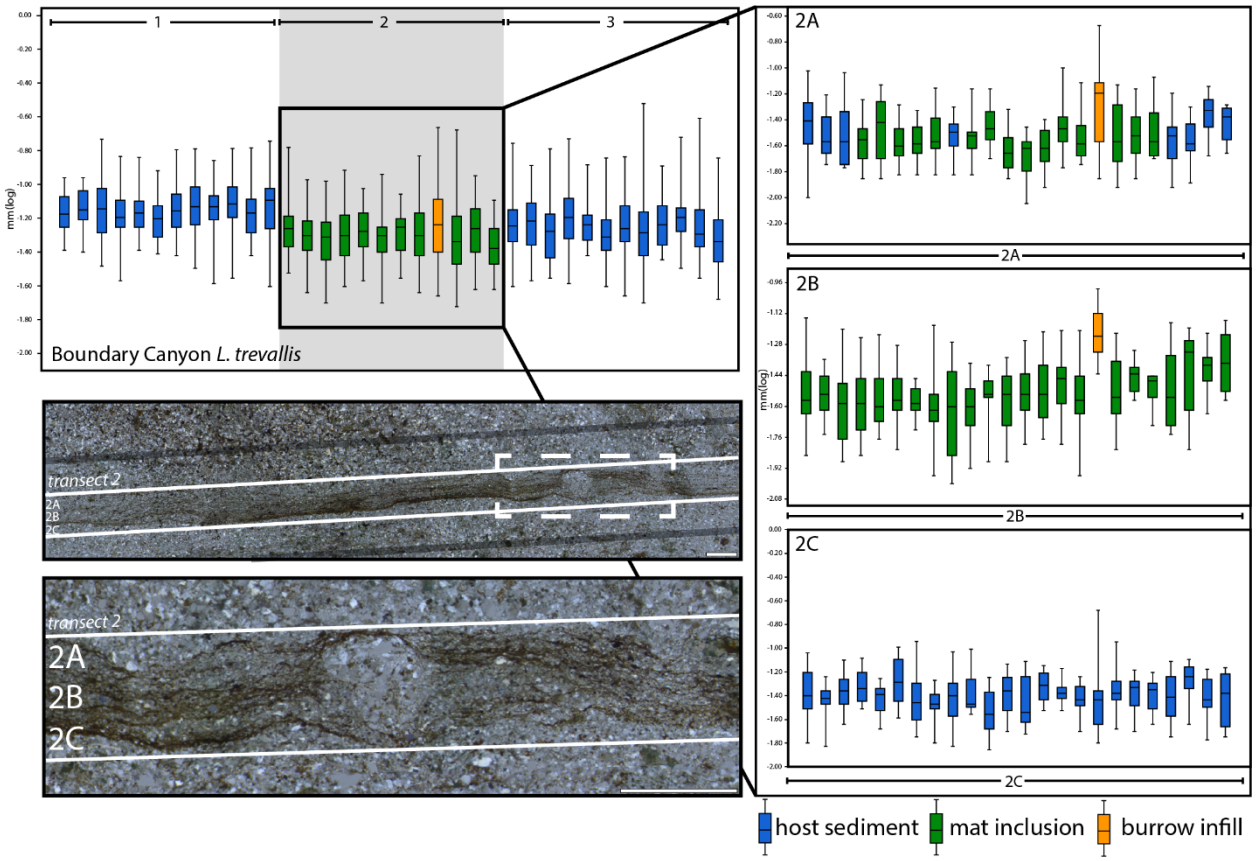

Figure 4.9. Boxplot analyses of grain size distributions within the Boundary Canyon sample. (Left) Boxplot using 1.5 mm^2 boxes, image of petrographic section with the second, burrow containing transect indicated by white lines, and enlargement of the burrow area marked dashed lines. (A–C) Boxplot analyses of 0.5 mm^2 boxes from the second transect. Scale = 1 mm.

4.7. Conclusion

Complex behaviors in terminal Ediacaran strata that were previously tied to the Cambrian substrate revolution are becoming more numerous and widespread, with the discovery of certain ichnotaxa from various localities worldwide. Many of the advanced bilaterian behaviors from the early Cambrian are now considered to have been present in the terminal Ediacaran (Darroch et al., 2018). Although the Wood Canyon Formation is considered to be fairly low in trace fossil diversity (O'Neil and Tackett, *in review*) in comparison to sites like the Nama Group of Namibia (Jensen et al., 2000, Macdonald et al., 2014, Buatois et al., 2018), the occurrence of *Lamonte trevallis* indicates that there was likely a more diverse trace-making community present in the Great Basin

region. The mottled nature of the sedimentary beds and the abundance of distinct surface burrows are likely to have obscured the identification of more complex behaviors, such as undermat mining. Petrographic analyses of sediments throughout a stratigraphic section facilitates identification of burrowing behaviors that are difficult to identify or distinguish on the rock surface.

Although *Lamonte trevallis* has surface characteristics (trails and three-dimensional infilled burrows) similar to other simple Ediacaran traces (Chen et al., 2013), the undermat mining targeted at the organic rich material is a much more purposeful behavior, and the transition between the varying behaviors indicates a complexity beyond what is considered typical for the Ediacaran. Further, the presence of mat-mining behaviors in Ediacaran sediments supports an earlier onset of biosubstrate infaunalization, in addition to increased mat-grazing prior to the Precambrian–Cambrian boundary.

4.8. References

Bottjer, D.J. 2010. "The Cambrian Substrate Revolution and Early Evolution of the Phyla." *Journal of Earth Science* 21:21–24.

Brasier, M.D., Cowie, J., and M. Taylor. 1994. "Decision on the Precambrian-Cambrian boundary stratotype." *Episodes* 17, 3–8.

Buatois, L.A., Gingras, M.K., Maceachern, J., Mangano, M.G., Zonneveld, J.-P., Pemberton, S.G., Netto, R.G., and A. Martin. 2005. "Colonization of brackish-water systems through time: Evidence from the trace-fossil record." *Palaios* 20:321–347.

Buatois, L.A., Almond, J., and M.G. Mángano. 2018. "Sediment disturbance by Ediacaran bulldozers and the roots of the Cambrian explosion." *Scientific Reports* 8:4514. Doi: 10.1038/s41598-018-22859-9.

Chakraborty, P.P., Das, P., Saha, S., Das, K., Mishra, S.R., and P. Paul. 2012. "Microbial mat related structures (MRS) from Mesoproterozoic Chhattisgarh and Khariar basins: Central India and their bearing on shallow marine sedimentation." *Episodes* 35(4):513–523.

Chen, Z., Zhou, C., Meyer, M., Xiang, K., Schiffbauer, J.D., Yuan, X., and S. Xiao. 2013. "Trace fossil evidence for Ediacaran bilaterian animals with complex behaviors." *Precambrian Research* 224:690–701.

Chen, Z., Zhou, C., and X. Yuan. 2019. "Death march of a segmented and trilobate bilaterian elucidates early animal evolution." *Nature* 573:412–415. Doi:10.1038/s41586-019-1522-7.

Corsetti, F.A. and J.W. Hagadorn. 2000. "Precambrian-Cambrian transition: Death Valley. United States." *Geology* 28:299–302. Doi: 10.1130/0091-7613(2000) 28<299:PTDVUS>2.0.CO;2.

Cribb, A., Kenchington, C., Koester, B., Gibson, B., Boag, T., Racicot, R., Mocke, H., Laflamme, M., and S.A.F. Darroch. 2019. "Increase in metazoan ecosystem engineering prior to the Ediacaran-Cambrian boundary in the Nama Group. Namibia." *Royal Society Open Science* 6:190548. Doi:10.1098/rsos.190548

Darroch, S.A.F., Smith, E.F., Laflamme, M., and D.H. Erwin. 2018. "Ediacaran extinction and Cambrian explosion." *Trends in Ecology and Evolution* 33:653–663. Doi:10.1016/j. tree.2018.06.003.

Droser, M.L., Gehling, J.G., and S. Jensen. 1999. "When the worm turned: Concordance of Early Cambrian ichnofabric and trace-fossil record in siliciclastic rocks of South Australia." *Geology* 27(7):625–628. Doi:10.1130/0091-7613(1999) 027<0625:WTWTCO>2.3.CO;2.

Gorin, G., Fiet, N., and M. Pacton. 2008. “Benthic microbial mats: a possible major component of organic matter accumulation in the Lower Aptian oceanic anoxic event.” *Terra Nova* 21(1):21–27. Doi:10.1111/j.1365-3121.2008.00848.x.

Hagadorn, J.W. and B. Waggoner. 2000. “Ediacaran fossils from the southwestern Great Basin. United States.” *Journal of Paleontology* 74:349–359. Doi:10.1666/ 0022-3360(2000)074<0349:EFFTSG>2.0.CO;2.

Harazim, D., Callow, R.H.T., and D. McIlroy. 2013. “Microbial mats implicated in the generation of intrastratal shrinkage (‘synaeresis’) cracks.” *Sedimentology* 60:1621–1638. Doi:10.1111/sed.12044.

Herringshaw, L.G., Callow, R.H.T., McIlroy, D., et al. 2017. “Engineering the Cambrian explosion: the earliest bioturbators as ecosystem engineers.” *Geological Society, London, Special Publications* 448:369–382. Doi: 10.1144/SP448.18

Jensen, S., Saylor, B.Z., Gehling, J.G., and G.J.B. Germs. 2000. “Complex trace fossils from the terminal Proterozoic of Namibia.” *Geology* 28:143–146. Doi:10.1130/ 0091-7613(2000)28<143: CTFFTT>2.0.CO;2

Jensen, S., Droser, M.L., and N.A. Heim. 2002. “Trace fossils and ichnofabrics of the lower Cambrian Wood Canyon Formation, southwest Death Valley area: Field trip guide book.” *Society for Sedimentary Geology* 93:123–135.

Landing, E. 1994. “Precambrian-Cambrian boundary global stratotype ratified and a new perspective of Cambrian time.” *Geology* 22:179–82. doi:10.1130/00917613(1994)022 < 0179:PCBGSR > 2.3.CO;2.

Loyd, S.J. and F.A. Corsetti. 2010. “The origin of the millimeter-scale lamination in the Neoproterozoic Lower Beck Spring Dolomite: Implications for widespread, fine-scale,

layer-parallel diagenesis in Precambrian carbonates." *Journal of Sedimentary Research* 80:678–687. Doi:10.2110/jsr.2010.063.

Macdonald, F.A., Pruss, S.B., and J.V. Strauss. 2014. "Trace Fossils with Spreiten from the Late Ediacaran Nama Group, Namibia: Complex Feeding Patterns Five Million Years Before The Precambrian-Cambrian Boundary." *Journal of Paleontology* 88(2):299–308. Doi:10.1666/13-042.

Mángano, M.G., and L.A. Buatois. 2016. "The Trace-Fossil Record of Major Evolutionary Events: Volume 1: Precambrian and Paleozoic." *Springer Netherlands*. ISBN 978-94017-9600-2.

Mata, S.A. 2012. "Paleoenvironments and the Precambrian-Cambrian transition in the Southern Great Basin: Implications for microbial mat development and the Cambrian Radiation." Ph.D Thesis, University of Southern California.

Meyer, M., Xiao, S., Gill, B.C., Schiffbauer, J.D., Chen, Z., Zhou, C., and X. Yuan. 2014. "Interactions between Ediacaran animals and microbial mats: Insights from *Lamonte trevallis*, a new trace fossil from the Dengying Formation of South China." *Palaeogeography. Palaeoclimatology, Palaeoecology* 396:62–74. Doi:10. 1016/j.palaeo.2013.12.026

Noffke, N. 2000. "Extensive microbial mats and their influences on the erosional and depositional dynamics of a siliciclastic cold water environment (Lower Arenigian, Montagne Noire, France)." *Sedimentary Geology* 136:207–215. Doi:10.1016/S00370738(00)00098-1.

Noffke, N., Eriksson, K.A., Hazen, R.M., and E.L. Simpson. 2006. “A new window into Early Archean life: Microbial mats in Earth's oldest siliciclastic tidal deposits (3.2 Ga Moodies Group, South Africa)” *Geology* 34(4):253–256. Doi;10.1130/ G22246.1

Pemberton, S.G. and R.W. Frey. 1982. “Trace fossil nomenclature and the *Planolites-Palaeophycus* dilemma.” *Journal of Paleontology* 56(4):843–881.

Sappenfield, A., Droser, M.L., Kennedy, M.J., and R. McKenzie, R. 2012. “The oldest Zoophycos and implications for Early Cambrian deposit feeding.” *Geological Magazine* 149(06):1–6. Doi:10.1017/S0016756812000313

Schiffbauer, J.D., Huntley, J.W., O’Neil, G.R., Darroch, S.A.F., Laflamme, M., and Y. Cai. 2016. “The Latest Ediacaran Wormworld Fauna: Setting the Ecological Stage for the Cambrian Explosion.” *GSA Today* 26(11):4–11. Doi: 10.1130/ GSATG265A.1.

Schiffbauer, J. 2016. “The age of tubes: A window into biological transition at the Precambrian-Cambrian boundary.” *Geology* 44:975–976. Doi:10.1130/ focus112016.1.

Seilacher, A., Buatois, L.A., and M.G. Mangano, 2005. “Trace fossils in the Ediacaran-Cambrian transition: Behavioral diversification, ecological turnover and environmental shift.” *Palaeogeography. Palaeoclimatology, Palaeoecology*:227, 323–356. Doi:10.1016/j.palaeo.2005.06.003.

Selly, T., Schiffbauer, J.D., Jacquet, S.M., Smith, E.F., Nelson,L.L., Andreasen,B.D., Huntley, J.W., Strange, M.A., O’Neil, G.R., Thater, C.A., Bykova, N., Steiner, M., Yang, B., and Y. Cai. 2019. “A New Cloudinid Fossil Assemblage from the Terminal Ediacaran of Nevada, USA.” *Journal of Systematic Palaeontology*. doi: 10.1080/14772019.2019.1623333.

Schindelin, J.;Arganda-Carreras, I., Frise, E. et al., 2012. “Fiji: an open-source platform for biological-image analysis.” *Nature methods* 9(7):676-682, PMID 22743772. doi:10.1038/nmeth.2019.

Smith, E.F., Nelson, L.L., Tweedt, S.M., Zeng, H., and J.B. Workman. 2017. “A cosmopolitan late Ediacaran biotic assemblage : new fossils from Nevada and Namibia support a global biostratigraphic link.” *Proceedings of the Royal Society Biology* 284:20170934. https://doi.org/10.1098/ rspb.2017.0934.

CHAPTER 5: THE DEATH VALLEY EDIACARAN–CAMBRIAN DEPOSITS AS A HOTBED FOR NAMA DIVERSITY

The placement of the terminal Ediacaran at the forefront of the Cambrian Explosion necessitates in depth exploration and research into Ediacaran fossil localities, new and established. This is the case for the Ediacaran–Cambrian deposits of the western United States, which have a rich paleontological history. The long established fossil sites, like Chicago Pass and Boundary Canyon, provide a unique opportunity for reinvestigation and the application of analytical techniques that have not been previously used. More recently, or newly, described fossil assemblages, like those of the Deep Spring Formation at Ancient Bristlecone Pine Forest, benefit from the already described fossil biota from established sites, but also provide an opportunity for sedimentological, taxonomic, and taphonomic comparisons to such sites. Thereby expanding our knowledge of the controls on diversity and preservation in Ediacaran exceptional preservation localities.

Although most studies focus primarily on the more exceptionally preserved fossils, much can also be attained from examining poorly preserved specimens. In the case of the tubular biota from Ancient Bristlecone Pine Forest, the fossils appear to have undergone the same taphonomic pathway as the tubular fossils from Mt. Dunfee, Montgomery Mountains, the Gaojiashan Lagerstätte, and the Miaohe biota, but under different, less desirable conditions. Identifying these conditions and their effect on the final fossil quality can lead to the addition of Wormworld fossil sites that contain poorly preserved remnants of fossils and would thus be otherwise be overlooked. Not only does the addition of these sites expand the known geographic extent of the Wormworld fauna, but may lead to the identification of classifiable taxa through the use of new analytical approaches.

Identifying taphonomic pathways in relation to sedimentology requires the ability to identify the mineralogical composition of the fossils, while measuring fossil diversity requires the ability to identify difficult to discern fossilized remnants. Advanced imaging and analyses, like scanning electron microscopy and microCT imaging has resulted in the ability to identify small, fragmented fossils encased in sediment that would otherwise be difficult to impossible to extract without damaging. It was also through the application of this technology that the oldest soft-tissue preservation in the fossil record was identified in the cloudinomorphs of the late Ediacaran Wood Canyon Formation (Schiffbauer et al., 2020). These technologies were also used to identify density and compositional differences within the fossils and the host rock sediments. Additionally, when applied to samples containing the common, known ichnotaxa from the Ediacaran, petrographic thin sectioning revealed evidence for complex feeding activity that was previously indistinguishable on the bed surfaces.

Investigations into trace fossil assemblages, like the Wood Canyon Formation at Chicago Pass and Boundary Canyon, provide a different view of the Wormworld organisms than what is attained from the tubular fossils. As the terminal Ediacaran contains the earliest evidence for established burrowing behaviors, the ability to quantify changes in complexity and frequency of trace making behaviors can provide information on the impact of early bioturbation on the previously quiescent substrate prior to the Cambrian Explosion. Further, the ability to correlate trace fossil assemblages with faunal turnovers in body fossil localities leads to a more complete picture of the community makeup and changes of terminal Ediacaran Wormworld communities. As with the tubular fauna, the use of analytical techniques (petrographic thin sectioning in the case of the Wood Canyon Fm. traces) on what appear to be common fossils can reveal concealed fossils,

like *Lamonte trevallis*, which represents the earliest complex burrowing behavior in the western United States fossil assemblages.

The ever-expanding diversity of faunal occurrences in the Deep Spring and Wood Canyon formations warrants the establishment of the western United States an Ediacaran fossil Lagerstätte. With the occurrence of cloudinomorphs, erniettomorphs, and early complex traces, the western United States fossil beds continue to produce fossil taxa that are representative of the terminal Ediacaran Nama assemblage, paralleling the established Lagerstätte localities in diversity and preservation. However, the unfortunate reality of studying Ediacaran organisms is that the overwhelming majority are completely lacking in readily preservable hard parts. Poorly preserved sections, like Ancient Bristlecone Pine Forest, may provide important information as to the preservation pathways used to preserve soft-tissues and how, in particular the pyritization-kerogenization-aluminosilicification, the same pathways with different abundances of resources can produce incredible preservation fossils in one locality and featureless fossil remnants in another. Identification of sedimentological units that are capable of preserving labile tissues are vital, and, even more so, is the understanding of the taphonomic processes behind soft-tissue preservation. Identifying preservational biases in relation to biological events, preserved in both body and trace fossil assemblages, that occurred within the Wormworld fauna and their impact on the marine ecosystem continues to provide clues into the driving forces behind the proliferation of metazoan life in the Cambrian.